# THE EFFECTS OF TENSILE LOADING AND EXTRACELLULAR ENVIRONMENTAL CUES ON FIBROBLASTIC DIFFERENTIATION AND EXTRACELLULAR MATRIX PRODUCTION BY MESENCHYMAL STEM CELLS

A Dissertation
Presented to
The Academic Faculty

by

Derek M. Doroski

In Partial Fulfillment
of the Requirements for the Degree
Doctor of Philosophy in the
School of Biomedical Engineering

Georgia Institute of Technology
May 2011

# THE EFFECTS OF TENSILE LOADING AND EXTRACELLULAR ENVIRONMENTAL CUES ON FIBROBLASTIC DIFFERENTIATION AND EXTRACELLULAR MATRIX PRODUCTION BY MESENCHYMAL STEM CELLS

Approved by:


Dr. Johnna S. Temenoff, Advisor
School of Biomedical Engineering
*Georgia Institute of Technology*

Dr. Barbara D. Boyan
School of Biomedical Engineering
*Georgia Institute of Technology*

Dr. Andres J. Garcia
School of Mechanical Engineering
*Georgia Institute of Technology*

Dr. Andrew Lyon
School of Chemistry and Biochemistry
*Georgia Institute of Technology*

Dr. Marc E. Levenston
School of Mechanical Engineering
*Stanford University*



Date Approved: March 10, 2011

To my wife and baby girl.

# ACKNOWLEDGEMENTS

This acknowledgment may seem weird at first.

Just read iambically; that would be best.

First I think I will thank my advisor.

Then I will take time to thank all the rest.

Dr. Johnna Temenoff was essential.

And my committee with science guidance.

Grad meetings with my lab members was key.

Especially when results made no sense.

My undergrads James Eames and Brian Nguyen.*

Provided help and data collections.

Johnafel Crowe trained me on confocal.

Aqua Asberry taught stains and sections.

Must not forget the old Levenston lab.

My early sterile technique came from there.

And to my wife and baby ‘specially.

Without them I might of pulled out my hair.

Finally, let’s thank the Bard and the Church.

Inspirations and strength during research.

* Note: Nguyen is pronounced “win.” With other pronunciations this line is not in pentameter.

# TABLE OF CONTENTS

# LIST OF TABLES

# LIST OF FIGURES

# LIST OF ABBREVIATIONS

| | |
|---|---|
| α-SMA | α-smooth muscle actin |
| ANOVA | Analysis of variance |
| A-PEG-SVA | acryl-PEG-succinimidyl valerate |
| APS | Ammonium persulfate |
| bMSC | bovine marrow stromal cell |
| $CaH_2$ | Calcium hydride |
| Da | Daltons |
| DAB | Diaminobenzidine |
| DNA | Deoxyribonucleic acid |
| $ddH_2O$ | Distilled, deionized water |
| DHLNL | Dihydroxylysinonorleucine |
| ECM | Extracellular matrix |
| FBS | Fetal bovine serum |
| FuCl | Fumaryl chloride |
| GAG | Glycosaminoglycan |
| GAPDH | Glyceraldehyde phosphate dehydrogenase |
| GPC | Gel permeation chromatography |
| GRGDS | Glycine-arginine-glycine-aspartate-serine |
| hACL | Human anterior cruciate ligament |
| HLNL | Hydroxylysinonorleucine |
| hMSCs | Human mesenchymal stem cells |
| IHC | Immunohistochemistry |
| kDa | Kilodaltons |

| | |
|---|---|
| MeCl | Methylene chloride |
| MMP | Matrix metalloproteinase |
| $M_n$ | Number molecular weight |
| mRNA | Messenger ribonucleic acid |
| MSC | Mesenchymal stem cell/marrow stromal cell |
| MW | Molecular weight |
| myoD | myogenic differentiation protein |
| NMR | Nuclear Magnetic Resonance |
| OCT | Optimal cutting temperature compound |
| OPF | Oligo(poly(ethylene glycol) fumarate |
| OPF-3K | OPF with a 3 kDa PEG chain |
| OPF-10K | OPF with a 10 kDa PEG chain |
| PBS | Phosphate buffered saline with $Ca^{2+}$ and $Mg^{2+}$ |
| PEG | Poly(ethylene glycol) |
| PEG-DA | Poly(ethylene glycol)-diacrylate |
| PI | Polydispersity Index |
| PLGA | Poly(lactic-co-glycolic acid) |
| PLLA | Poly-L-lactic acid |
| PPARγ | Peroxisome proliferator-activated receptor-gamma 2 |
| RGD | Arginine-glycine-aspartate |
| RT-PCR | Reverse transcriptase polymerase chain reaction |
| TEA | Triethylamine |
| TEMED | N,N,N',N'-tetramethylethylenediamine |
| $W_d$ | Weight of the hydrogel after vacuum-drying |
| $W_w$ | Weight of the hydrogel after culture and before drying |

# SUMMARY

Ligament/tendon tissue engineering has the potential to provide therapies that overcome the limitations of incomplete natural healing responses and inadequate graft materials. While ligament/tendon fibroblasts are an obvious choice of cell type for these applications, difficulties associated with finding a suitable cell source have limited their utility. Mesenchymal stem cells/marrow stromal cells (MSCs) are seen as a viable alternative since they can be harvested through routine medical procedures and can be differentiated toward a ligament/tendon fibroblast lineage. Further study is needed to create an optimal biomaterial/biomechanical environment for ligament/tendon fibroblastic differentiation of MSCs. The overall goal of this dissertation was to improve the understanding of the role that biomechanical stimulation and the biomaterial environment play, both independently and combined, on human MSC (hMSC) differentiation toward a ligament/tendon fibroblast phenotype.

Specifically, the effects of cyclic tensile stimuli were studied in a biomaterial environment that provided controlled presentation of biological moieties. The influence of an enzymatically-degradable biomaterial environment on hMSC differentiation was investigated by creating biomaterials containing enzymatically-cleavable moieties. The role that preculture may play in tensile responses of hMSCs was also explored. Together, these studies provided insights into the contributions of the biomaterial and biomechanical environment to hMSC differentiation toward a ligament/tendon fibroblast phenotype.

# CHAPTER 1

# INTRODUCTION

## 1.1 Motivation

Ligaments and tendons are tissues that are important in inducing and guiding joint movement.[1] Thousands of people seek medical attention each year for injuries to these tissues.[2] Acute ruptures of ligaments and tendons stimulate a natural healing response that often fails to provide complete regeneration.[3,4] In modern repair, autografts from the patient can result in painful donor site morbidity while allografts from cadavers can provoke immune responses, disease transmission, and are in limited supply.[5-9] Often neither graft type completely restores pre-injury functionality.[5] Therefore, tissue engineered grafts that employ a biomaterial scaffold, cells, and bioactive factors are being investigated to overcome these significant challenges. Fibroblasts, the major cell type of ligaments and tendons,[4] are a major candidate cell type for these studies. However, difficulties associated with finding an acceptable source of autologous ligament/tendon fibroblasts has led to the investigation of mesenchymal stem cells/marrow stromal cells (MSCs) as a possible alternative cell type.[10] MSCs have been employed in many biomaterial environments and are often cultured under tensile strain to promote differentiation toward a ligament/tendon fibroblast phenotype.[11] However, understanding of how the local extracellular environment, in combination with mechanical loading, influences cellular differentiation and production of appropriate extracellular matrix is limited. Therefore, controlled experiments that elicit the effects of the composition of the extracellular environment on MSC phenotype in the presence and absence of tensile

stimulation can provide fundamental knowledge needed for the rational design of future *ex vivo* systems to promote fibrous differentiation of MSCs.

## 1.2 Research Objectives

The objective of the research presented in this dissertation was to investigate the role that the biomaterial environment has on the response of human MSCs (hMSCs) to cyclic tensile strains. A model system with well-controlled presentation of bioactive extracellular cues to encapsulated hMSCs was employed to investigate the effects of tensile loading on the promotion of a ligament fibroblast phenotype. In addition, an enzymatically-degradable biomaterial environment was employed to explore the influence of cell-mediated, localized carrier degradation on the production of major ligament/tendon extracellular matrix (ECM) proteins by encapsulated hMSCs. These enzymatically-degradable biomaterials were used with a preculture period or without preculture to create diverse cell-biomaterial environments that facilitated the study of the contribution of preculture on hMSC responses to short duration (1 day) tensile strain. The goal of these studies was to improve the understanding of the role of the local extracellular environment and biomechanical loading on hMSC differentiation toward a ligament/tendon fibroblast phenotype. The **central hypothesis** was that culture in an enzymatically-cleavable biomaterial carrier would increase relevant ligament/tendon ECM production by encapsulated hMSCs and increase key ligament/tendon gene expression levels in response to cyclic tensile strain. This hypothesis was explored through three specific hypotheses and research aims.

**Hypothesis I:** Cyclic tensile loading will promote a ligament/tendon fibroblastic phenotype in hMSCs encapsulated in OPF hydrogels over 21 days of *in vitro* culture.

**Specific Aim I:** Investigate the effect of cyclic tensile loading on hMSCs in an OPF-based biomaterial environment.

While tensile stimulation has previously been used to encourage differentiation of hMSCs toward a ligament/tendon fibroblastic phenotype, optimization of MSC differentiation to ligament/tendon fibroblasts has been hampered by a lack of knowledge of how biomechanical cues regulate this process. For these experiments, hMSCs were encapsulated in a hydrogel environment consisting of OPF and PEG-diacrylate (PEG-DA). This PEG-based biomaterial presents an environment with limited biological interaction, but with the inclusion of a tethered adhesive peptide glycine-arginine-glycine-aspartate-serine (GRGDS), the material could be designed for specific interaction with integrin cell surface receptors. hMSC-seeded hydrogels containing GRGDS were exposed to cyclic tensile strain (10% strain, 1Hz, 3 hours of cyclic tensile stimulation followed by 3 hours without stimulation) over 21 days using a custom tensile culture bioreactor. After days 1, 7, 14 and 21 of culture, cell number, gene expression, and protein production was examined. Comparisons were made with static controls to characterize the effect of tensile stimulation on hMSCs in OPF-based hydrogels.

**Hypothesis II:** Culture in an enzymatically-degradable biomaterial environment will promote the production of major ligament/tendon extracellular matrix (ECM) proteins by encapsulated hMSCs over 21 days of culture.

**Specific Aim II:** Determine whether hMSCs in hydrogels that are susceptible to enzymatic degradation are induced toward expression and production of a ligament/tendon ECM compared to hMSCs in hydrogels that are not susceptible to enzymatic degradation.

Remodeling of the ECM is an important part in the normal maturation of ligament/tendon tissues. Collagenases such as matrix metalloproteinase-1 (MMP-1) and MMP-13 can degrade fibrous ECMs and thus play an important role in tissue reorganization. Synthetic biomaterials, such as OPF, are not susceptible to cell-mediated enzymatic degradation. This insensitivity to enzymatic cleavage along with a relatively small mesh size may limit the ability of encapsulated cells to produce a ligament/tendon ECM throughout the hydrogel. Since degradation of the external environment is integral to natural tissue formation, it was hypothesized that a biomaterial carrier that is susceptible to enzymatic cleavage could encourage gene expression and ECM production in hMSCs that is characteristic of a ligament fibroblastic phenotype. To explore this possibility, hMSCs were encapsulated in enzymatically-cleavable hydrogels that were designed to be susceptible to MMP-mediated degradation. A range of enzymatically-cleavable sequence concentrations (0%, 25%, 75%, or 100%) were used to create biomaterial environments with different levels of susceptibility to enzyme-mediated degradation. After days 1, 7, 14, and 21 of culture, cell number and viability, cell morphology, MMP production, gene expression, and protein production were examined. The behavior of the hMSCs was compared across hydrogel types and to human anterior cruciate ligament (hACL) fibroblasts encapsulated in similar environments in order to determine whether hMSCs would exhibit upregulation of gene expression and ECM

production similar to an hACL fibroblast phenotype in hydrogels containing enzymatically-cleavable motifs compared to non-enzymatically cleavable hydrogels.

**Hypothesis III:** Preculture of hMSCs in enzymatically-cleavable hydrogels will upregulate gene expression of ligament/tendon fibroblastic genes (collagen I, collagen III, tenascin-C) in response to short-term tensile strain.

**Specific Aim III:** Examine the effect of preculture on the response of encapsulated hMSCs to short-term tensile strain (24 hours).

Multiple weeks of strain can be required before upregulation of characteristic ligament/tendon fibroblastic genes are seen in hMSCs. During this time period gene expression patterns in hMSCs can change and ECM proteins can be secreted even in static cultures. Since these and other changes in the local extracellular environment occur in a cell-biomaterial system exposed to multiple weeks of tensile culture, it is unclear whether multi-week strain periods are required for characteristic gene expression changes to manifest or if shorter strain periods are interacting with changes in the cell-biomaterial environment that occur after over multiple weeks of culture. Because this enzyme-sensitive biomaterial promoted ECM deposition by embedded MSCs over 21 days of static culture, it was hypothesized that a static preculture period before exposure of hMSCs to short term strain would stimulate ligament/tendon fibroblast phenotypic gene expression responses that are normally seen with longer tensile culture periods. To investigate this hypothesis hMSCs were encapsulated in 100% enzymatically-cleavable hydrogels with a preculture period or without preculture. Differences in baseline gene expression levels and ECM production between precultured and non-precultured samples were confirmed. After baseline culture, constructs were exposed to 24 hours of cyclic

tensile strain (10% strain, 1Hz, 3 hours without stimulation followed by 3 hours of cyclic tensile stimulation). Constructs cultured statically at 0% strain were used as controls. Gene expression of major ligament/tendon ECM proteins was examined to determine whether a preculture period, would affect MSC responses to short-term tensile strains.

### 1.3 Significance and Scientific Contributions

The studies detailed in this dissertation provide insights into how the interactions of mechanical and biomaterial cues affect the promotion of a characteristic ligament/tendon fibroblast phenotype in hMSCs. The controlled environment of the PEG-based hydrogel systems allowed addition of specific bioactive moieties to provide adhesive cues and localized matrix degradation in systems where needed. This controlled environment also facilitated mechanical stimulation of hydrogel constructs that may be needed to promote a ligament/tendon fibroblast phenotype in hMSCs while minimizing confounding effects from biological signaling that is seen with natural scaffolds. The use of preculture to create diverse cell-biomaterial environments facilitated the investigation of how changes in the local extracellular environment that occur even without mechanical stimulation may be interacting with cyclic tensile strains to produce observed cell responses.

In addition to elucidating effects of preculture and tensile loading on hMSC phenotype, behavioral differences between hMSCs and hACL fibroblasts were uncovered that may be related to the susceptibility of the biomaterial environment to enzymatic degradation. These results highlight the need for biomaterial systems that can adapt to the distinct biomaterial environments that may be needed for differentiating stem cells and terminally differentiated cells. Together, these findings provide a strong framework

for further elucidation of hMSC responses to biomaterial and mechanical environments and furnish information needed for the design of next generation biomaterials and bioreactors that may be needed to pre-differentiate MSCs to a ligament/tendon fibroblast-like phenotype. As such, results from this thesis contribute important key concepts that must be addressed to move toward the goal of making stem cells a feasible source for regeneration of tendons and ligaments. Therefore, these findings may have significant clinical applications in overcoming the limitations currently associated with harvesting autologous ligament/tendon fibroblasts for tendon/ligament tissue engineering applications.

# CHAPTER 2

# BACKGROUND AND LITERATURE REVIEW[†]

## 2.1 Tendon and Ligament

### 2.1.1 Function

Tendons and ligaments are dense, regularly arranged, connective tissues that induce or guide joint movement.[1] Tendons attach muscle to bone and are what couples the force of a muscle to a movement in the skeletal structure.[12] Ligaments attach bone to bone in order to regulate and guide the movement of bones with respect to each other and also provide support for the internal organs.[12] Both tissues function primarily in tension and therefore have similar structural characteristics.[12,13]

### 2.1.2 Structure and Composition

Tendon and ligament tissues are comprised of a cellular component and an extracellular matrix (ECM) component.[14] The cellular component consists of fibroblasts with small amounts of other cell types, while the ECM is primarily composed of collagen, proteoglycans, tenascin-C, and small amounts of other proteins.[13]

The largest component of the ECM of tendon and ligament tissue is collagen (primarily types I and III).[1,12,15] Collagen is the most abundant protein in the body, comprising one-third of the total protein mass.[16] There are at least nineteen different

---

[†] Portions of this chapter are adapted from Doroski, D.M., Brink, K.S., Temenoff, J.S. Techniques for biological characterization of tissue-engineered tendon and ligament. Biomaterials **28**, 187-202, 2007.

types,[1] with collagen type I being the most common.[17] In normal cruciate ligament tissue, the ratio of collagen I ECM to collagen III ECM is about 9:1.[18]

The ability of collagen to provide strength to tissues is an important characteristic, and is directly related to the structure of the molecule. Collagen forms a right-handed superhelix in a coiled-coil structure. In fibrillar collagens, such as collagen I and III, these superhelices form long fibers,[19] whose organization and diameter modulate tissue strength and stiffness.[20] The superhelix consists of three smaller left-handed helices whose structure provides high tensile strength through their rigidity and relative inelasticity.[12] The basic peptide sequence of these smaller helices consists of glycine-X-Y repeats, where X and Y are proline and hydroxyproline, respectively, in 10% of these repeats.[1] The small size of the glycine amino acid allows for close packing of the collagen helices[3] while the proline and hydroxyproline components of collagen influence the coil structure, thereby affecting the rigidity of the protein.[1]

Another important aspect of collagen is its ability to form cross-links. Cross-links mechanically stabilize the fibers and improve the tensile strength of the tissue.[21,22] Disulfide bonds are a cross-link that forms at cysteine residues and are found in type III and other collagens.[23] Other important cross-links include the immature cross-links dihydroxylysinonorleucine (DHLNL) and hydroxylysinonorleucine (HLNL). DHLNL cross-links are formed by condensation of a lysine-derived aldehyde with hydroxylysine or a hydroxylysine derived aldehyde with lysine. HLNL cross-links are formed by condensation of hydroxyallysine and hydroxylysine.[24] The degree of hydroxylation of their lysine residue correlates to the stability of the cross-link.[22]

Both of these cross-links are reducible by sodium borohydride[1] and are generally found in younger collagen. Over time, these reducible cross-links are converted to non-reducible pyridinoline and pyrrole forms.[22,25] Pyridinoline cross-links are proposed to form by condensation between two divalent keto-amine cross-links[26] while pyrrole cross-links are proposed to form from a lysine aldehyde and an immature cross-link.[27]

Proteoglycans are another important component of the tendon and ligament ECM due to their contribution to viscoelastic and other mechanical properties of the tissue.[13] Proteoglycans consist of at least one glycosaminoglycan (GAG) chain attached to a protein core. One of the functions of proteoglycans in ligament tissues is to attract water through the GAG chains and thus lubricate the tissue and enhance gliding function.[1] This hydration causes the proteoglycans to swell and become trapped among the collagen in the matrix leading to compressive strength and allowing rapid diffusion of water soluble molecules.[20] As such, proteoglycans add viscous properties to the matrix in the form of a hydraulic damper.[17]

The most abundant proteoglycan in tendon tissue is decorin.[20,28] Decorin inhibits formation of large collagen fibrils,[20,28,29] and thus prevents abnormal packing of collagen that can lead to reduced tensile strength.[30] Another proteoglycan, aggrecan, is found abundantly in areas where the tissue is subject to compressive forces,[20,28,29] such as where the tendon wraps around bone or at tendon to bone insertion sites.[28] Aggrecan's large size and negative charge creates an osmotic gradient that allows it to hold water and swell the collagen network, promoting a structure that resists compressive loading.[20,28] Other proteoglycans such as biglycan, fibromodulin, lumican, and versican can also influence a

wide range of the tissue properties, including fibril diameter, cellular proliferation and migration, and the viscoelasticity of the pericellular matrix.[20,29]

Tendon and ligament tissue also contains other proteins such as the matricellular protein tenascin-C. Tenascin-C associates with fibronectin[31] and its expression is upregulated in response to mechanical loading.[10] It has been shown to modulate growth factor activity[31] and inhibit $\beta_1$ integrin-dependent cell adhesion.[32] Since this protein is found in higher amounts in tendons and ligaments than in other orthopedic tissues, it has been used as a tissue specific marker.[10]

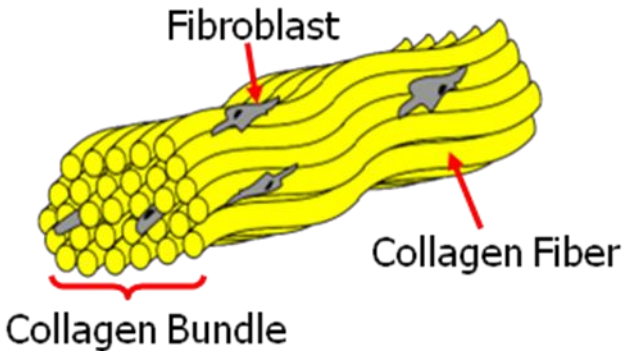


**Figure 2.1. The relationship between a collagen bundle and fibroblasts. The collagen bundle is comprise of individual collagen fibrils that tightly surround the cells.**

The ECM components described above are organized in a hierarchical fashion in tendon and ligament tissue, primarily to improve the tensile properties of the matrix.[12] The overall tissue structure consists of fibroblasts surrounded by collagen fibrils along with small amounts of proteoglycans.[1,12] The collagen fibrils comprise a collagen fiber (Fig. 2.1), which in turn constitutes a fiber bundle.[12] Fascicles, the main subdivision of the tissue, are groups of fiber bundles. These structures are aligned parallel to each other along the direction of principal force. The sinusoidal wave-like structure of the collagen

fascicles is known as the "crimp" structure and is thought to allow the tissue to elongate without causing damage.[1] The presence of the highly-hydrated proteoglycans provides further damping and lubrication in the tissue, as well as allowing the fascicles to slide past each other.[28]

While all tendons and ligaments have these basic structural components, characteristics of each component can vary between different tendon and ligament tissues. For example, the size and morphology of the fibroblasts is not consistent for all tendons and ligaments.[3] The collagen bundle width, amplitude and period of the crimp, and ratio of type I to type III collagen may also vary.[3]

### 2.1.3 Cells

The main cell type found in tendon and ligament tissue is the fibroblast. Fibroblasts have a spindle-shaped morphology, are sparsely distributed throughout the tissue, and align in columns along the direction of the collagen fibers (Figure 2.1).[4] While the fibroblasts themselves do not comprise a large volume of tendon/ligament tissue, they are responsible for secreting and maintaining the ECM that makes up the remainder of the tissue. However, the relatively low numbers of fibroblasts, along with their low mitotic activity, leads to a relatively low tissue turnover rate and may explain why some tendons and ligaments seem to possess a poor capacity for natural healing.[4]

### 2.1.4 Pathology

Pathologies of ligament and tendon tissue can be classified as acute or chronic according to the persistence of the pathological factors and as intrinsic or extrinsic according to the source of the injury stimulus.[33] Acute injuries are generally caused by extrinsic factors that lead to tissue rupture such as rapid twisting, high forces, or other

trauma.[34] This rupture may lead to further degeneration of the tissue.[35] Chronic disorders of ligament/tendon, are often caused by both intrinsic and extrinsic factors such as repetitive loading of the tissue beyond its physiological threshold[36] or microtrauma due to non-uniform stress fields within the tissue.[37] These factors can result in degeneration that includes inflammation of the sheath and degradation of the tissue.[33]

Over 800,000 people seek medical attention each year for injuries to ligaments, tendons, or the joint capsule.[2] Ruptures and other damage to tendons and ligaments can cause great pain and decrease the functionality of the joint complex.[33] There are numerous areas throughout the body where tendons and ligaments experience such injuries. These include the patellar tendon,[38] the anterior cruciate ligament,[12] the posterior cruciate ligament,[39] and the medial collateral ligament[40] in the knee; the Achilles tendon[4] at the heel; the anterior talofibular ligament[41] and the calcaneofibular ligament[42] in the ankle; the radial ulnohumeral ligament[43] and the lateral ulnar collateral ligament[44] in the elbow; the digital flexor tendon[4,12] and the ulnar collateral ligament[45] in the hand; the scapholunate ligament[46] in the wrist; the rotator cuff tendons[12], the acromioclavicular ligament[47], the coracoclavicular ligament[48], and the coracohumeral ligament[49] at the shoulder; and the gluteus medius tendon[50] at the hip.

In chronic ligament/tendon injuries natural repair mechanisms appear to involve constant regeneration of the tissue through ligament/tendon fibroblasts.[33] In acute tendon injuries three overlapping phases of healing are seen: inflammation, cellular proliferation with initial matrix deposition, and remodeling.[34] The inflammation phase of healing is characterized by the migration of inflammatory cells to the injury site. The cellular proliferation phase is characterized by an increase in the number of fibroblasts.[34,51] The

fibroblasts initially produce a provisional matrix consisting mainly of collagen III with some collagen I also present.[33,34,52] In the remodeling stage, a decrease in the cellularity of the wound site is seen and the ECM is reorganized as greater amounts of collagen I are produced to replace the collagen III matrix.[53] Remodeling is facilitated through an increase in the levels of matrixmetalloproteinases (MMPs) after injury.[54] While the intensity of healing responses can vary, natural healing is often insufficient since many tendons and ligaments possess a limited capacity to regenerate.[3,4]

### 2.1.5 Current Treatment Options

In the absence of sufficient natural healing, surgical interventions are commonly used to repair ruptured ligaments and tendons. While certain ligaments and tendons can be repaired by suturing the injured tissue back together, some heal poorly in response to this type of surgery, so the use of grafts is required.[55] While there has been a lot of success in restoring functionality after ligament/tendon injury,[9] complications related to graft choice often arise. Autografts from the patient may result in donor site morbidity and laxity of the joint, while cadaveric allografts may cause a harmful response from the immune system, retroviral transmission, and are not readily avialable.[5-9] Both autografts and allografts often fail to restore the full strength of undamaged tissue.[5]

## 2.2 Engineered Tendon and Ligament

### 2.2.1 Previous Approaches

In response to the shortcomings of current treatment options, a number of synthetic graft materials have been investigated from as early as the 1970s.[56] Early prostheses included polyethylene terephthalate, polytetrafluroethylene, and polyethylene

terephthalate-polypropylene.[57] While the high strength of these grafts lead to initial success, poor integration with existing tissue eventually led to abrasion and failure of the grafts. The design of ligament/tendon replacements was advanced with the invention of a polypropylene graft designed to promote tissue ingrowth.[56] However, inflammation caused by the non-degradable graft material caused eventual failure of this prosthesis. While newer grafts that facilitate tissue ingrowth such as the "LARS" artificial ligament have showed some encouraging results,[58] the past failures of synthetic grafts have prevented widespread use of tissue engineered tendons and ligaments except as an experimental treatement.[59]

### 2.2.2 Current Tissue Engineering Strategies

While many approaches for the tissue engineering of ligaments and tendons are being investigated, current tissue engineering strategies often involve the use of a biomaterial carrier, cells, and/or bioactive factors to promote tissue healing by harnessing the regeneration potential of natural processes in the body.[60] The biomaterial carrier is usually a three dimensional scaffold used in an effort to direct pre-seeded cells to create viable tendon/ligament tissue.[61-65] Scaffolds are often chosen/designed to be degradable in order to adapt to tissue production inside the scaffold and to encourage cellular recruitment and external tissue ingrowth.[2] In addition, to ensure final clinical use, biomaterials are selected that are not harmful to the surrounding tissue and do not result in unresolved inflammation or other deleterious biological responses.

### 2.2.3 Biomaterials

A number of scaffold materials, both natural and synthetic, have been explored. One advantage of natural scaffolds is that they are inherently bioactive and facilitate

interactions with seeded cells that may be necessary for tissue engineering strategies. Another advantage of is that components of the natural ECM can be used.[66] The use of ECM components facilitates the presentation of bioactive moieties that are similar to those present in the tissue that is being engineered. Given that collagen is the largest component of tendon and ligament tissues, it is no surprise that the most commonly used natural scaffolds are primarily composed of collagen.[67-80] Other natural scaffolds include porcine small intestine submucosa,[81-84] chitosan-based scaffolds,[62,63,85] silk fibers,[64,86,87] semitendonous tendon,[88] and fibronectin/fibrinogen fibers.[89] Unfortunately, the inherent bioactivies of natural scaffolds can present a complex signaling environment that is not well defined. Consequently, control of bioactive moieties presented in natural matrices is limited. In addition, issues related to biocompatibility can arise depending on the source of the scaffold material.[56]

In contrast, synthetic materials provide greater control over the chemical and physical properties of the scaffold with a high degree of reproducibility.[66] One way to tailor the properties of the biomaterial are the polymer used. For example, polymers can be produced with specific molecular weights, cross-linking modes, degradation characteristics, and mechanical properties.[66,90] A large number of synthetic scaffolds are being investigated for tendon and ligament tissue engineering. The most commonly used synthetic scaffolds are made of poly-L-lactic acid (PLLA)[10,61,65,71,91-93] or poly(lactic-co-glycolic acid) (PLGA).[65,94,95] Synthetic materials lack the inherent biological activity that natural scaffolds possess and may require the introduction of biological moieties to facilitate suitable cellular interactions. In addition, synthetic scaffolds may need to be replaced by natural tissue over time, possibly through degradation of the scaffold.[56]

While the lack of biological moieties can be a disadvantage of synthetic materials, they also provide a well-defined environment that can facilitate controlled experiments examining the effects of biological moieties that are introduced in a discrete manner.

Biomaterial fibers that are organized using textile structures are a common type of graft that is explored for ligament/tendon tissue engineering.[96] Both natural and synthetic materials have been used with these structures. The main types of textile structures are woven structures such as the Leeds-Keio PET graft,[97] knitted structures such as the Stryker-Dacron PET graft,[98] and braided structures such as the Gore-Tex PTFE graft.[99] The polymer fibers provide a structure that is similar to ligament/tendon tissue and the textile organization can increase the elastic modulus and ultimate tensile strength of the graft to a point where it approaches that of natural tissue.[96] While the high tensile strength of these grafts makes them attractive as a possible ligament/tendon substitute, they may not be able to serve as long term solutions as they can be susceptible to abrasion, undergo fatigue failure, and their wear products can cause inflammation.[59]

Hydrogels, which can be fabricated from natural or synthetic polymers, are also used for ligament/tendon tissue engineering.[100] Hydrogels are highly hydrated scaffolds (at least 30% by weight) that are formed through cross-linking between polymer chains.[66] These scaffolds can be used to encapsulate cells in a three dimensional environment that can be formed *in situ* in a minimally invasive manner.[101] While hydrogels do not generally possess the mechanical properties that woven, knitted, or braided fibers can achieve, they are often designed to be replaced by natural tissue as they degrade.[66,96] Since hydrogels are often intended to be transient structures, the initial mechanical strength of the scaffold may not be a disadvantage.

This work employed synthetic hydrogel scaffolds to create a biomaterial model system. Specifically, oligo(poly(ethylene glycol) fumarate (OPF) was used with poly(ethylene glycol)-diacrylate (PEG-DA) as a cross-linker (Fig. 2.2). These synthetic, PEG-based polymers can be cross-linked to form hydrogels with cross-linking accomplished though a chain-growth polymerization mechanism.[102] OPF-based hydrogels can be used as a injectable,[103] in-situ thermally cross-linkable,[103] hydrolytically degradable[104] biomaterial scaffold. In addition, this polymer and its degradation products have been found to be cytocompatible in *in vitro* studies.[105,106]

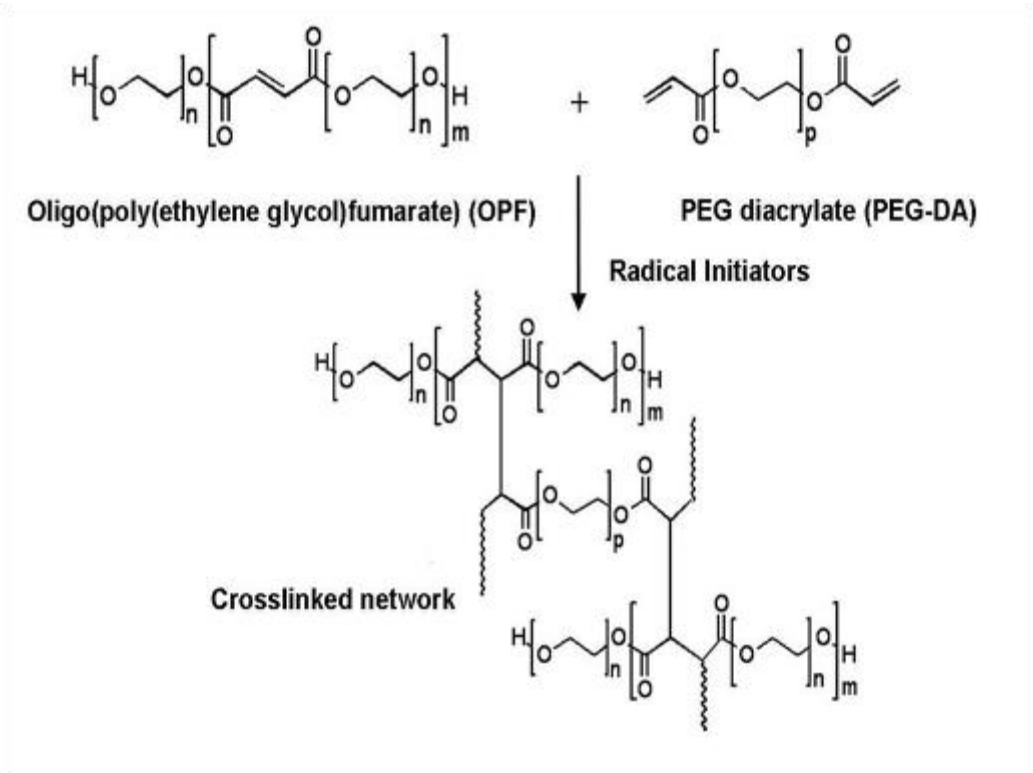


**Figure 2.2. Cross-linking of OPF and PEG-DA. Step growth of the polymer network is achieved through the use of thermal radial initiators.**

Both OPF and PEG-DA contain PEG repeat units. The number of repeats is represented in the figure by the letter "n". OPF-3K, PEG-DA-3K, OPF-10K, etc. are named according to the size of these repeats- i.e. OPF with PEG chain of 10 kDa results

in OPF-10K and OPF with a PEG chain of 3 kDa results in OPF-3K. The size of this PEG chain can be modified to influence swelling, degradation, and mechanical properties of the resultant OPF hydrogels.[104,106,107] These PEG-repeat units are responsible for the resistance to protein and cell adhesion that has been demonstrated with both OPF[108] and PEG-DA.[109]

Encapsulation experiments have shown that cells remain in the constructs after a four week period that can continue to produce matrix proteins.[110] The ability encapsulate cells into these synthetic hydrogels and to present bioactive factors provides a versatile synthetic model system. Since the OPF biomaterial does not promote cell adhesion or other biochemical responses it can be used as a "blank slate" that does not introduce confounding biological signals into controlled experiments. Biological functionalities, can later be added in a discrete, controlled manner to effect cellular responses. One commonly employed functionality is the RGD peptide which has been used to modulate cell adhesion in a dose dependent manner.[111] Enzymatically-degradable sequences have also been incorporated in PEG-based biomaterials to facilitate remodeling of the hydrogel environment and migration of encapsulated cells.[112,113]

To enable cell-mediated degradation of the biomaterial environment the enzymatically-degradable peptide, glycine-glycine-glycine-leucine-glycine-proline-alanine-glycine-glycine-lysine (GGGL↓GPAGGK) was conjugated on both ends to 3,400 Da MW A-PEG-SVA (Fig. 2.3). The GGGL↓GPAGGK peptide is cleaved between L and G.[114] Cleavage of this peptide is believed to occur through matrix metalloproteinases (MMPs) and can be achieved by collagenase from *Clostridium histolyticum*.[113] This cleavage can be inhibited by N-[(2R)-2-(Hydroxamidocarbonylmethyl)-4-

methylpentanoyl]-L-tryptophan methylamide] (GM6001).[113] GM6001 is a broad based MMP inhibitor that is known to reduce the activity of a number of MMPs (including 1, 2, 3, 7, 8, 9, 10, 12, 13, 14, 15, 17, 20, 21, 26).[115] The inhibition by GM6001 suggests that the GGGL↓GPAGGK peptide is indeed sensitive to MMP-mediated degradation although the susceptibility to any specific MMP is uncertain. GM6001 can also inhibit other enzymes including ADAMs[115] so it is possible that non-MMP enzymes that may be present in the bacterial collagenase used are actually responsible for cleavage. Since the GGGLGPAGGK peptide can be degraded enzymatically, its incorporation into hydrogel networks provides a synthetic model system where the total susceptibility to enzymatic degradation can be controlled.


**Fig. 2.3. Chemical structure of acrylated GGGLGPAGGK peptide (LGPA).**

### 2.2.4 Cells

Multiple cell types have been seeded within scaffolds in an effort to promote cell-mediated tissue regeneration. The most common cell types employed are ligament/tendon fibroblasts[62,63,70,72,74-77,84,85,94,95,116-122] and mesenchymal stem cells/marrow stromal cells (MSCs).[10,64,67-69,84,86,91,93,119,123] Since fibroblasts are the predominant cell type in tendon/ligament tissue they are often used for these applications.[4] Unfortunately, allogeneic ligament/tendon fibroblasts can provoke a foreign body response by the host and often there is not a suitable source of autologous cells.[10] MSCs are seen as a promising alternative since they can be harvested from

adults using a routine needle biopsy, expanded to large numbers,[10] and differentiated into ligament/tendon fibroblasts.[11,124]

### 2.2.5 Tensile Loading

Tensile loading is often employed with ligament/tendon tissue engineering constructs in order to promote a ligament fibroblast phenotype in MSCs.[11] This approach has seen some success in promoting upregulation of genes commonly associated with ligament/tendon fiboroblasts.[11,125] Strain regimens are often oscillatory in nature and are characterized by the strain amplitude, frequency of strain, and the timeframe of strain cycles and rest periods without strain. While a large variety of strain protocols have been investigated,[11,126-137] certain values for different parameters are often employed. A peak to peak amplitude of 10% and a frequency of 1 Hz are commonly used in an effort to simulate a physiological loading regimen.[129,130] Increased gene expression and protein production of collagen I in tendon fibroblasts has also been correlated to increasing the peak to peak amplitudes up to 10%.[138] A loading protocol consisting of 3 hours of cyclic strain followed by 3 hours of 0% strain has been employed, to upregulate collagen I gene expression and overall collagen content in fibrin constructs with encapsulated MSCs.[139] While preculture periods for strain regimens have not been widely investigated, a static preculture period of 1-2 days after cell seeding, but before strain is initiated, has been used in order to provide time for cells to spread and attach to the biomaterial matrix.[129,130]

### 2.2.6 Matrix Metalloproteinases

Normal maturation of ligament/tendon ECM requires degradation of the environment for reorganization of ECM components.[4,51,140] MMPs are one category of proteases that play an important role in natural degradation processes. MMPs, also

known as matrixins,[141] are a family of enzymes secreted by fibroblasts and MSCs that facilitate ECM reorganization,[141] making them crucial for normal embryonic development[141,142] and the maintenance of healthy tissue.[142-144] MMPs play a major role in the cleavage of ECM molecules, although other proteases can also facilitate ECM degradation.[145] After ligament injuries MMPs are upregulated and may play an important role in the healing process.[146] While the structure of these enzymes can vary, all MMPs contain sequence homology to the catalytic domain of MMP-1[145] and include a propeptide and a catalytic domain.[147] These proteases are generally secreted in a latent form and are activated extracellularly.[141] Activation occurs through cleavage of the propeptide or its displacement from the catalytic site.[148] These enzymes require a metal ion $Zn^{2+}$ cofactor[141] for activity which is where they get the name 'metalloproteinases.'

Regulation of MMPs occurs through many mechanisms. MMP amounts are regulated at both the transcriptional and post-transcriptional level.[149] In addition, the activity of MMPs can be controlled through the activation of latent MMPs or through the inhibition of active MMPs.[150] One of the major inhibitors of active MMPs is $\alpha_2$-macroglobulin.[151] $\alpha_2$-macroglobulin is a glycoprotein found in blood and tissue fluids[151] that entraps enzymes within the macroglobulin. As a result it will inhibit most endopeptidases.[152] Tissue inhibitors of metalloproteinases (TIMPs) are the other major class of MMP inhibitors[151] which prevent the function of a wide range of MMPs.[153] In addition to the regulation of MMP production and activity, the spatial localization of MMPs can also be regulated by cells.[147]

There are 23 different MMP genes in the human genome.[145] These MMPs are grouped into different categories according to their domain organization and substrate

preferences.[145] The categories are collagenases (MMP-1 aka interstitial collagense or collagenase 1, MMP-8 aka neutrophil collagenase or collagenase 2, MMP-13 aka collagenase 3), gelatinases (MMP-2 aka gelatinase A, MMP-9 aka gelatinase B), stromolysins (MMP-3 aka stromelysin 1, MMP-10 aka stromelysin 2), matrilysins (MMP-7 aka matrilysin 1, MMP-26 aka matrilysin 2, MMP-11 aka stromelysin 3), transmembrane-type MMPs (MMP-14 aka MT1-MMP, MMP-15 aka MT2-MMP, MMP-16 aka MT3-MMP, MMP-24 aka MT5-MMP), GPI-anchored membrane type MMPs (MMP-17 aka MT4-MMP, MMP-25 aka MT6-MMP), and others (MMP-12 aka macrophage elastase, MMP-19, MMP-20 aka enamelysin, MMP-21, MMP-23 aka CA-MMP, MMP-27, MMP-28 aka epilysin).

Collagenases may be important in ligament/tendon tissue as they target a number of collagens including collagen I and collagen III[145,147] which are the most prevalent components of ligament/tendon tissue.[154] The collagenases function by unwinding the triple helical fibrillar collagen chains[155] before cleaving the chains into characteristic ¾ and ¼ fragments.[145] Collagenases, such as MMP-1 and MMP-13 contain propetide, catalytic and hemopexin domains.[145] Both MMP-1 and MMP-13 are known to target collagen I, collagen II, collagen III, collagen X, gelatin, aggrecan, tenascin, and MMP-9 (Table 2.1).[147] However, there is variation between other known substrates of MMP-1 (collagen VII, collagen VIII, proteoglycan link protein, versican, entactin, α1-PI, ILb-1, pro-TNF, IGFBP-3, MMP-2) and MMP-13 (collagen IV, collagen IX, collagen XIV, perlecan, fibronectin, osteonectin, MMP-9, plasminogen activator inhibitor-2). In addition, when MMP-1 and MMP-13 target the same substrate their specificities can vary greatly.[156] MMP-1 and MMP-13 also possess different levels of susceptibility to

inhibitors which are related to structural differences in the S1' subsite of the catalytic domain.[157,158] In addition to collagenases, gelatinases may be important in ligaments/tendons as they target denatured collagen.[145] MMPs from other categories may also play a role in ligament/tendon tissue as they have shown some specificity to collagen III and in some cases collagen I.[147]

**Table 2.1. Comparison of MMP-1 and MMP-13**

| | **MMP-1** | **MMP-13** |
|---|---|---|
| Alternate names | Collagenase-1, Interstitial collagenase | Collagenase-3 |
| Chromosomal location | 11q22-q23 | 11q22.3 |
| s1' subsite structure | Small, closed | Long, open |
| ECM substrate | Collagens (I, II, III, VII, X), gelatin, proteoglycan link protein, aggrecan, versican, tenascin, entactin | Collagens (I, II, III, IV, IX, X, XIV), gelatin, aggrecan, perlecan, large tenascin-C, fibronectin, osteonectin |
| Non ECM substate | $\alpha_1$-PI, ILb-1, pro-TNF, IGFBP-3, MMP-2, MMP-9 | MMP-9, plasminogen activator inhibitor-2 |
| Activated by | MMP-3, MMP-10, plasmin, kallikrein, chymase | MMP-2, MMP-3, MMP-10, MMP-14, MMP-15, plasmin |
| Activator of | MMP-2 | MMP-2, MMP-9 |

This table is compiled from information from the cited references.[145,147,158]

# CHAPTER 3[‡]

# CYCLIC TENSILE CULTURE PROMOTES LIGAMENT/TENDON FIBROBLASTIC DIFFERENTIATION OF MARROW STROMAL CELLS ENCAPSULATED IN POLY(ETHYLENE GLYCOL)-BASED HYDROGELS

## 3.1 Introduction

Over 800,000 people seek medical attention each year for injuries to ligaments, tendons, or the joint capsule.[159] Tendon and ligament tissues, composed of collagen bundles organized in a hierarchical fashion, function primarily in tension to induce or guide joint movement.[12] Fibroblasts maintain this ECM, but their low cell numbers and low mitotic activity lead to a reduced tissue turnover rate that may explain the poor natural healing of some tendons and ligaments.[4] While tissue grafts can improve function after injury, current graft fixation procedures do not completely recapitulate normal joint mechanics, leading to potential for secondary pathologies such as osteoarthritis.[160] Thus, there is a need for new regenerative medicine-based strategies to improve healing of tendon/ligament injuries and provide alternatives to current autograft transplantation techniques.

Over the past 15 years, a variety of tissue engineering approaches have been explored for tendon and ligament regeneration. Many of these center on combining cells

---

[‡] This chapter has been adapted from Doroski, D.M., Levenston, M.E., Temenoff, J.S. Cyclic tensile culture promotes fibroblastic differentiation of marrow stromal cells encapsulated in poly(ethylene glycol)-based hydrogels. Tissue Eng Part A **16**, 3457-66, 2010.

with a 3-dimensional biomaterial scaffold,[161,162] and may also add exogenous bioactive factors, such as growth factors or mechanical (usually tensile) stimulation.[162-164] Progenitor cells, such as MSCs, are often selected as the cell source for these studies[162,165] since this overcomes the difficulty of isolating autologous tendon/ligament fibroblasts in sufficient numbers to seed on scaffolds for eventual clinical applications.[10] MSCs can be expanded many times[166] and subsequently differentiate into multiple lineages associated with orthopedic tissues, including tendon/ligament fibroblasts.[124] In addition, this flexibility provides the future possibility of using a single cell source to form all the tissues associated with tendon/ligaments and their insertions to bone/muscle, and thus potentially provides a true counterpart to the bone-ligament-bone autografts currently employed in reconstruction procedures.[167] However, optimization of MSC differentiation to tendon/ligament fibroblasts for these applications has been hampered by lack of knowledge of how both loading and biochemical cues simultaneously regulate this process. A well-controlled model system with the ability to alter both external loading parameters and local extracellular cues to better study MSC response to both stimuli concurrently was therefore developed.

For these studies, an OPF-based biomaterial was combined with a custom tensile culture bioreactor (Fig. 3.2A and 3.2B). Tensile strain has been employed to stimulate MSC differentiation toward a tendon/ligament fibroblast phenotype.[11] This system has the advantage of being able to develop strains in a three dimensional environment, which may be important since cells respond differently in two dimensional compared to three dimensional culture.[168] In addition, the tensile constructs are designed to create a

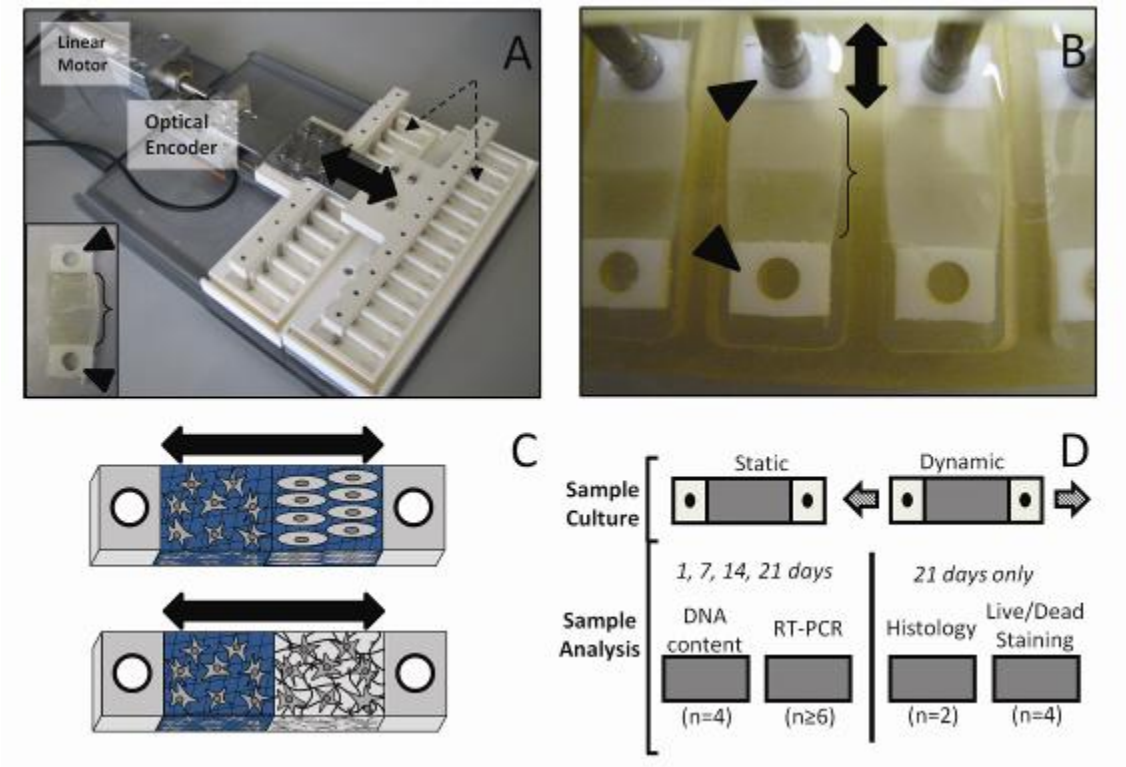


**Figure 3.1. A: Custom tensile culture system. Up to 24 biomaterial constructs can be cultured in tensile wells (dotted line arrows) and strained by the tensile rakes (double arrow shows direction of tensile strain) at the same time. The rake is moved by a linear motor with positional accuracy monitored by an optical encoder. Inset: Individual construct with hydrogel (bracket) flanked by end blocks (arrowhead). B: Laminated hydrogel constructs in culture wells. Polyethylene end blocks (arrowhead) are interfaced with the tensile rake to allow mechanical stimulation to be transduced to the hydrogel section (bracket) and create a uniform strain field in the construct during culture. Double arrow indicates direction of strain. C: Diagram demonstrating possibilities for future use of this culture system with laminated hydrogels. For example, this permits co-culture of two different cell types (top) or two biomaterial environments with different bioactive factors (bottom). Double arrow represents direction of strain. D: Overall experimental design for hMSC loading studies.**

uniform strain field across the hydrogel[169] to provide a well-defined mechanical environment.

While the long-term goal is to employ this model system to examine the formation of ligaments/tendons as well as their interfaces with surrounding tissues, a first step was to determine if layered (laminated) acellular OPF hydrogels would withstand

cyclic loading over 28 days *in vitro*. After this was ascertained, differentiation of hMSCs encapsulated in non-laminated OPF hydrogels in response to cyclic tensile loading was examined as a proof-of-concept before moving to more sophisticated co-culture conditions in future experiments. In particular, for these experiments, hMSCs were encapsulated in a mixture of OPF and PEG-DA with the tethered adhesive peptide GRGDS using a radical-induced gelation process[170] and cultured in a cyclic tensile bioreactor for 21 days. Based on previous work with tensile stimulation of MSCs,[11,171,172] constructs were cultured under a repeating cyclic strain regimen of 10% strain, 1 Hz, and 3 hours of strain followed by 3 hours without strain. After days 1, 7, 14 and 21 of culture, cell number, gene expression (particularly collagen I, III, and tenascin-C), and protein production was compared between constructs containing encapsulated hMSCs exposed to tensile stimulation and MSCs embedded in identical OPF hydrogels without mechanical stimulation to investigate the effects of cyclic tension on cellular differentiation in this hydrogel environment. More specifically, the hypothesis of this study was that cyclic tensile loading would promote a ligament/tendon fibroblastic phenotype in encapsulated hMSCs over 21 days of *in vitro* culture.

## 3.2 Materials and Methods

### 3.2.1 Polymer Synthesis

OPF with a 3 kDa PEG chain (OPF-3K) or a 10 kDa PEG chain (OPF-10K) was synthesized according to previous protocols.[173] Briefly, calcium hydride ($CaH_2$, Thermo Fisher Scientific, Waltham, MA) was mixed with methylene chloride (MeCl, Thermo Fisher Scientific) and distilled to produce anhydrous MeCl. To produce the OPF polymer, fumaryl chloride (FuCl, Sigma-Aldrich, St. Louis, MO) and triethylamine

(TEA, Sigma-Aldrich)) were slowly added dropwise to PEG (3 kDa; $M_n$: 3,300 ± 10 Da, PI: 1.1 or 10 kDa; $M_n$: 12,400 ± 20 Da, PI: 1.1, Sigma-Aldrich) that had been azeotropically distilled in toluene (Thermo Fisher Scientific) and dissolved in MeCl. FuCl and TEA were added at molar ratios of 0.9:1 FuCl:PEG and 1:2 FuCl:TEA under nitrogen gas and cooled over ice. MeCl was removed from the resultant OPF product by rotovapping (Buchi, New Castle, DE). Recrystalization of the OPF was carried out twice in ethyl acetate (Thermo Fisher Scientific) to remove salts produced by the conjugation reaction. Ethyl acetate was removed by three consecutive washes in ethyl ether (Thermo Fisher Scientific). Polymers were vacuum dried to remove ethyl ether and stored at -20°C before use. The molecular weight of the OPF polymer was determined through gel permeation chromatography (GPC, Shimadzu, Columbia, MD). The resultant OPF-3K polymer was found to have a molecular weight ($M_n$) of 8,900 ± 530 with a polydispersity index of 3.1 ± 0.4 and the OPF-10K had an approximate $M_n$ of 18,300 ± 90 with a polydispersity index of 4.8 ± 0.2. NMR spectra of similar OPF macromers and the number of double bonds present in the macromer has been reported previously.[108,173] The same batch of OPF-3K and OPF-10K was used for all hydrogels in these experiments. Further details regarding this synthesis are found in appendix A.1.

### 3.2.2 Peptide Conjugation

To allow presentation of arginine-glycine-aspartate (RGD) ligands to encapsulated cells, the GRGDS adhesion peptide (PeproTech, Rocky Hill, NJ) was conjugated to a 3,400 Da MW acrylated-PEG-succinimidyl valerate spacer (A-PEG-SVA, Laysan Bio, Arab, AL) according to previous protocols.[108] Briefly, conjugation was achieved by adding the A-PEG-SVA to the GRGDS adhesion peptide dissolved in a

sodium bicarbonate (Sigma-Aldrich) buffer solution under gentle stirring over a three hour period. The mixed solution was transferred into 1,000 Da molecular weight cut-off dialysis tubing (Spectrum Laboratories, Rancho Dominguez, CA) and dialyzed for two days to remove unreacted peptides. Conjugated peptide was then lyophilized (Labconco, Kansas City, MO) and stored at -20°C. Further details regarding this conjugation are found in appendix A.4.

### 3.2.3 Tensile Culture Bioreactor

The tensile culture device employed in this study is a modification of one previously used with fibrin hydrogels.[174] Major components include a linear motor, optical encoder, tension rakes, and stationary culture chambers (Fig. 3.1A and 3.1B). Movement of the tensile rake is imparted through the linear motor. The linear motor is computer controlled by a user defined displacement protocol and is monitored through readings of the optical encoder. This system facilitates simultaneous culture of up to 24 constructs in individualized tensile culture wells (Fig. 3.2B). In addition, the components that interface with the tensile constructs (rakes and culture chambers) can be autoclaved for easy sterilization.

The tensile constructs are fabricated by injecting polymer solutions into a mold between two polyethylene end blocks (75-110 μm pore size, Interstate Specialty, Sutton, MA). The polymer solution invades the porous end blocks and forms an integrated tensile construct hydrogel after cross-linking. The final tensile construct (Fig. 3.2A, inset) contains a cell-hydrogel section (12.5 mm x 9.5 mm, 1.6 mm) flanked by the porous end blocks. One end block is placed over a stationary peg in the culture wells and the other end block interfaces with the tensile rake of this bioreactor (Fig. 3.2B). The

high stiffness of the end blocks compared to the hydrogel allows a uniform strain field to be imparted across the sample during tensile culture.[169,174]

### 3.2.4 Hydrogel Degradation Study

To examine hydrogel degradation under tensile loading, OPF (3K or 10K) and PEG-DA (nominal MW 3400, Laysan Bio) were combined in a 1:1 wt/wt ratio. Polymers suspended (75 wt% liquid) in phosphate buffered saline with $Ca^{2+}$ and $Mg^{2+}$ (PBS, Invitrogen, Carlsbad, CA) were injected into a custom fabricated mold and cross-linked for 10 min at 37°C with 0.018 M of the thermal radical initiators ammonium persulfate (APS, Sigma-Aldrich) and N,N,N',N'-tetramethylethylenediamine (TEMED, Sigma-Aldrich). For laminated hydrogels, an OPF-10K solution was injected into one half of the mold and cross-linked for 6 min at 37°C. Subsequently, the OPF-3K solution was injected into the other half of the mold and cross-linked for an additional 6 min to form the laminated construct (seen in Fig. 3.2B and 3.2C). After fabrication, constructs were loaded under a sinusoidal cyclic strain regimen of 10% strain (5% offset, 5% amplitude) at 1 Hz for 12h, followed by 12h at 0% strain. After 1, 7, 14, and 28 days of culture, constructs were removed ($n \geq 3$). Fold swelling was calculated by $W_w/W_d$ where $W_w$ is the weight of the hydrogel after culture and before drying, and $W_d$ is the weight of the hydrogel after vacuum-drying.

### 3.2.5 Cell Culture

hMSCs (PT-2501, Lonza) obtained at passage 0 were seeded into tissue culture flasks at 3,333 cells/$cm^2$ and grown in mesenchymal stem cell growth medium (Lonza, Switzerland). Cells were passaged after reaching approximately 80% confluency using a one to three expansion. At passage 5 (p5), cells were cryopreserved for future use.

Culture medium was changed every 2-3 days. hMSCs from four unique donors were pooled in equal numbers at p5 and cultured in Dulbecco's modified Eagle's medium with 4.5 g/L glucose and sodium pyruvate (Mediatech, Manassas, VA), 10% fetal bovine serum (FBS, Thermo Fisher Scientific), 1% non-essential amino acids (Mediatech), and 1% antibiotic/antimycotic (Mediatech). Four different donors were used in order to minimize effects that could be due to variation between donors. Donor information as provided by the supplier is listed in Table 3.1. Medium was changed every 2-3 days (Note: FBS was pre-screened for the highest promotion of cell growth and collagen I, collagen III, and tenascin-C gene expression, with cell growth being the primary criteria). Ascorbic acid (50 µg/ml, Sigma-Aldrich) was added to the medium composition described above for the immunohistochemistry studies.

**Table 3.1. hMSC donor demographics**

| Age | Race | Gender |
|---|---|---|
| 22 | B | Female |
| 22 | B | Female |
| 43 | C | Male |
| 21 | B | Male |

### 3.2.6 Cell Encapsulation in Constructs

For experiments involving encapsulated hMSCs, constructs were fabricated from OPF-3K and PEG-DA hydrogel solutions with acrylated-PEG GRGDS adhesion peptide at a concentration of (1 µmol GRGDS)/(g of hydrogel after swelling). After the solutions were filter sterilized using a 0.2 µm filter (Nalgene, Rochester, NY) hMSCs were added at $10 \times 10^6$ cells/ml and the hydrogel solution was cross-linked as described above. After

fabrication, the tensile constructs were placed into 6-well plates in culture medium and allowed to swell overnight.

### 3.2.7 Tensile Culture

After swelling overnight, constructs with encapsulated hMSCs were loaded into the tensile culture bioreactor (Fig. 3.2A and 3.2B). A loading regimen for these studies was chosen based on parameters commonly used in tendon/ligament tissue engineering and parameters previously used with this system to promote collagen expression and production.[171,172] Specifically, constructs were maintained under a sinusoidal cyclic strain regimen of 10% strain (5% offset, 5% amplitude) at 1 Hz for 3h, followed by 3 hours at 0% strain, repeated continuously. Control hydrogels were loaded into a similar culture system, but held at 0% strain. Culture medium was replaced every 2-3 days.

### 3.2.8 Cell Viability

After 21 days of culture, constructs were removed from the device and soaked in PBS for 1h to remove medium. After medium was removed, the hydrogels were incubated in the LIVE/DEAD fluorescent staining solution (1 nM calcein AM, 1 nM ethidium homodimer-1 in PBS; Invitrogen) for 1h. After staining, hydrogel constructs were removed from the LIVE/DEAD solution and washed in PBS for 10 minutes to remove excess dye before imaging. Images from the center of each hydrogel were acquired (n=4, Fig. 3.2D) using a confocal microscope (Zeiss Axiovert 100M with LSM 510 software, Thornwood, NY).

### 3.2.9 Cell Number

At 1, 7, 14, and 21 days after initiation of mechanical stimulation, constructs were removed from the tensile device and washed in PBS. After washing, the end blocks were removed and the wet weight of the hydrogel was recorded. Hydrogel portions were mechanically disrupted using a pellet grinder (VWR International, West Chester, PA) and suspended in 750 µl of distilled, deionized water ($ddH_2O$). To disrupt cells and release DNA into solution, samples were subjected to three cycles of freezing at -80°C for 1h, thawing at room temperature for 30 min., and sonicating for 30 min. DNA content, which can be correlated to cell number, was determined (n=4, Fig. 3.2D) by assaying the resulting supernatant via PicoGreen (Invitrogen) with lambda DNA used for standards (included in kit). The PicoGreen assay uses the Hoescht 33258 fluorophore which binds to double stranded DNA. The fluorescent signal, which is proportional to the amount of double stranded DNA, was measured and compared to standards. The results were normalized to the weight of the hydrogel after culture to account for potential differences in the mass of individual hydrogels. Further details regarding the lab protocol used for this assay are found in appendix A.7.

### 3.2.10 Gene Expression

At 1, 7, 14, and 21 days after initiation of tensile stimulation, constructs were removed from the tensile device for gene expression analysis. After washing with PBS, the end blocks were removed and the hydrogel portion of the construct was mechanically disrupted using a DNase, RNase-free pellet grinder. RNA was isolated from the hydrogels with the QiaShredder column (Qiagen, Valencia, CA). Purification of RNA was achieved using the RNeasy mini kit (Qiagen). cDNA was synthesized with

Superscript III RT (Invitrogen) in the presence of a nucleotide mix (Promega, Madison, WI).

Amplification of cDNA through real time reverse transcriptase polymerase chain reaction (real time RT-PCR) was performed using custom designed primers and SYBR Green (Applied Biosystems, Foster City, CA). To design primers, a search for the gene sequence of interest was conducted using the National Center for Biotechnology Information (NCBI, http://www.ncbi.nlm.nih.gov/guide/) database. After the gene sequence was obtained, the sequence was input into Primer3 (http://fordo.wi.mit.edu/primer3/), a primer design tool. Default values were used to create candidate primer sequences. Candidate sequences were examined using the NCBI BLAST nucleotide database (http://blast.ncbi.nlm.nih.gov/) for known homologies with other genes. Pairs of primers were chosen to limit homology with other genes. Primers where both pairs in the set registered homology to the same non-target gene were not considered. After design, candidate primer pairs were obtained (Invitrogen) and used to create melt curves from cDNA previously isolated from hMSCs. Primer pairs that produced melt curves with multiple peaks were rejected. Amplification of cDNA and melt curve production was conducted and recorded using the StepOnePlus$^{TM}$ Real-Time PCR System (Applied Biosystems). A cycle time (Ct) value for a given gene was determined based on when the amplification curve crossed a threshold value. The threshold was set at the same value for all runs.

For statistical analysis, dCt values (cycle time for glyceraldehyde phosphate dehydrogenase (GAPDH) subtracted from the cycle time for the given gene) were used ($n \geq 6$). For a given gene, if half or more of the samples in a group did not amplify, that

group was recorded as not amplifying and excluded from figures. Genes examined included collagen I, collagen III, and tenascin-C as markers for tendon/ligament fibroblast gene expression.[11] To explore the potential for differentiation down alternate pathways, genes from other lineages were examined including collagen II (chondrogenic differentiation[175]), osteocalcin (osteoblastic differentiation[175]), α-smooth muscle actin (α-SMA, myofibrogenic differentiation[176]), and peroxisome proliferator-activated receptor-gamma 2 (PPARγ, adipocytic differentiation[177]). Sequences for the forward and reverse primers used are listed in Table 3.2. Further details regarding the lab protocol used for this assay are found in appendix A.10.

**Table 3.2. Primer sequences used for real time RT-PCR analysis.**

| Gene | Forward Primer | Reverse Primer |
|---|---|---|
| Collagen I | gaaaacatcccagccaagaa | gccagtctcctcatccatgt |
| Collagen III | tacggcaatcctgaacttcc | gtgtgtttcgtgcaaccatc |
| TNC | ccacaatggcagatccttct | gttaacgccctgactgtggt |
| Collagen II | accccaatccagcaaacgtt | atctggacgttggcagtgttg |
| Osteocalcin | gtgcagagtccagcaaaggt | agcagagcgacaccctagac |
| myoD | gtcgagcctagactgcctgt | gtatatcgggttggggttcg |
| α-SMA | gcctgagggaaggtcctaac | ggagctgcttcacaggattc |
| PPARγ2 | tccatgctgttatgggtgaa | gggagtggtcttccattacg |
| GAPDH | gagtcaacggatttggtcgt | ttgattttggagggatctcg |

### 3.2.11 Histology

After 21 days, samples cultured in medium with ascorbic acid were collected for histological staining. After washing in PBS, the end blocks were removed and the hydrogel portion of the construct was held under a -20 mmHg vacuum in optimal cutting

temperature compound (OCT, VWR) for 4 hours to enhance penetration, then frozen over dry ice and stored at -80°C until sectioning. OCT-embedded hydrogels were cut into 30 μm sections on glass slides. Sections were fixed using acetone and immunohistochemistry was performed for genes that were significantly upregulated in real time RT-PCR (n=2, Fig. 3.1D). Primary antibody binding to proteins of interest was accomplished using monoclonal IgG mouse anti-human antibodies (Abcam, Cambridge, MA). Secondary antibody binding to primary antibodies was accomplished using polyclonal goat anti-mouse IgG antibodies conjugated to horseradish peroxidase (Abcam). Sections were exposed to diaminobenzidine (DAB) chromogen (Abcam) for 15 minutes to elicit a color change. Negative controls included samples immunostained with the primary antibody omitted.

### 3.2.12 Statistics

Results are reported as mean ± standard deviation. A Box-Cox transformation for normality was used on dCt values of gene expression data. Data were analyzed using a two-way ANOVA. If both factors were significant, but interactions were not significant, a Tukey's post hoc test with significance set at $p \leq 0.05$ was used for pairwise comparisons. If only one factor was significant and interactions were not significant one-way ANOVAs were run on the significant factor with each level of the non-significant factor fixed. A Tukey's post hoc test with significance set at $p \leq 0.05$ was used for pairwise comparisons. If interactions were significant, one way ANOVAs were run on the first (or second) factor with each level of the second (or first) factor fixed. A Tukey's post hoc test with significance set at $p \leq 0.05$ was used for pairwise comparisons. For the hydrogel degradation study, the factors were day and hydrogel type. For the cell number

study and gene expression analysis, the factors were day and mechanical condition. Statistical analysis was carried out using Systat (Chicago, IL).

## 3.3 Results

### 3.3.1 Hydrogel Degradation

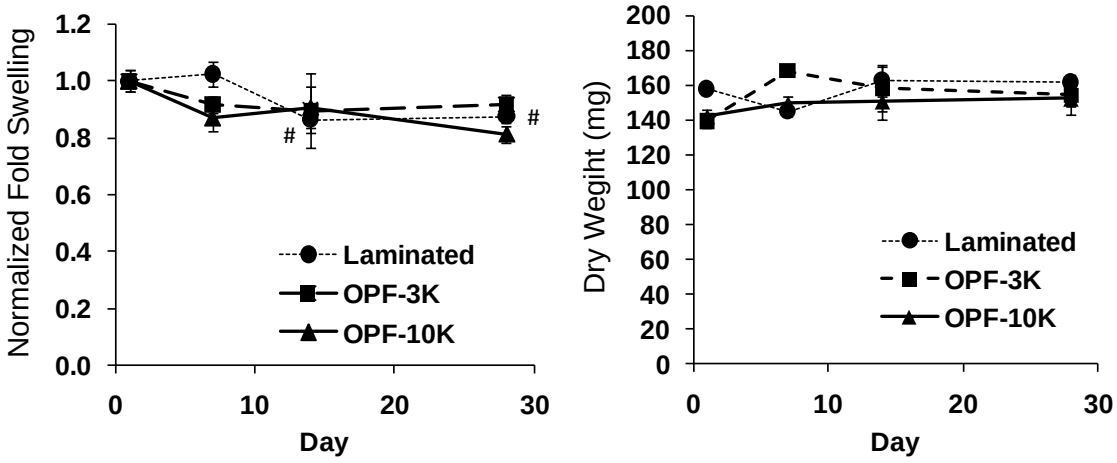


**Figure 3.2. OPF-3K, OPF-10K, and laminated hydrogel constructs all maintained structural integrity over 28 days of cyclic tensile culture with minimal degradation (n≥3 ± std. dev.). Fold swelling (left) was normalized to day 1 for each construct type. Dry weight is shown in the right graph. #Indicates significance difference for laminated constructs vs. d1 ($p<0.05$).**

**Table 3.3. Non-normalized fold swelling values for OPF-3K, OPF-10K, and laminated hydrogel constructs over 28 days of cyclic tensile culture (n≥3 ± std. dev.).**

| | Laminated | OPF-3K | OPF-10K |
|---|---|---|---|
| d1 | 4.8±0.2 | 4.1±0.0 | 4.5±0.2 |
| d7 | 4.9±0.2 | 3.8±0.1 | 3.9±0.2 |
| d14 | 4.2±0.2 | 3.7±0.5 | 4.1±0.3 |
| d21 | 4.2±0.1 | 3.8±0.2 | 3.7±0.1 |

OPF-3K, OPF-10K, and 3K-10K laminated hydrogels remained well integrated with their end blocks with no visible breaks through 28 days. This is particularly noteworthy because it has been shown in previous work that OPF-10K hydrogels swell significantly more than OPF-3K gels.[170] The maintenance of hydrogel integrity over 28 days suggests that the laminated gels were sufficiently bonded to withstand internal pressures generated from differential swelling, as well as strains imparted in tensile culture. Fold swelling of laminated constructs was significantly lower on days 14 and 28 compared to day 1 (Fig. 3.2 and Table 3.3), however, there was no significant change in dry weight after 28 days for any construct type (Fig. 3.2 and Table 3.3), indicating no loss of material over time.

### 3.3.2 Cell Viability and Number

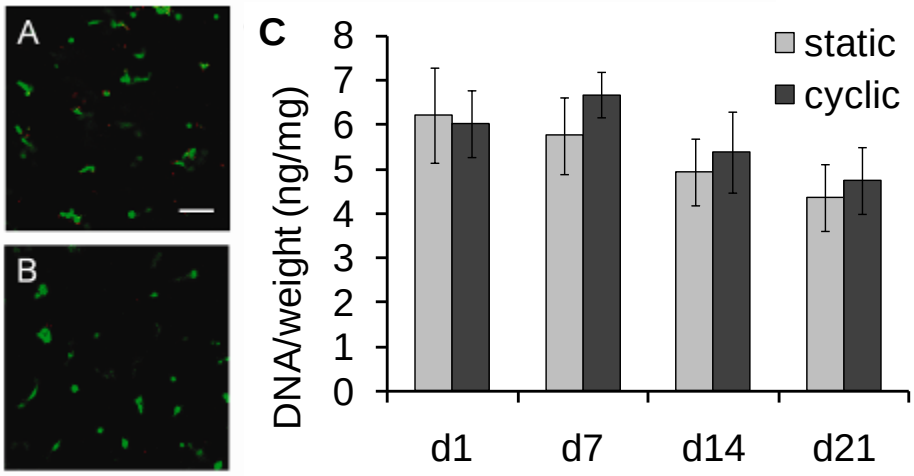


**Figure 3.3. A majority of live (green cells) was observed, in both cyclically (3.4A) and statically (3.4B) cultured OPF hydrogels over 21 days (n=4). No significant difference in cell number was found between static conditions and cyclic strain or across time (n=4 ± std. dev). Scale bar = 100 µm.**

Cells in both cyclically (Fig. 3.3A) and statically (Fig. 3.3B) cultured hydrogels generally demonstrated green staining, indicating viability. DNA content/hydrogel wet weight (an indicator of cell number per construct) showed no significant differences between samples cultured under cyclic tension compared to those cultured statically (Fig. 3.3C). Overall, DNA content was relatively constant in both static and cyclic hydrogel constructs over 21 days, with only the comparison between day 7 and day 21 cyclic constructs showing significance.

### 3.3.3 Gene Expression

**Table 3.4 RELATIVE GENE EXPRESSION LEVELS (FOLD CHANGE VS GAPDH, n≥6 ± STD.**

| | | d1 | d7 | d14 | d21 |
|---|---|---|---|---|---|
| Col I | static | 1.4±0.12 | 1.5±0.52 | 1.7±0.73 | 2.4±1.1 |
| | cyclic | 1.4±0.33 | 2.5±0.37*# | 3.0±0.67*# | 5.6±1.2*# |
| Col III | static | 0.76±0.051 | 0.81±0.42 | 1.4±0.23 | 2.3±1.0# |
| | cyclic | 0.93±0.28 | 1.1±0.19 | 1.7±0.27*# | 6.9±1.7*# |
| TNC | static | 0.10±0.032 | 0.31±0.11# | 0.71±0.19# | 0.37±0.12# |
| | cyclic | 0.10±0.025 | 0.37±0.052# | 1.0±0.19*# | 0.97±0.28*# |
| Col II | static | $1.8\times10^{-5}\pm3.9\times10^{-6}$ | $2.9\times10^{-5}\pm2.5\times10^{-5}$ | $1.4\times10^{-4}\pm1.4\times10^{-4\#}$ | $2.2\times10^{-4}\pm1.1\times10^{-4\#}$ |
| | cyclic | $2.5\times10^{-5}\pm5.2\times10^{-6}$ | $8.0\times10^{-5}\pm9.1\times10^{-5}$ | $1.7\times10^{-4}\pm1.5\times10^{-4\#}$ | $2.3\times10^{-4}\pm8.6\times10^{-5\#}$ |
| α-SMA | static | $2.6\times10^{-3}\pm6.6\times10^{-4}$ | $5.5\times10^{-3}\pm1.8\times10^{-3}$ | $1.2\times10^{-2}\pm3.5\times10^{-3\#}$ | $8.1\times10^{-3}\pm2.8\times10^{-3\#}$ |
| | cyclic | $3.4\times10^{-3}\pm1.0\times10^{-3}$ | $6.6\times10^{-3}\pm1.3\times10^{-3}$ | $1.0\times10^{-2}\pm3.9\times10^{-3\#}$ | $9.5\times10^{-3}\pm1.7\times10^{-3\#}$ |
| OCN | static | $1.2\times10^{-3}\pm1.5\times10^{-4}$ | $2.6\times10^{-3}\pm4.5\times10^{-4\#}$ | $4.0\times10^{-3}\pm1.0\times10^{-3\#}$ | $3.6\times10^{-3}\pm1.4\times10^{-3\#}$ |
| | cyclic | $1.3\times10^{-3}\pm8.3\times10^{-4}$ | $1.9\times10^{-3}\pm1.7\times10^{-4\#}$ | $4.6\times10^{-3}\pm9.0\times10^{-4\#}$ | $3.9\times10^{-3}\pm7.2\times10^{-4\#}$ |
| PPARγ | static | $7.8\times10^{-6}\pm2.9\times10^{-6}$ | | | |
| | cyclic | $6.0\times10^{-6}\pm4.2\times10^{-6}$ | | | |

***Significantly different from static constructs at same time point ($p \leq 0.05$).**
**#Significantly different from d1 for the same sample type ($p \leq 0.05$).**
**Col I, collagen I; col III, collagen III; TNC, tenascin-C; col II, collagen II; α-SMA, α-smooth muscle actin; OCN, osteocalcin; PPARγ, peroxisome proliferator-activated receptor-gamma 2. Values for day 7, day 14 and day 21 are not listed for PPARγ as this gene did not amplify at those time points for most samples.**

No significant difference was seen in mRNA expression between cyclically and statically cultured constructs for the non-tendon/ligament fibroblast genes (collagen II, α-

SMA, osteocalcin, PPARγ - Table 3.3 and Fig. 3.5) at each time point. PPARγ was not expressed at detectable levels after day 1 as it did not amplify in most samples after that time point. In addition, collagen II demonstrated no significant differences in expression across time. Similarly, α-SMA expression showed no significant change across time in cyclic samples, although upregulation was seen in static samples on days 14 and 21 compared to day 1. Upregulation was also seen in osteocalcin in both static and cyclic samples on days 14 and 21 compared to day 1.

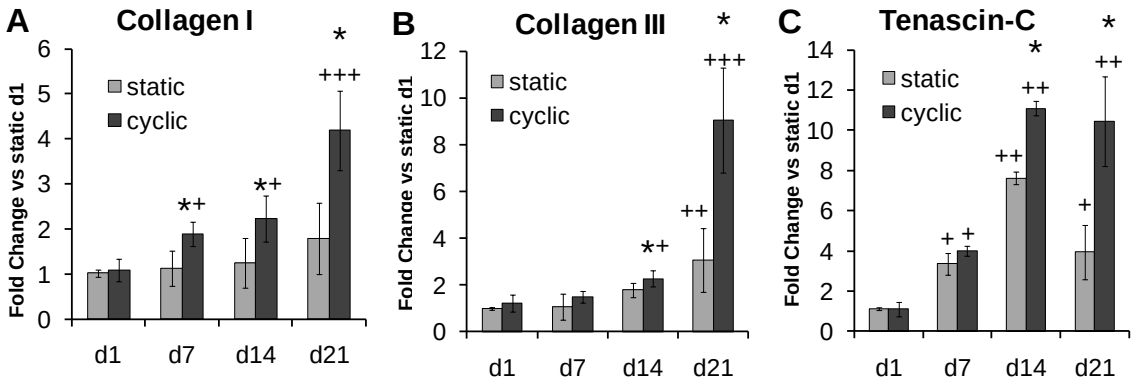


**Figure 3.4. Collagen I (A), collagen III (B), and tenascin-C (C), markers for tendon/ligament fibroblastic differentiation, were upregulated in hMSCs encapsulated in constructs under cyclic tensile strain compared to static constructs by day 21 (n≥6 ± std. dev.). Expression normalized to GAPDH was then normalized to d1 static results for all genes (note: y-axis is different for each graph). *Indicates significance over static constructs at same time point ($p \leq 0.05$). Significant from d1 (+); d1 and d7 (++); or d1, d7, and d14 (+++); for the same sample type ($p \leq 0.05$).**

In contrast with non-tendon/ligament fibroblast genes, significant differences were seen for tendon/ligament fibroblast lineage genes between cyclic and static culture, particularly at later time points. Specifically, collagen I mRNA was significantly upregulated in cyclically strained constructs on days 7, 14, and 21 as compared to static constructs, although no difference was observed on day 1 (Fig. 3.4A). Upregulation of collagen I mRNA was also observed in both strained and static samples at day 21 and in

strained samples on day 7 in comparison to day 1. Collagen III mRNA was significantly upregulated in cyclically strained constructs on day 21 as compared to static constructs (Fig. 3.4B). Upregulation of collagen III mRNA was also observed in both strained and static samples on days 14 and 21 in comparison to day 1. Tenascin-C mRNA was significantly upregulated in cyclically strained constructs on day 21 as compared to static constructs at that time point (Fig. 3.4C). Upregulation of tenascin-C was also found in both strained and static samples on days 7, 14, and 21 compared to day 1.

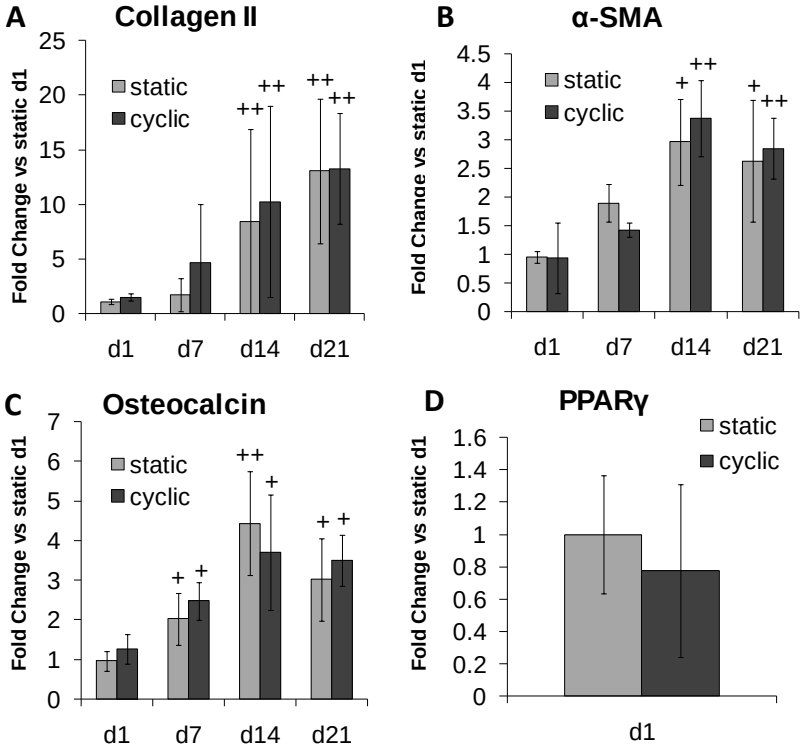


**Figure 3.5. Gene expression levels of hMSCs for collagen II (A), α-SMA (B), osteocalcin (C), and PPARγ (D) in constructs under cyclic tensile strain compared to static constructs over 21 days (n≥6 ± std. dev.). Expression normalized to GAPDH was then normalized to d1 static results for all genes (note: y-axis is different for each graph). Significant from d1 (+); d1 and d7 (++); or d1, d7, and d21 (+++); for the same sample type ($p \leq 0.05$).**

### 3.3.4 Histology

Immunohistochemistry revealed the presence of collagen I and tenascin-C after 21 days of culture in both static and cyclic constructs (Fig. 3.6), indicating that gene expression of these tendon/ligament fibroblast markers was translated into protein production in the hydrogel constructs. Minimal staining for collagen III (Fig. 3.6C and 3.6F) was also detected. As seen in Fig. 3.6, staining generally appeared to be concentrated pericellularly and tenascin-C seemed to be more prevalent in cyclic constructs. No staining was evident in control sections with the primary antibody omitted (Fig. 3.6 inset) suggesting that there was no significant non-specific binding of the secondary antibody or endogenous staining from the contrast agent. However it should be noted that no isotype control was used so the possibility of non-specific binding of the primary antibody can not be eliminated.

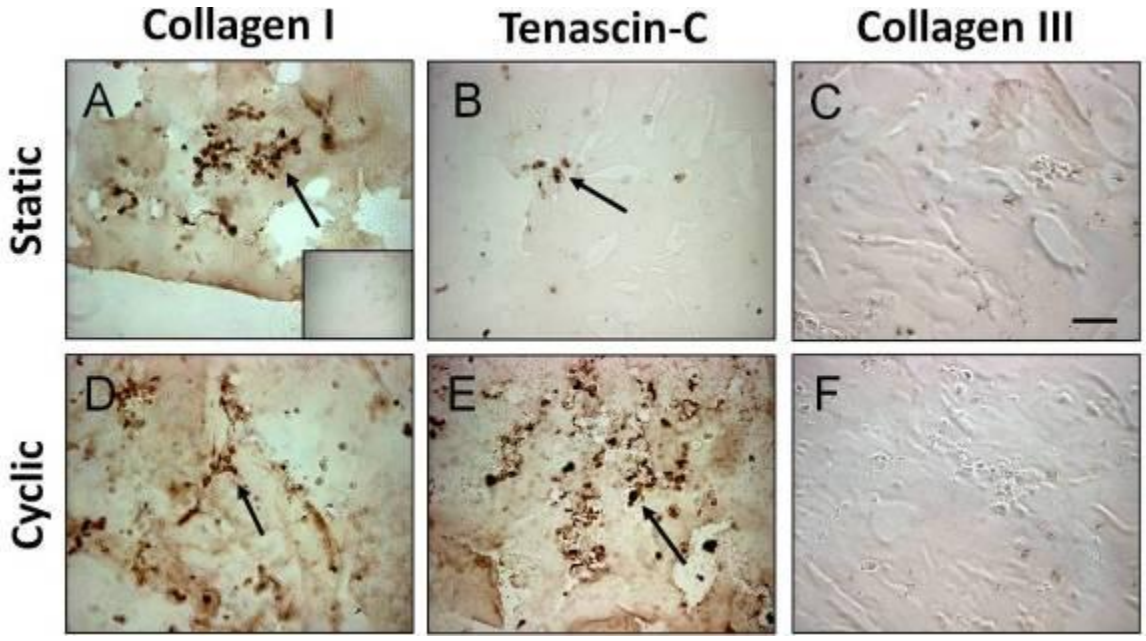


**Figure 3.6. Immunohistochemistry (n=2) for collagen I (A and D), tenascin-C (B and E), and collagen III (C and F) after 21 days of culture in both static and cyclic constructs. Collagen I and tenascin-C were detected mainly pericellularly (arrows). No staining was evident for collagen III or in control sections with the primary antibody omitted (inset). Scale bar = 100 µm.**

## 3.4 Discussion

Our three dimensional OPF hydrogels and novel tensile culture system provide a versatile scaffold-bioreactor system for the study of biological and mechanical influences on cells. The ability to incorporate ECM moieties and create hydrogel laminates that are stable through at least 28 days of cyclic tensile culture (Fig. 3.2) provides a versatile system for studying the formation of tendons/ligaments as well as their interfaces with muscle/bone. While culture periods longer than 3-4 weeks can lead to hydrolytic degradation of OPF-based hydrogels, minimal degradation was seen in this system after 4 weeks, in agreement with prior reports.[178] As a result the mechanical properties (i.e. elastic modulus) of the hydrogel constructs and presentation of adhesive motifs would not be expected to change due to degradation of the polymers. This stability provides an advantage in these studies as no change in loading of the embedded cells would be expected due to polymer degradation, although other changes in the cell-biomaterial environment, such as ECM production, could change the loading transferred to individual cells. In addition, these OPF-based hydrogels provided a biomaterial environment where no alteration in construct geometry (shrinkage) was observed up to 21 days in the presence of cells, as has been reported previously with naturally-based polymers.[179,180]

For these experiments, our custom bioreactor system was used to examine the differentiation of hMSCs in OPF hydrogels modified with RGD adhesion peptides over 21 days of culture. OPF-3K based hydrogels were specifically chosen due to their greater ability to facilitate cell adhesion in 2D culture compared to OPF-10K hydrogels (Supplementary Fig. B.1). These data were in agreement with previous work which showed that cells can detect and adhere to RGD in OPF hydrogels.[108] This peptide was

employed in these studies to avoid the lowered viability seen with hMSCs in hydrogels without RGD.[181] This provided the foundation for a scaffold that would permit cell survival so this study could focus on the effect of cyclic strain on encapsulated cells. As expected, the system demonstrated high cell viability (Fig. 3.3A and 3.3B), with no significant change in cell number between day 1 and day 21 constructs in either static or strained conditions (Fig. 3.3C). It should be noted that, neither samples without RGD peptides, nor samples containing a scrambled peptide (such as RDG), were used in these studies so the specific contribution of the RGD adhesion peptides to the cell viability or to other cell responses can not be specified for this system.

While this study showed no change in cell number due to strain, other groups have reported that strain promotes higher[182,183] or lower[184,185] cell numbers over time. Cell proliferation in this study may have been prevented by the small mesh size of these hydrogels. Mesh sizes of between 76 and 160 Å have previously been reported for similar OPF hydrogels[186] and sizes ranging from 20-60 Å were calculated for PEG-DA hydrogels.[187,188] While OPF hydrogel mesh size increases with the molecular weight of the PEG chain, the mesh size of an OPF-10K hydrogel is still orders of magnitude smaller than a cell,[186] allowing only limited space for cellular division in the dense polymer matrix. Modifications of the hydrogel environment to facilitate local cell-mediated degradation may be a target for further studies in an effort to provide the void space needed for proliferation inside the gel.

Upregulation of collagen I, collagen III, and tenascin-C gene expression was observed in the constructs, particularly under cyclic loading (Fig. 3.4). This upregulation is in agreement with previous findings that have used three-dimensional

constructs.[11,100,189] The upregulation of collagen I, collagen III, and/or tenascin-C mRNA is often used as a marker for a tendon/ligament fibroblast phenotype due to the prevalence of these proteins in tendon/ligament tissue.[4,10,190] Collagens make up the majority of tendon/ligament and give the tissue its high tensile strength.[12] Tenascin-C is an antiadhesive protein and may increase tissue elasticity in response to heavy loading.[191] Other work using collagen I gels to encapsulate hMSCs has shown an upregulation of collagen III, but not collagen I, in response cyclic strain.[179] The differences in the response of collagen I may be due in part to variations in the cyclic strain regimen, since the studies that reported upregulation of collagen I in response to cyclic strain employed higher amplitudes and durations of strain.[11,100,189] Overall, the upregulation of collagen I, collagen III, and tenascin-C in cyclic constructs compared to static samples by day 21 suggests that, under the loading conditions chosen for this study, cyclic strain promoted a ligament/tendon fibroblastic phenotype in hMSCs by 21 days. While some upregulation was seen over time in certain non-tendon/ligament fibroblast genes (Table 3.3), the lack of upregulation of any of these genes under cyclic conditions suggest that cyclic strain did not promote differentiation down alternative pathways.

Collagen I gene expression in this study correlated with pericellular matrix deposition (Fig. 3.4A, 3.6A and 3.6D), although differences in staining were not apparent between cyclically- and statically-cultured hydrogels, in contrast with previous results.[100] In addition, in our experiments, little collagen III staining was observed at day 21, despite upregulation of collagen III expression levels at this time point. Previous reports have demonstrated collagen III production in response to cyclic strains when marrow stromal cells were cultured in collagen I gels.[11,100] However, in these prior studies, the presence

of the collagen-based scaffold, as well as differences in the exact loading parameters used, which in some cases applied a combination of translation and rotational forces,[11] could have affected the level of deposition of both collagen I and III around the cells. One possible explanation for the minimal collagen III staining in our system is that a large fold change in gene expression was not observed until day 21, and therefore there may not have been enough time to observe increased production of this molecule in this study. While the collagen production seen may indicate that the cells are not following a normal healing response, where collagen III is deposited initially and later replaced by collagen I,[33] the results are encouraging since collagen I is more prevalent than collagen III in mature tissue.[140] Further work, including studies to examine the time course of collagen production in this system, will be required to better understand and optimize culture conditions to promote optimal ratios of collagen I and collagen III.

Tenascin-C was also observable by immunostaining at day 21, especially in cyclically cultured constructs (Fig. 3.6B and 3.6E). During development, tenascin-C is expressed highly at insertion sites of ligaments and tendons to bone[192] and is localized immediately surrounding cells,[192] similar to the pericellular staining that was observed. Culture methods that encourage production of both collagen I and tenascin-C, similar to our system, may be promising avenues for pursuit of tissue engineering of insertion sites of ligament and tendon to bone.

One factor that may have played an important role in the distribution and ratios of the proteins produced is the physical constraints imposed by the biomaterial environment. Hydrogels with small mesh sizes and limited degradability, similar to the OPF hydrogels used in this study, have produced a pericellular matrix deposition[101] like that observed in

this system. In those experiments, degradation of the scaffold led to larger mesh sizes that facilitated a change in the ratio and distribution of matrix proteins, most likely by allowing greater diffusion of the proteins that make up the ECM. Investigation of the effect of PEG-based hydrogels with larger mesh sizes or degradation of the OPF hydrogel matrix may be necessary to facilitate a distribution of matrix proteins throughout the construct as seen in more mature tendon/ligament tissue.[192]

## 3.5 Conclusions

In addition to confirming the responsiveness of hMSCs to tensile loading, the studies described here demonstrate the feasibility of this novel system in examining cellular differentiation under tensile loading in response to controlled physicochemical changes in the extracellular environment, including the possibility of co-culture using the laminated structures tested in these experiments. Significant additional work is required to find the correct combination of cell types, bioactive factors, and loading parameters to regenerate both fibrous tissue and its interfaces. However, such a model system may prove valuable in identifying key parameters for next-generation tissue engineering approaches to recreating these complex structures.

# CHAPTER 4

# HUMAN MARROW STROMAL CELLS PRODUCE COLLAGENOUS EXTRACELLULAR MATRIX IN ENZYMATICALLY-DEGRADABLE HYDROGELS

## 4.1 Introduction

A variety of synthetic biomaterial scaffolds using MSCs have been employed for ligament/tendon tissue engineering.[193,194] These systems often seek to promote a phenotype in MSCs that is similar to that of ligament/tendon fibroblasts which are the most prevalent cell type in ligament/tendon tissues.[4] Collagen I, collagen III, and tenascin-C are major ligament/tendon ECM components that are often examined as signs of this differentiation.[11,193,195] Unfortunately, the elaboration of such ECM components by encapsulated cells may be hindered if the scaffold does not undergo sufficient degradation as matrix proteins are produced.[56,101] While a low rate of degradation can hinder ECM production, degradation that occurs too quickly could result in a loss of scaffold integrity before sufficient replacement tissue is produced.[66] Normal maturation of the ligament/tendon ECM takes advantage of cell-mediated enzymatic degradation.[4,51,140] A biomaterial carrier that is susceptible to biological enzymatic cleavage may provide a natural balance of degradation and ECM production since the encapsulated cells would control the degradation rate. While there has been some study on the effect of hydrolytic degradation on ECM production,[101] there has not been much study on the effect of the susceptibility of the biomaterial carrier to cell-mediated

enzymatic degradation on the deposition of matrix proteins, which is the main objective of this study.

Before investigating the effects on encapsulated cells of a biomaterial carrier susceptible to enzymatic degradation, hydrogels were created with increasing proportions of covalently incorporated, enzymatically-cleavable GGGLGPAGGK peptides (see section 2.2.4). In particular, in these studies, hydrogels were created without any GGGLGPAGGK sequences (0%), or with 25%, 75%, or 100% of the hydrogel composed of polymers containing these enzymatically-cleavable peptides by weight. To determine whether increasing the portion of the GGGLGPAGGK sequences used to create hydrogels would raise the total susceptibility of the construct to enzymatic degradation, the hydrogels were cultured in bacterial collagenase or in saline. Results from these preliminary experiments suggested that the various ratios of enzymatically-degradable peptides provided hydrogels with different total amounts of degradation when exposed to exogenous bacterial collagenase.

After variations in total susceptibility that resulted from the hydrogel formulations were elucidated, hMSCs were encapsulated in each of these formulations. After days 1, 7, 14, and 21 of culture, cell number and viability, cell morphology, MMP production (specifically MMP-1 and MMP-13), gene expression (particularly collagen I, collagen III, and tenascin-C), and protein production were examined. The behavior of the hMSCs was compared across hydrogel types and to hACL fibroblasts encapsulated in similar environments. The particular hypothesis of this study was that culture in an enzymatically-degradable biomaterial environment would promote increased ECM production in encapsulated hMSCs over 21 days of culture, with the most ECM

production expected in the most degradable hydrogel, and decreaseing ECM amounts expected as the total degradability of the hydrogel decreased.

## 4.2 Materials and Methods

### 4.2.1 Polymer Synthesis

OPF-3K was synthesized according to previous protocols.[173] Briefly, $CaH_2$ was mixed with MeCl and distilled to produce anhydrous MeCl. To produce the OPF polymer, FuCl and TEA were slowly added dropwise to PEG (3 kDa; $M_n$: 3,300 ± 10 Da, PI: 1.1) that had been azeotropically distilled in toluene and dissolved in MeCl. FuCl and TEA were added at molar ratios of 0.9:1 FuCl:PEG and 1:2 FuCl:TEA under nitrogen gas and cooled over ice. MeCl was removed from the resultant OPF product by rotovapping. Recrystalization of the OPF was carried out twice in ethyl acetate to remove salts produced by the conjugation reaction. Ethyl acetate was removed by three consecutive washes in ethyl ether. Polymers were vacuum dried to remove ethyl ether and stored at -20°C before use. The molecular weight of the OPF polymer was determined through GPC. The resultant OPF-3K polymer was found to have a molecular weight ($M_n$) of 8,900 ± 530 with a polydispersity index of 3.1 ± 0.4. NMR spectra of similar OPF macromers and the number of double bonds present in the macromer has been reported previously.[108,173] The same batch of OPF-3K that was synthesized and used in the previous study (Chapter 3) was also used in this study. Further details regarding this synthesis are found in appendix A.1.

To synthesize PEG-DA, $CaH_2$ was mixed with MeCl and distilled to produce anhydrous MeCl. Under nitrogen gas, TEA was added to PEG(3 kDa; $M_n$: 3,300 ± 10 Da, PI: 1.1) that had been dissolved in MeCl at a molar ratio of 2:1 TEA:PEG. Acryloyl

chloride (AcCl) dissolved in MeCl was slowly added dropwise at a molar ratio of 2:1 AcCl:PEG under nitrogen gas in order to acrylate the PEG. After allowing the reaction to proceed overnight, 2M $K_2CO_3$ was added to remove TEA-Cl by forming KCl and allowing it to separate out in the aqueous phase overnight. The solution of PEG-DA was separated from the aqueous phase of KCl and $MgSO_4$ was added to remove any additional aqueous solution. PEG-DA was then precipitated in ethyl ether and stored at -20°C before use. The resultant PEG-DA has a typical molecular weight of 3,759±18 with a polydispersity index of 1.071 ± 0.001. Further details regarding this synthesis are found in appendix A.2.

### 4.2.2 Peptide Conjugation

To allow presentation of arginine-glycine-aspartate (RGD) ligands to encapsulated cells, the GRGDS adhesion peptide was conjugated to a 3,400 Da MW acrylated-PEG-succinimidyl valerate spacer (A-PEG-SVA, Laysan Bio, Arab, AL) according to previous protocols.[108] Briefly, conjugation was achieved by adding the A-PEG-SVA to the GRGDS adhesion peptide dissolved in a sodium bicarbonate buffer solution under gentle stirring over a three hour period. The mixed solution was transferred into 1,000 Da molecular weight cut-off dialysis tubing and dialyzed for two days to remove unreacted peptides. Conjugated peptide was then lyophilized and stored at -20°C. The same batch of acrylated GRGDS peptide was used in all of these studies. Further details regarding this conjugation are found in appendix A.4.

To enable cell-mediated degradation of the biomaterial environment the enzymatically-degradable peptide, glycine-glycine-glycine-leucine-glycine-proline-alanine-glycine-glycine-lysine (GGGL↓GPAGGK) was conjugated on both ends to 3,400

Da MW A-PEG-SVA (Fig. 2.3) using the peptide conjugation protocol mention above. Briefly, conjugation was achieved by adding A-PEG-SVA to the GGGL↓GPAGGK peptide dissolved in a sodium bicarbonate buffer solution under gentle stirring over a three hour period. The mixed solution was transferred into 3,500-5,000 Da molecular weight cut-off dialysis tubing (Spectrum Laboratories, Rancho Dominguez, CA) and dialyzed for two days to remove unreacted peptides. Conjugated GGGL↓GPAGGK peptide (LGPA) was then lyophilized and stored at -20°C. All batches of LGPA were subjected to fold swelling measurements to screen out poorly conjugated batches. The exact same set of LGPA batches were used when possible and at least 4 batches of LGPA were used in each group of hydrogels in order to minimize the effects of batch to batch variability. Further details regarding this conjugation are found in appendix A.3.

### 4.2.3 Hydrogel Degradation Study

To confirm the availability of the enzymatically-degradable GGGL↓GPAGGK sequences for enzyme mediated degradation, hydrogel formulations were chosen that were expected to provide a wide range of susceptibility to enzymatic-degradation. OPF-3K:PEG-DA in a 1:1 ratio and LGPA were combined to create polymer mixtures containing 0%, 25%, 75%, or 100% LGPA by weight (Fig. 4.1 and Table 4.1). Polymers suspended at high or low saline content (75wt% PBS or 90wt% PBS) were injected into a custom fabricated mold and cross-linked in the shape of a thin disc (30 µl, 6 mm dia) for 10 min at 37°C with 0.018 M of the thermal radical initiators APS and TEMED. After cross-linking the hydrogels were placed into wells of a 12-well plate containing 2 ml of a collagenase II solution consisting of PBS with collagenase II (1 mg/ml, Invitrogen), $CaCl_2$ (3 mM, Thermo Fisher Scientific), and 1% antibiotic/antimycotic and placed on an

orbital shaker plate (VWR) in an incubator (Heracell® 150, Thermo Fisher Scientific). Hydrogels cultured in PBS alone were used as a control. Solutions were changed every day.

**Table 4.1. Hydrogel Formulations.**

| % LGPA | Saline Content | LGPA:OPF:PEG-DA (wt%) | PBS:Total Polymer (wt%) |
|---|---|---|---|
| 0% | Low (75 wt%) | 0:50:50 | 75:25 |
| 25% | Low (75 wt%) | 25:37.5:37.5 | 75:25 |
| 75% | Low (75 wt%) | 75:12.5:12.5 | 75:25 |
| 100% | Low (75 wt%) | 100:0:0 | 75:25 |
| 0% | High (90 wt%) | 0:50:50 | 90:10 |
| 25% | High (90 wt%) | 25:37.5:37.5 | 90:10 |
| 75% | Hight (90 wt%) | 75:12.5:12.5 | 90:10 |
| 100% | High (90 wt%) | 100:0:0 | 90:10 |

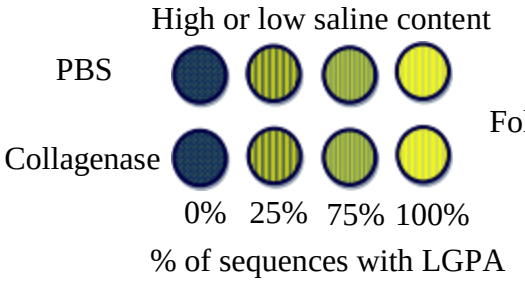


Sample Analysis (d7)
Fold Swelling = Wet Weight/Dry Weight (n=5)
Mesh size (n=5)

**Figure 4.1. Research design for hydrogel degradation study.**

After 7 days of culture, constructs were removed (n=5). Fold swelling was calculated by $W_w/W_d$ where $W_w$ is the weight of the hydrogel after culture and before drying, and $W_d$ is the weight of the hydrogel after vacuum-drying. The mesh size of the hydrogels, which is an indicator of the distance between crosslinks, or how tightly the polymer network was formed, was calculated using polymer theory according to previously reported methods.[186,196] Briefly, a hanging pan balance was used to measure

hydrogel weight in air after cross-linking ($W_{a,r}$), weight in non-solvent hexane after cross-linking ($W_{n,r}$), weight in air after swelling in PBS overnight ($W_{a,s}$), weight in hexane after swelling in PBS ($W_{n,s}$), weight in air swelling then vacuum drying ($W_{a,d}$), and weight in hexane after vacuum drying ($W_{n,r}$). Mesh size ($\xi$) was calculated according to (1).

$$(1)\quad \xi = v_{2,s}^{-1/3}(r^2_0)^{1/2}$$

To calculate $\xi$ (2) and (3) are required.

$$(2)\quad v_{2,s}=V_p/V_{g,s}$$

$$(3)\quad r^2_0=C_nNL^2$$

To calculate $v_{2,s}$ (4) and (5) are required.

$$(4)\ V_p=(W_{a,d}-W_{n,d})/\rho_n$$

$$(5)\ V_{g,s}=(W_{a,s}-W_{n,s})/\rho_n$$

$\rho_n$ is the density of hexane (0.66 g/cm$^3$). To calculate $r^2_0$ (6) is required. $C_n$ is the characteristic ratio (4.1 in this case) and L is the weighted bond length of the polymer (1.47 Å).

$$(6)\ N = \#M_c/M_r$$

To calculate N (7) is required. # is the number of bonds in the repeat unit of the polymer (3 bonds). $M_r$ is the molecular weight of the repeat unit (44 g/mol).

$$(7)\ )\ 1/M_c=2/M_n-(vbar/V_1)[\ln(1-v_{2,s})+v_{2,s}+Xv^2_{2,s}]/(v_{2,r}[(v_{2,s}/v_{2,r})^{1/3}-1/2(v_{2,s}/v_{2,r})])$$

To calculate $M_c$ (8) and (9) are required. vbar is the specific volume of the polymer (0.871 ml/g). $V_1$ is the molar volume of the swelling agent (18.1 ml/mol). X is the Flory OPF-water interaction parameter (0.426).

$$(8)\quad v_{2,s}=V_p/V_{g,s}$$

$$(9)\ v_{2,r}=V_p/V_{g,r}$$

Equations (4) and (5) can be used to calculate $V_p$ and $V_{g,s}$ and are listed above. To calculate $V_{g,r}$ (10) is required.

$$(10)\ V_{g,r} = (W_{a,r}-W_{n,r})/\rho_n$$

### 4.2.4 Cell Culture

hMSCs obtained at passage 0 were seeded into tissue culture flasks at 3,333 cells/cm$^2$ and grown in mesenchymal stem cell growth medium. Cells were passaged after reaching approximately 80% confluency using a one to three expansion. At passage 5 (p5), cells were cryopreserved for future use. Culture medium was changed every 2-3 days. hMSCs from four unique donors were pooled in equal numbers at p5 and cultured in Dulbecco's modified Eagle's medium with 4.5 g/L glucose and sodium pyruvate, 10% fetal bovine serum, 1% non-essential amino acids, 1% HEPES buffer (VWR), 1% antibiotic/antimycotic, and ascorbic acid (50 µg/ml). Four different donors (Table 3.1) were used in order to minimize effects that could be due to variation between donors. Medium was changed every 2-3 days (Note: FBS was pre-screened for the highest promotion of cell growth and collagen I, collagen III, and tenascin-C gene expression, with cell growth being the primary criteria).

Human anterior cruciate ligament (hACL) fibroblasts were isolated from the ACL of a human donor undergoing knee surgery. The ACL tissue was cut into approximately 1-3 mm$^3$ pieces and distributed into T-75 flasks (Thermo Fisher Scientific) with a collagenase solution. The collagenase solution consisted of Dulbecco's modified Eagle's medium with 4.5 g/L glucose and sodium pyruvate, 10 ml/L of penicillin/streptomycin (EMD biosciences, Darmstadt Germany), 10 ml/L kanamycin sulfate (EMD biosciences), 1 ml/L gentamicin sulfate (VWR), 1 ml/L fungizone antimycotic (Invitrogen), and 40

mg/L collagenase type II (Invitrogen). After 1-2 days of gentle agitation, when the tissue was fully degraded, the solution was removed and filtered through a syringe filter holder (Pall Corporation) with a 74 μm nylon mesh (Small Parts). Cells in the resultant solution were pelleted and frozen down for future use. For experiments involving encapsulation of hACL fibroblasts, these cells were thawed and cultured in cultured in Dulbecco's modified Eagle's medium with 4.5 g/L glucose and sodium pyruvate, 10% fetal bovine serum, 1% non-essential amino acids, 1% HEPES buffer, 1% antibiotic/antimycotic, and ascorbic acid (50 μg/ml). Medium was changed every 2-3 days (Note: FBS was pre-screened for the highest promotion of cell growth and collagen I, collagen III, and tenascin-C gene expression, with cell growth being the primary criteria).

### 4.2.5 Cell Encapsulation

For experiments involving encapsulated cells, polymers were prepared with the same compositions used for low saline content hydrogels in the degradation study (above) with the addition of acrylated-PEG GRGDS adhesion peptides at a concentration of (1 μmol GRGDS)/(g of hydrogel after swelling). After the solutions were filter sterilized using a 0.2 μm filter (Nalgene, Rochester, NY) cells were added at 10 x $10^6$ cells/ml and the hydrogel solution was cross-linked into 30 μl samples in the shape of a thin disc (30 μl, 6 mm dia) as described above. Experiments involving hMSCs used polymer mixtures containing 0%, 25%, 75%, or 100% LGPA by weight (Fig. 4.2). Experiments involving human ACL fibroblasts used polymer mixtures containing 0% or 100% LGPA by weight. After fabrication, the hydrogels were placed into 24-well plates in culture medium. Cell culture medium was change every 2-3 days.

### 4.2.6 Cell Viability and Morphology

After 1, 7, 14, 21 days of culture, the hydrogels were removed from their wells and soaked in PBS for 1h to remove medium. After medium was removed, the samples were incubated in the LIVE/DEAD fluorescent staining solution (1 nM calcein AM, 1 nM ethidium homodimer-1 in PBS; Invitrogen) for 1h. After staining, hydrogels were removed from the LIVE/DEAD solution and washed in PBS for 10 minutes to remove excess dye before imaging. An image stack through the entire thickness at the center of each hydrogel were acquired (n≥3, Fig. 4.2) using a confocal microscope with a vertical distance between sequential images of 10 µm.

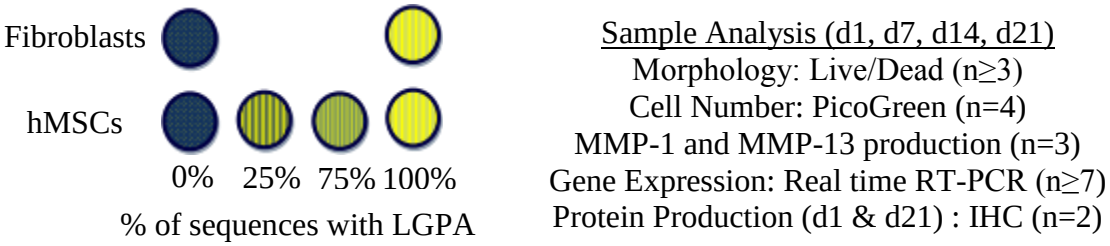


**Figure 4.2. Research design for studies involving encapsulated cells in low saline content hydrogels.**

To analyze the cellular morphology for evidence of localized degradation, cellular perimeter and area of image stacks (5 images/stack) was analyzed. Cell perimeter and area was calculated for the region 200-400 µm from the surface of the sample (subsurface region) or for a deeper 200 µm region in the middle of the sample (core region; usually ~400 µm from both surfaces). Image stacks were imported into ImageJ (NIH, Bethesda, MD) for morphological analysis. Five equally spaced slices (50 µm apart) were analyzed. Slices 50 µm apart were used instead of sequential slices in order to minimize the possibility of counting a single cell more than once. Data values for all cells in slices of a given sample were averaged. To calculate spreading, a circularity analysis was done

with circularity = $4*\pi*\text{area}/(\text{perimeter})^2$, where a circularity value of 1 correlates to a perfect circle and values approaching zero indicate increasing spreading.

### 4.2.7 Cell Number

After 1, 7, 14, and 21 days of culture, hydrogels were removed from their wells and washed in PBS. After washing, the wet weight of the hydrogel was recorded. Hydrogels were mechanically disrupted using a pellet grinder and suspended in 750 µl of $ddH_2O$. To disrupt cells and release DNA into solution, samples were subjected to three cycles of freezing at -80°C for 1h, thawing at room temperature for 30 min., and sonicating for 30 min. DNA content, which can be correlated to cell number, was determined (n=4, Fig. 4.2) by assaying the resulting supernatant via PicoGreen with lambda DNA used for standards (included in kit). The PicoGreen assay uses the Hoescht 33258 fluorophore which binds to double stranded DNA. The fluorescent signal, which is proportional to the amount of double stranded DNA, was measured and compared to standards. Further details regarding the lab protocol used for this assay are found in appendix A.7.

### 4.2.8 Matrix Metalloproteinase Production

The production of MMP-1 and MMP-13, along with their active forms, was examined. MMP-1 and MMP-13 are collagenases that are known to target collagen I and collagen III,[147] the most prevalent components of ligament/tendon tissue[154] and were examined as potential mediators of enzymatic degradation in this system (see section 2.2.6 for more information on MMPs). Six hydrogels per sample type were used in these assays. Medium from the wells of 24 well plates containing hydrogel samples was collected on days 1, 3, 5, 7, 9, 11, 14, 16, 18, and 21 of culture for MMP analysis (Fig.

4.2). Cumulative production of total and active amounts of MMP-1 and MMP-13 proteins was assessed at 1, 7, 14, and 21 days of culture (n=3) using fluorokine kits (R&D Systems, Minneapolis, MN). As appropriate, medium on different days of culture was pooled to assess the production of MMPs during a given range of time. More specifically, to measure MMP production after 1 day of culture, medium from only day 1 was used. For MMP production from day 2 to day 7 of culture, medium collected on day 3, day 5, and day 7 was pooled. For MMP production from day 8 to day 14 of culture, medium collected on day 9, day 11, and day 14 was pooled. For MMP production from day 15 to day 21 of culture, medium collected on day 16, day 18, and day 21 was pooled.

Details regarding the protocol used to assay active and total amounts of MMP-1 and MMP-13 using the fluorokine kits are found in appendix A.9. Briefly, medium from samples was added to 96 well plates. The MMP of interest (MMP-1 or MMP-13 as needed) is specifically bound by monoclonal antibodies immobilized on the surface of the wells. The wells are washed repeatedly in a buffer solution to remove any unbound substances. After washing is complete, p-aminophenylmercuric acetate (APMA), an activator of MMPs is added to sample wells that will be used to measure total levels of the MMP. APMA is not added to wells used to measure active MMP. After incubation with APMA, sample wells were washed repeatedly to remove APMA. After washing a fluorogenic substrate is added to sample wells. The substrate contains a fluorophore and a quencher that are connected by a peptide sequence. When the fluorophore and quencher are held in close proximity by the peptide linker a resonance energy transfer occurs between the two molecules and prevents fluorescence. Active MMP present in sample wells will cleave the peptide sequence and separate the fluorophore and the

quencher, thus creating a fluorescent signal. This signal is read in a plate reader and compared to standards of the MMP being examined to determine MMP levels. For statistical analysis the cumulative amount of MMP produced by a given day was used.

### 4.2.9 Gene Expression

After 1, 7, 14, and 21 days of culture, samples were removed from their wells for gene expression analysis (Fig. 4.2). After washing with PBS, the hydrogels were mechanically disrupted using a DNase, RNase-free pellet grinder. RNA was isolated from the hydrogels with the QiaShredder column. Purification of RNA was achieved using the RNeasy mini kit. cDNA was synthesized with Superscript III RT in the presence of a nucleotide mix.

Amplification of cDNA through real time RT-PCR was performed using custom designed primers and SYBR Green. To design primers, a search for the gene sequence of interest was conducted using the National Center for Biotechnology Information (NCBI, http://www.ncbi.nlm.nih.gov/guide/) database. After the gene sequence was obtained, the sequence was input into Primer3 (http://fordo.wi.mit.edu/primer3/), a primer design tool. Default values were used to create candidate primer sequences. Candidate sequences were examined using the NCBI BLAST nucleotide database (http://blast.ncbi.nlm.nih.gov/) for known homologies with other genes. Pairs of primers were chosen to limit homology with other genes. Primers where both pairs in the set registered homology to the same non-target gene were not considered. After design, candidate primer pairs were obtained (Invitrogen) and used to create melt curves from cDNA previously isolated from hMSCs. Primer pairs that produced melt curves with multiple peaks were rejected. Amplification of cDNA and melt curve production was

conducted and recorded using the StepOnePlus™ Real-Time PCR System. A cycle time (Ct) value for a given gene was determined based on when the amplification curve crossed a threshold value. The threshold was set at the same value for all runs ($n \geq 7$). For a given gene, if half or more of the samples in a group did not amplify, that group was recorded as not amplifying and excluded from figures. Genes examined included collagen I, collagen III, and tenascin-C as markers for ligament/tendon fibroblast gene expression.[11] To explore the potential for differentiation down alternate pathways, genes from other lineages were examined including collagen II (chondrogenic differentiation[175]), osteocalcin (osteoblastic differentiation[175]), myogenic differentiation (myoD, myogenic differentiation[176]), and PPARγ (adipocytic differentiation[177]). Sequences for the forward and reverse primers used are listed in Table 3.2. Further details regarding the lab protocol used for this assay are found in appendix A.10.

### 4.2.10 Histology

After 1 and 21 days of culture, samples with hMSCs were collected for histological staining (Fig. 4.2). IHC was not conducted on hACL fibroblast samples. After washing in PBS for 1h to remove excess media, the hydrogels were fixed in formalin (Thermo Fisher Scientific) overnight. Samples were put into PBS for 20 minutes to wash out the formalin, then manually dehydrated using the following schedule: 70% dehydration alcohol (VWR) overnight, 80% dehydration alcohol overnight, 90% dehydration alcohol overnight, 95% dehydration alcohol overnight, 100% dehydration alcohol overnight. After dehydration samples were held under a -20 mmHg vacuum in paraffin (Thermo Fisher Scientific) for 4 hours to enhance penetration, then embedded. Paraffin-embedded hydrogels were cut into 10 μm sections and placed on

glass slides. Immunohistochemistry was performed (see appendix A.11 for further details) on these sections for genes that were significantly upregulated in real time RT-PCR (n=2). Primary antibody binding to proteins of interest was accomplished using monoclonal IgG mouse anti-human antibodies. Secondary antibody binding to primary antibodies was accomplished using polyclonal goat anti-mouse IgG antibodies conjugated to biotin (Abcam). Further amplification of signal was achieved using the Vectastain elite ABC peroxidase kit (Thermo Fisher Scientific). This amplification is achieved through an avidin conjugated horseradish peroxidase which binds to the biotinylated secondary antibody. Sections were exposed to diaminobenzidine (DAB) chromogen (Abcam) for 5 minutes to elicit a color change. Negative controls included samples immunostained with the primary antibody omitted.

### 4.2.11 Statistics

Results are reported as mean ± standard deviation. A Box-Cox transformation for normality was used on dCt values of gene expression data. Data were analyzed using a two-way ANOVA or three-way ANOVA as appropriate. If both factors were significant, but interactions were not significant, a Tukey's post hoc test with significance set at $p \leq 0.05$ was used for pairwise comparisons. If only one factor was significant and interactions were not significant one-way ANOVAs were run on the significant factor with each level of the non-significant factor fixed. A Tukey's post hoc test with significance set at $p \leq 0.05$ was used for pairwise comparisons. If interactions were significant, one way ANOVAs were run on the first (and then second) factor with each level of the second (and then first) factor fixed. A Tukey's post hoc test with significance set at $p \leq 0.05$ was used for pairwise comparisons.

For morphological analyses, the factors were day, hydrogel type, and region of the hydrogel when comparisons were made across hydrogel type, day, or between morphologies in the subsurface or middle regions. The factors were hydrogel type, day, and cell type when comparisons were made between cell types. For the hydrogel degradation study, cell number study, and gene expression analysis, the factors were day and hydrogel type. For the MMP production study the factors were day, hydrogel type, and MMP-activity when comparisons were made within a given cell type while the factors were day, hydrogel type, and cell type when comparisons were made between cell types. For gene expression analysis the factors were day and hydrogel type. Statistical analysis was carried out using Systat.

## 4.3 Results

### 4.3.1 Hydrogel Degradation Study

All hydrogel formulations cultured in PBS remained intact during the entire culture period. Both high and low saline content hydrogels consisting entirely of enzymatically-cleavable sequence (100%) degraded in collagenase within 2 days (Fig. 4.3). Interestingly, 75% enzymatically-cleavable hydrogels in collagenase degraded within 7 days when they were fabricated with a high saline content, but not at a low saline content. Hydrogels without any enzymatically-cleavable sequences (0%) or with only 25% of the polymers consisting of enzymatically-cleavable sequences remained intact in collagenase during the entire length of the 7 day culture. Fold swelling was significantly higher in high saline content hydrogels compared to low saline content hydrogels for all groups except 100% enzymatically-cleavable hydrogels in collagenase. Fold swelling was also significantly higher in hydrogels cultured in collagenase compared to those cultured in

PBS for all groups except low saline content hydrogels containing no enzymatically-cleavable sequences (0%).

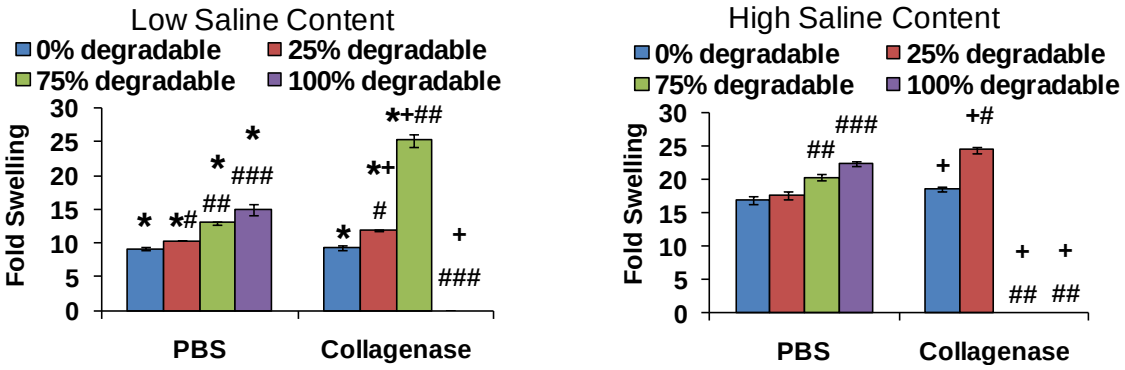


**Figure 4.3. Fold swelling of enzymatically-cleavable hydrogels with a low or high initial saline content (75wt% PBS or 90wt% PBS) cultured in PBS or collagenase, n=5 ±SD. $p<0.05$ compared to high saline content hydrogels (*). $p<0.05$ compared to PBS (+). $p<0.05$ compared to the 0% (#), 0% and 25% (##), or 0%, 25%, and 75% (###) hydrogels.**

Fold swelling showed a generally increasing trend as the amount of enzymatically-cleavable sequences in the hydrogel formulation increased. Specifically, in low saline content hydrogels cultured in PBS, fold swelling comparisons between hydrogels containing different amounts of enzymatically-cleavable sequences revealed that all comparisons between the four formulations were significant. Similarly, fold swelling of low saline content hydrogels cultured in collagenase was significantly different for every comparison between hydrogels with different enzymatically-cleavable sequence concentrations. For high saline content hydrogels in PBS, fold swelling was significantly different for every comparison between hydrogels with different enzymatically-cleavable sequence concentrations except for 0% enzymatically-cleavable hydrogels compared to 25% enzymatically-cleavable hydrogels. For high saline content hydrogels in collagenase, fold swelling was significantly different for every comparison between hydrogels with different enzymatically-cleavable sequence concentrations

except for 75% enzymatically-cleavable hydrogels compared to 100% enzymatically-cleavable hydrogels, with both undergoing complete degradation within two days of culture.

Mesh size of high saline content hydrogels was significantly higher than low saline content hydrogels in all samples except 100% enzymatically-cleavable hydrogels in collagenase (Fig. 4.4). Mesh size was also significantly different in low saline content 100% enzymatically-cleavable hydrogels in collagenase compared to PBS and in high saline content hydrogels with 0%, 75%, or 100% enzymatically-cleavable sequences in collagenase compared to PBS.

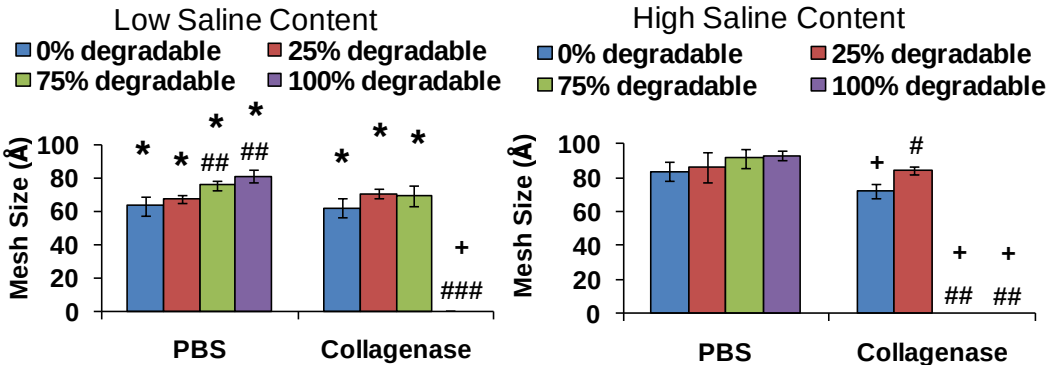


**Figure 4.4. Mesh size of enzymatically-cleavable hydrogels with a low or high initial saline content (75wt% PBS or 90wt% PBS) cultured in PBS or collagenase, n=5 ±SD. p<0.05 compared to high sailine hydrogels (*). (+) p<0.05 compared to PBS (+). p<0.05 compared to the 0% (#); 0% and 25% (##); or 0%, 25%, and 75% (###) hydrogels.**

For low saline content hydrogels mesh size was significantly different between 100% enzymatically-cleavable hydrogels and 0%, 25%, and 75% enzymatically-cleavable samples in collagenase. For low saline content hydrogels in PBS, differences were seen for 75% and 100% enzymatically-cleavable hydrogels compared to 0% and 25% enzymatically-cleavable hydrogels. For high saline content hydrogels significant differences were seen between all sample types except between 75% and 100%

enzymatically-cleavable hydrogels which were both fully degraded. No differences were seen in high saline content hydrogels in PBS between hydrogel types.

### 4.3.2 Cell Viability and Morphology

Both hMSCs and hACL fibroblasts generally demonstrated green staining throughout the entire 21 day culture period, indicating viability (Fig. 4.5G-J and 4.6G-J). There were no significant differences in circularity of hMSCs across time, due to hydrogel type, or in different regions of the hydrogels (Fig.4.5C, D, E, F). Similarly, there were no significant differences in the circularity of hACL fibroblasts across time or due to hydrogel type in the middle region of the hydrogels. Circularity of hACL fibroblasts in subsurface regions was significantly lower in 100% enzymatically-cleavable hydrogels on day 21 compared to day 7 (Fig. 4.6E) although no other comparisons of circularity in these cells were significant in the subsurface region.

Cellular area of hMSCs in middle regions was significantly different in 75% and 100% enzymatically-cleavable hydrogels compared to 0% enzymatically-cleavable hydrogels on day 7. Cellular area of hMSCs in middle regions was also significantly different in 0% and 25% enzymatically-cleavable hydrogels on day 7 compared to day 1 and in 100% enzymatically-cleavable hydrogels on day 7 and day 14 compared to day 1. In contrast, cellular area of encapsulated hACL fibroblasts in subsurface regions was significantly higher in 100% compared to 0% enzymatically-cleavable hydrogels on day 14 (Fig. 4.6C) and cell area was also higher in 100% enzymatically-cleavable hydrogels on day 21 and day 14 compared to day 7.

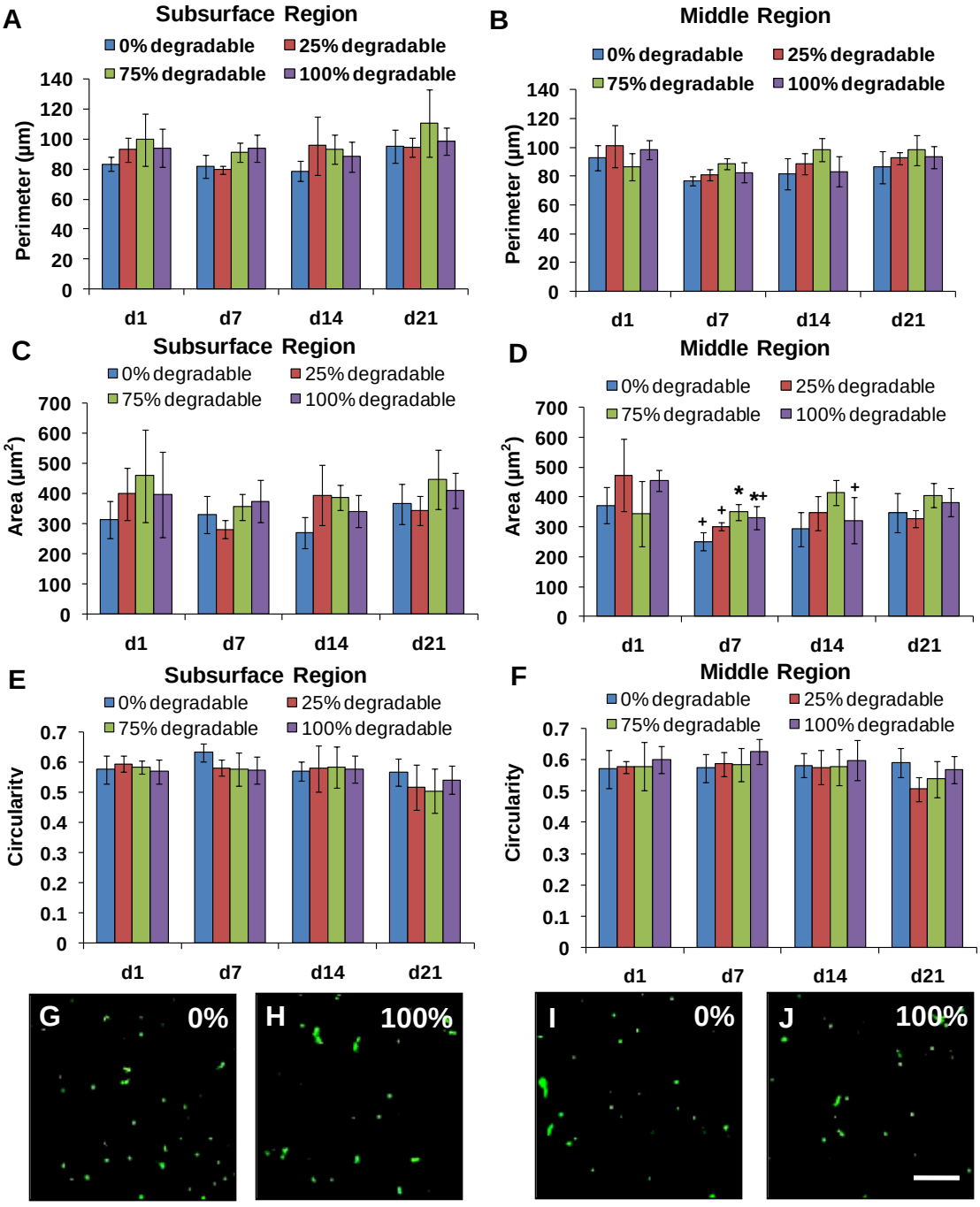


**Figure 4.5. Cellular perimeter (A, B), area (C, D) , or circularity (E, F) of encapsulated hMSCs in subsurface (A, C, E) or middle (B, D, F) regions of the hydrogels over 21d of culture (n≥3±SD). LIVE/DEAD images of hMSCs in subsurface (G, H) or middle (I, J) regions in 0% (G, I), or 100% (H, J) enzymatically-cleavable hydrogels at d21. $p<0.05$ compared to d1 (+). $p<0.05$ compared to the 0% (*). Scale bar = 100 μm.**

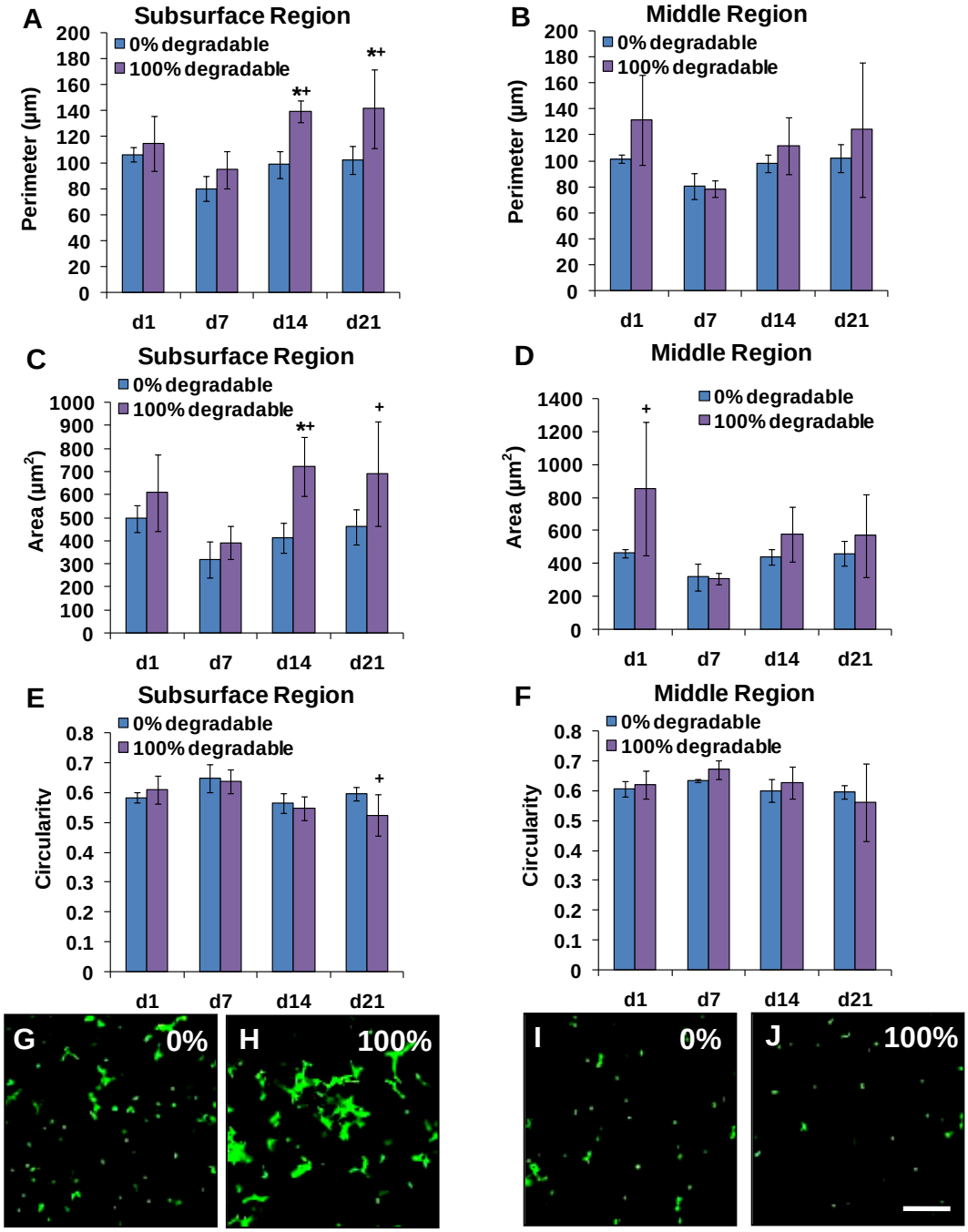


**Figure 4.6. Cellular perimeter (A, B), area (C, D), or circularity (E, F) of encapsulated hACL fibroblasts in subsurface (A, C, E) or middle (B, D, F) regions over 21d of culture (n≥3±SD). LIVE/DEAD images of hACL fibroblasts in subsurface (G, H) or middle (I, J) regions of 0% (G, I) or 100% (H, J) enzymatically-cleavable hydrogels at d21. p<0.05 compared to non-cleavable, 0% degradable hydrogels (*). p<0.05 compared to d7 hydrogels(+). Scale bar = 100 µm.**

There were no significant differences in perimeter seen with hMSCs across time, due the hydrogel type, or in different regions of the hydrogel (Fig. 4.5A&B). In contrast, cellular perimeter of encapsulated hACL fibroblasts in subsurface regions of the hydrogel was significantly higher in 100% compared to 0% enzymatically-cleavable hydrogels by day 14 (Fig. 4.6A). In addition, perimeter of hACL fibroblasts was significantly higher in 100% enzymatically-cleavable hydrogels on day 14 and day 21 compared to day 7. There were no significant differences in hACL fibroblast perimeter in middle regions or between different regions of the hydrogel (Fig. 4.6A&B). Images of hMSCs and hACL fibroblasts in the hydrogels matched well with the quantitative data (Fig. 4.5G-J and 4.6G-J).

### 4.3.3 Cell Number

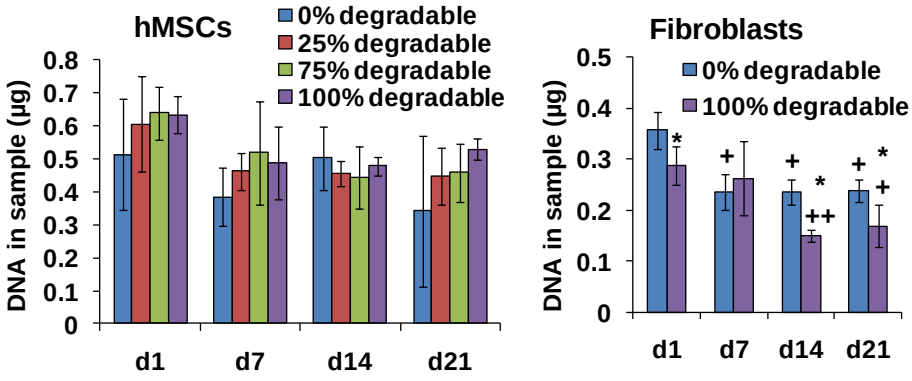


**Figure 4.7. DNA content of enzymatically-cleavable hydrogels with hMSCs or fibroblasts (n=5 ±SD). p<0.05 compared to non-enzymatically cleavable, 0% LGPA hydrogels (*). p<0.05 compared to d1 hydrogels(+). p<0.05 compared to d1 and d7 hydrogels (++).**

No differences in cell number of hMSCs were seen across time or due to hydrogel type (Fig. 4.7). Conversely, hACL fibroblasts showed a decrease in cell number on day 1, day 14, and day 21 in 100% enzymatically-cleavable hydrogels compared to 0% enzymatically-cleavable hydrogels. A decrease in cell number was also seen in hACL

fibroblasts on day 7, day 14, and day 21 compared to day 1 in 0% enzymatically-cleavable hydrogels. In addition, decreases in cell number were seen with hACL fibroblasts in 100% enzymatically-cleavable hydrogels on day 14 compared to day 1 and day 7 and on day 21 compared to day 1.

### 4.3.4 Matrix Metalloproteinase Production

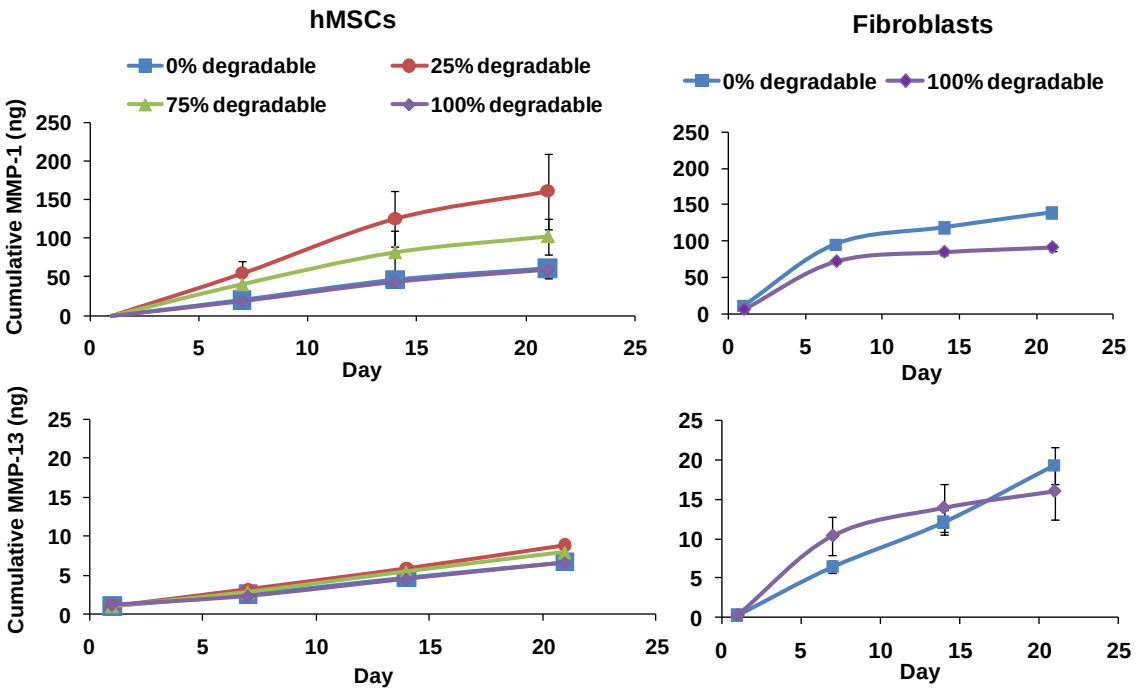


**Figure 4.8. Cumulative production of <u>total</u> MMP-1 and MMP-13 in hMSCs and hACL fibroblasts in enzymatically-cleavable hydrogels over 21d of culture (n=3 ±SD). Statistical significance is listed in tables 4.2 and 4.3.**

hMSCs produced detectable levels of MMP-1 by day 7 while hACL fibroblasts produced detectable MMP-1 by day 1 (Fig. 4.8). hACL fibroblasts produced higher amounts of MMP-1 than hMSCs in both 0% and 100% enzymatically-cleavable hydrogels at all time points. Levels of MMP-1 produced by hMSCs were significantly higher by day 21 compared to day 1 and day 7 and on day 14 compared to day 1 in all hydrogel types. MMP-1 was also significantly higher on day 14 compared to day 7 and

on day 7 compared to day 1 in 0% and 100% enzymatically cleavable hydrogels. The MMP-1 produced by hACL fibroblasts rose significantly at each time point, peaking at day 21, except in 100% enzymatically cleavable hydrogels from day 14 to day 21.

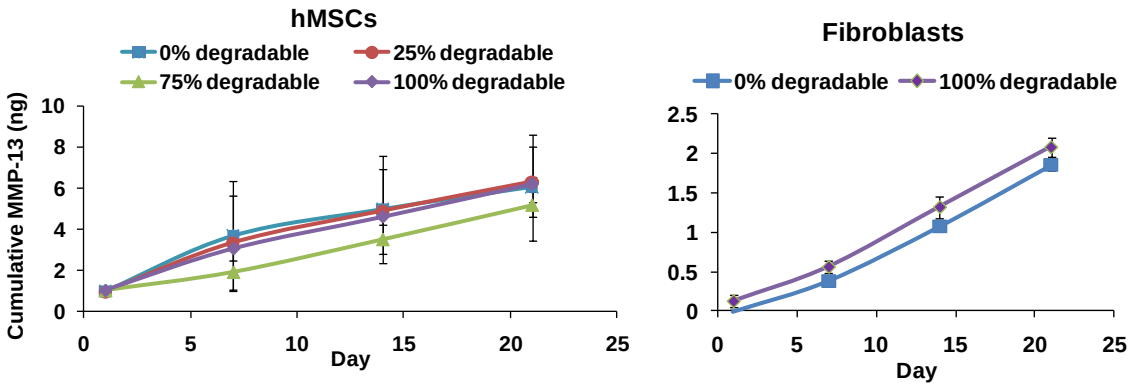


**Figure 4.9. Cumulative production of <u>active</u> MMP-13 in hMSCs and hACL fibroblasts in enzymatically-cleavable hydrogels over 21d of culture (n=3 ±SD). Statistical significance is listed in tables 4.2 and 4.3.**

**Table 4.2. Table of statistical significance for cumulative production of MMP-1 and MMP-13 by hMSCs in enzymatically-cleavable hydrogels over 21d of culture (n=3 ±SD). p<0.05 compared to fibroblasts (*). p<0.05 compared to d1 (+), d7 (++), d14 (+++), or d21 (++++). p<0.05 compared to 0%(#), 25% (##), 75% (###), or 100%(####). p<0.05 compared to active MMP ($).**

| hMSC | | Total MMP-1 | Total MMP-13 | Active MMP-1 | Active MMP-13 |
|---|---|---|---|---|---|
| d1 | 0% | *,++,+++,++++,$ | *,++,+++,++++,$ | | *,++++ |
| | 25% | +++,++++,$ | ++,+++,++++ | | ++++ |
| | 75% | +++,++++,$ | +,++,+++ | | |
| | 100% | *,++,+++,++++ | *,++,+++,++++ | | *,++++ |
| d7 | 0% | *,##,+,+++,++++,$ | *,##,+,+++,++++ | | |
| | 25% | #,####,++++,$ | #,####,+,+++,++++ | | |
| | 75% | ++++,$ | +,+++,++++,$ | | |
| | 100% | *,##,+,+++,++++,$ | *,##,+,+++,++++ | | |
| d14 | 0% | *,##, +,++,$ | *,##,+,++ | | * |
| | 25% | #,####,+,$ | #,####,+,++ | | |
| | 75% | +,$ | ####,+,++,$ | | |
| | 100% | *,##,+,++,$ | *,##,###,+,++,++++ | | |
| d21 | 0% | *,##,+,++,$ | *,##,###,+,++ | | *,+ |
| | 25% | #,####,+,++,$ | #,###,####,+,++ | | + |
| | 75% | +,++,$ | #,##,####,+,++,$ | | |
| | 100% | *,##,+,++,$ | *,##,###,+,++,+++ | | *,+ |

hMSCs cultured in 25% enzymatically-cleavable hydrogels produced significantly higher levels of MMP-1 on days 7, 14, and 21 than hMSCs in 0% or 100% enzymatically-cleavable hydrogel formulations. While hMSCs did not show significant differences in MMP-1 production between 100% enzymatically-cleavable and 0% enzymatically-cleavable hydrogels at any time point, hACL fibroblasts produced significantly less MMP-1 in 100% enzymatically-cleavable hydrogels compared to 0% by day 7. Neither hMSCs nor hACL fibroblasts produced detectable levels of active MMP-1 at any time in the culture period. As a result of the lack of active MMP-1 production, total levels of MMP-1 were significantly higher than active MMP-1 with hMSCs and hACL fibroblasts in all hydrogel types by day 7.

**Table 4.3. Table of statistical significance for cumulative production of MMP-1 and MMP-13 by hACL fibroblasts in enzymatically-cleavable hydrogels over 21d of culture (n=3 ±SD). p<0.05 compared to d1(+), d7(++), d14(+++), or d21 (++++). p<0.05 compared to 0%(#) or 100%(####). p<0.05 compared to active MMP($).**

| Fibroblast | | Total MMP-1 | Total MMP-13 | Active MMP-1 | Active MMP-13 |
|---|---|---|---|---|---|
| d1 | 0% | ++,+++,++++,$ | ++,+++,++++,$ | | ++,+++,++++ |
| | 100% | ++,+++,++++,$ | ++,+++,++++,$ | | ++,+++,++++ |
| d7 | 0% | +,+++,++++,$ | +,+++,++++,$ | | +,+++,++++ |
| | 100% | +,+++,++++,#,$ | +,$ | | +,+++,++++,# |
| d14 | 0% | +,++,++++,$ | +,++,++++,$ | | +,++,++++ |
| | 100% | +,++,#,$ | +,$ | | +,++,++++ |
| d21 | 0% | +,++,+++,$ | +,++,+++,$ | | +,++,+++ |
| | 100% | +,++,#,$ | +,$ | | +,++,+++ |

While no active MMP-1was produced by either cell type, both hMSCs and hACL fibroblasts produced modest levels of active MMP-13 (Fig. 4.9). Interestingly, there was no significant difference in the amount of active MMP-13 and total MMP-13 produced by hMSCs except in 75% enzymatically-cleavable hydrogels on days 7, 14, and 21. This

suggests that the MMP-13 secreted by hMSCs was in an active form in most cases. Conversely, hACL fibroblasts produced significantly more total MMP-13 than active MMP-13 in both hydrogel types at all time points. hACL fibroblasts produced significantly more total MMP-13 than hMSCs in all hydrogel types by day 7. While hACL fibroblasts generally produced more total MMP-13, hMSCs often produced more MMP-13 in an active form. Specifically, hMSCs produced more active MMP-13 than hACL fibroblasts in 0% and 100% enzymatically-cleavable hydrogels on day 1 and day 21 and in 0% enzymatically-cleavable hydrogels on day 14.

Active MMP-13 was significantly higher with hMSCs in 0%, 25%, and 100% enzymatically cleavable hydrogels on day 21 compared to day 1. No significant differences were seen with active MMP-13 in hMSCs due to the hydrogel type. The total MMP-13 produced by hMSCs rose significantly at each time point, peaking at day 21, except from day 14 to day 21 in 0%, 25%, and 75% enzymatically-cleavable hydrogels. In addition, total MMP-13 produced by hMSCs was significantly different between 25% enzymatically-cleavable hydrogels compared to 0% and 100% enzymatically-cleavable samples on days 7, 14, and 21; between 75% enzymatically-cleavable hydrogels compared to 100% enzymatically-cleavable samples on days 14 and 21; and between 75% enzymatically-cleavable hydrogels compared to 0% and 25% enzymatically-cleavable samples on day 21.

The active MMP-13 produced by hACL fibroblasts rose significantly at each time point, peaking at day 21 in both 0% and 100% enzymatically-cleavable hydrogels. In addition, total MMP-13 produced by hACL fibroblasts in 0% enzymatically-cleavable hydrogels rose significantly at each time point, peaking at day 21. Total MMP-13

produced by hACL fibroblasts in 100% enzymatically-cleavable hydrogels was significantly higher on days 7, 14, and 21 compared to day 1. There were no differences in total or active MMP-13 production by hACL fibroblasts across hydrogel types except for active MMP-13 on day 7.

### 4.3.5 Gene Expression

Neither hMSCs nor hACL fibroblasts showed any significant differences in GAPDH gene expression (Ct) at any time point due to the hydrogel formulation (Supplementary Fig. B.2). In addition, there was no significant difference in GAPDH expression between hMSCs and hACL fibroblasts on day 7, day 14, or day 21. However, hMSCs had a significantly higher Ct values for GAPDH compared to hACL fibroblasts on day 1.

Collagen I gene expression was higher (Fig. 4.10A, 4.10B) in hACL fibroblasts compared to hMSCs in 0% and 100% enzymatically-cleavable hydrogels on day 1, day 7, and day 21. Collagen III gene expression was significantly different (Fig. 4.10C, 4.10D) in hACL fibroblasts compared to hMSCs in 0% enzymatically-cleavable hydrogels on day 1, day 7, day 14, and day 21 and in 100% enzymatically-cleavable hydrogels on day 1, day 7, and day 14.

Tenascin-C gene expression was significantly different (Fig. 4.10E, 4.10F) in hACL fibroblasts compared to hMSCs in 0% and 100% enzymatically-cleavable hydrogels at all time points.

hMSCs showed significantly different collagen I gene expression on day 14 and day 21 compared to day 1 and day 7 in 0%, 25%, and 75% enzymatically-cleavable hydrogels (Fig. 4.10A). Significant differences in 100% enzymatically-cleavable

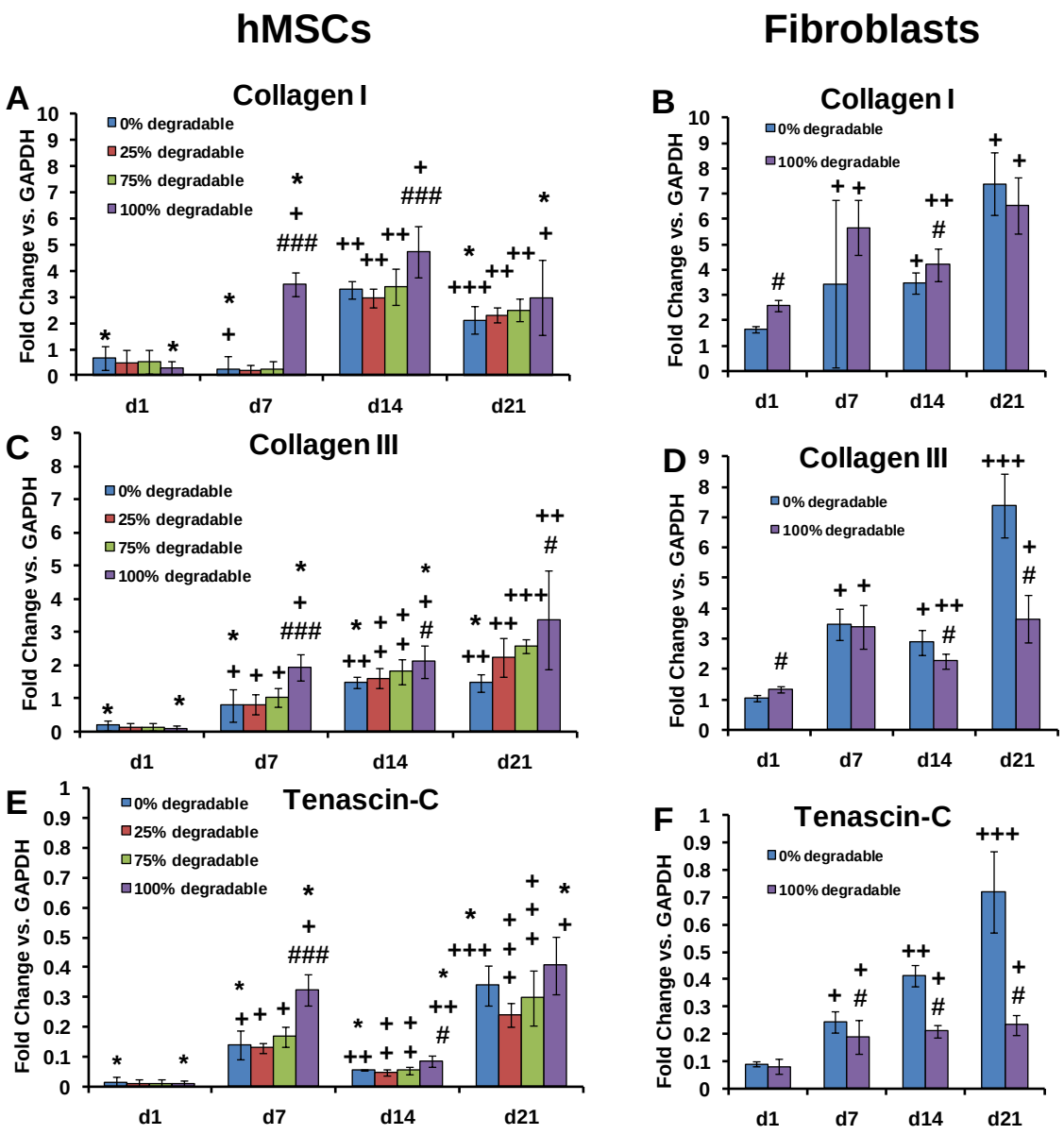


**Figure 4.10. Collagen I (A, B), collagen III (C, D), and tenascin-C (E, F) gene expression in hMSCs (A, C, E) or fibroblasts (B, D, F) in enzymatically-degradable hydrogels (n≥7 ±SD). p<0.05 compared to the 0%(#); 0% and 25%(##); or 0%, 25%, and 75%(###) hydrogels; respectively, for the given time point. p<0.05 compared to d1(+); d1 and d7(++); or d1, d7, and d14(+++); respectively, for the given hydrogel type. p<0.05 compared to fibroblasts (*) for the given day and hydrogel type.**

hydrogels with hMSCs were seen on day 7, day 14, and day 21 compared to day 1; and day 21 compared to day 14. Collagen I was upregulated in hACL fibroblasts in 0% enzymatically-cleavable hydrogels on day 21 compared to day 1 and day 14, and on days

7 and 14 compared to day 1, and in 100% enzymatically-cleavable hydrogels on day 7 compared to day 1, on day 14 compared to day 1 and day 7, and on day 21 compared to day 14 and day 1 (Fig. 4.10B).

hMSCs showed upregulation of collagen III gene expression on day 7, day 14, and day 21 compared to day 1 in all hydrogel types (Fig. 4.10C). In addition, collagen III was upregulated in hMSCs in 0%, 25%, and 75% enzymatically-cleavable hydrogels on day 14 and day 21 compared to day 7, in 75% enzymatically-cleavable hydrogels on day 21 compared to day 14, and in 100% enzymatically-cleavable hydrogels on day 21 compared to day 7. Collagen III was upregulated in hACL fibroblasts in 0% enzymatically-cleavable hydrogels on day 7, day 14, and day 21 compared to day 1 and on day 21 compared to day 7 and day 14 (Fig. 4.10D). Collagen III was significantly different in hACL fibroblasts in 100% enzymatically-cleavable hydrogels on day 7, day 14, and day 21 compared to day 1, day 14 compared to day 7, and day 21 compared to day 14.

All comparisons of tenascin-C gene expression across time points were statistically significant in hMSCs for all hydrogel types except in 100% enzymatically-cleavable hydrogels on day 21 compared to day 7 (Fig. 4.10E). Tenascin-C was upregulated in hACL fibroblasts in 0% MMP hydrogels on day 7, day 14, and day 21 compared to day 1, day 14 and day 21 compared to day 7, and day 21 compared to day 14 (Fig. 4.10F). Upregulation was seen in hACL fibroblasts in 100% enzymatically-cleavable hydrogels on day 7, day 14, and day 21 compared to day 1.

hMSCs showed upregulation of collagen I gene expression on day 7 and day 14 in 100% enzymatically-cleavable hydrogels compared to 0%, 25%, and 75% enzymatically-

cleavable hydrogels (Fig. 4.10A). hACL fibroblasts showed upregulation of collagen I gene expression on day 1 and day 14 in 100% enzymatically-cleavable hydrogels compared to 0% enzymatically-cleavable hydrogels (Fig. 4.10B).

hMSCs generally showed upregulation of collagen III gene expression in response to increase concentrations of MMP-cleavable peptides (Fig. 4.10C). Specifically, collagen III was upregulated in hMSCs on d7 in 100% MMP-cleavable hydrogels compared to 0%, 25%, and 75% enzymatically-cleavable hydrogels and on day 14 and day 21 in 100% enzymatically-cleavable hydrogels compared to 0% enzymatically-cleavable hydrogels. Conversely, collagen III was downregulated in hACL fibroblasts on day 14 and day 21 in 100% enzymatically-cleavable hydrogels compared to 0% cleavable hydrogels (Fig. 4.10D). Collagen III was also downregulated in hACL fibroblasts on day 1 in 0% enzymatically-cleavable hydrogels compared to 100% cleavable hydrogels.

hMSCs showed upregulation of tenascin-C on day 7 in 100% enzymatically-cleavable hydrogels compared to 75%, 25%, and 0% enzymatically-cleavable hydrogels, on day 14 in 100% enzymatically-cleavable hydrogels compared to 0% enzymatically-cleavable hydrogels, and on day 21 in 100% enzymatically-cleavable hydrogels compared to 25% enzymatically-cleavable hydrogels (Fig. 4.10E). Tenascin-C was downregulated in hACL fibroblasts on day 7, day 14, and day 21 in 100% enzymatically-cleavable hydrogels compared to 0% enzymatically-cleavable hydrogels (Fig. 4.10F).

Collagen II, osteocalcin, myoD, and PPARγ were generally expressed at low transcript levels (Fig. 4.11 and 4.12) with some samples failing to reach detectable levels. Specifically, in hMSCs collagen II was not detected on day 14 of 25% enzymatically-cleavable hydrogels, on day 21 of 75% enzymatically-cleavable hydrogels; osteocalcin

was not detected on day 1 in any samples; and PPARγ was not detected on day 1 or day 21 in any samples, on day 7 in 0% or 75% enzymatically-cleavable hydrogels, or on day 14 in 0% or 100% enzymatically-cleavable hydrogels. PPARγ was not detected in any hydrogels containing hACL fibroblasts at any time point.

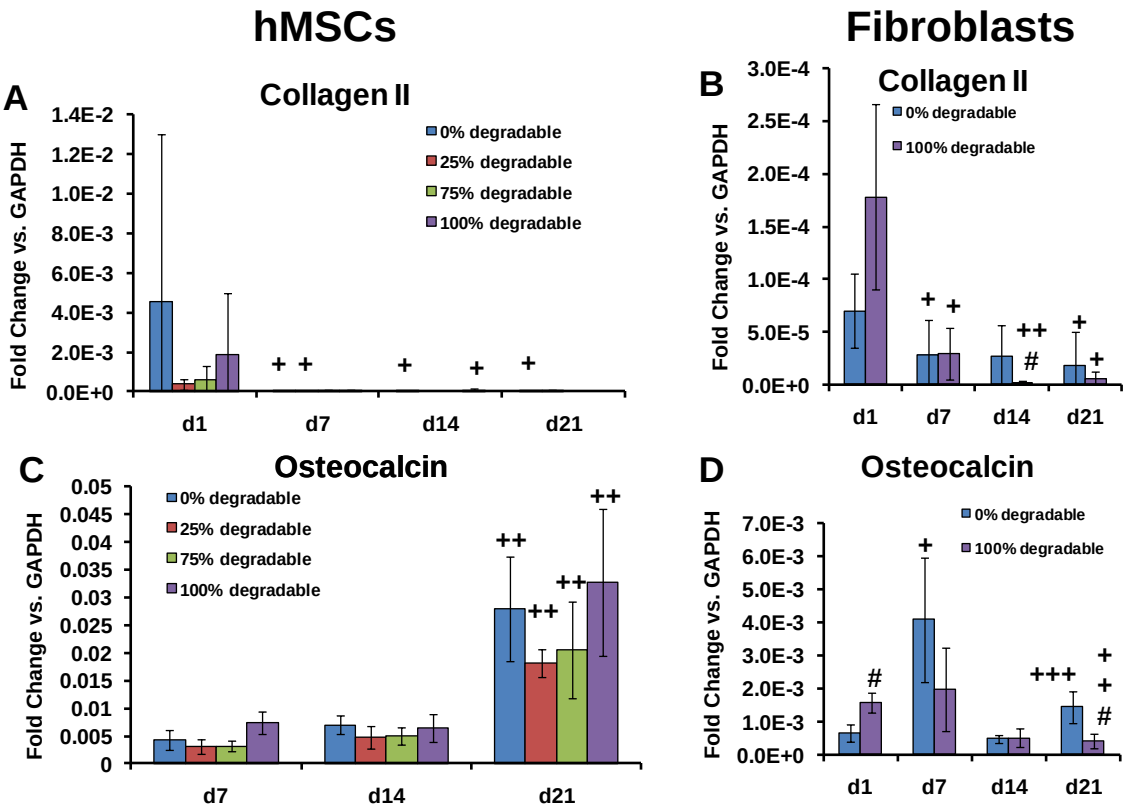


**Figure 4.11. Collagen II (A, B) and osteocalcin (C, D) gene expression in hMSCs (A, C) or fibroblasts (B, D) in enzymatically-degradable hydrogels (n≥7 ±SD). p<0.05 compared to fibroblasts (*), p<0.05 compared to the 0% hydrogels (#), for the given time point. p<0.05 compared to d1(+); d1 and d7(++); or d1, d7, and d14(+++); respectively, for the given hydrogel type.**

hMSCs showed downregulation of collagen II in 0% enzymatically-cleavable hydrogels on day 7, day 14, and day 21 compared to day 1; in 25% enzymatically-cleavable hydrogels on day 7 compared to day 1; and in 100% enzymatically-cleavable hydrogels on day 14 compared to day 1 (Fig. 4.11A). hACL fibroblasts showed downregulation of collagen II in 0% enzymatically-cleavable hydrogels on day 7 and day

21 compared to day 1; in 100% enzymatically-cleavable hydrogels on day 7, day 14, and day 21 compared to day 1, and on day 14 compared to day 7; and on d14 in 100% enzymatically-degradable hydrogels compared to 0% enzymatically degradable hydrogels (Fig. 4.11B).

hMSCs showed upregulation of osteocalcin gene expression on day 21 in all hydrogel types compared to day 7 and day 14 (Fig. 4.11C). In addition, osteocalcin was upregulated in hMSCs on day 7 in 100% enzymatically-cleavable hydrogels compared to 25% and 75% enzymatically-cleavable samples. Osteocalcin was upregulated in hACL fibroblasts in 0% enzymatically-cleavable hydrogels on day 7 compared to day 1, day 14, and day 21; and on day 21 compared to day 1 and day 14 (Fig. 4.11D). In addition, osteocalcin was upregulated in hACL fibroblasts in 100% enzymatically-cleavable hydrogels on day 1 and day 7 compared to day 21; on day 1 in 100% compared to 0% enzymatically-cleavable hydrogels; and on day 21 in 0% compared to 100% enzymatically-cleavable hydrogels.

hMSCs showed significant differences in myoD gene expression in 0% enzymatically-cleavable hydrogels on day 7 and 14 compared to day 1, and on day 21 compared to day 7; in 25% enzymatically-cleavable hydrogels on day 7 compared to day 1, day 14, and day 21; in 75% enzymatically-cleavable hydrogels on day 7, day 14, and day 21 compared to day 1; and in 100% enzymatically-cleavable hydrogels on day 7 compared to day 1 (Fig. 4.12A). hACL fibroblasts showed significant differences in myoD gene expression in 0% enzymatically-cleavable hydrogels on day 14 compared to day 1, day 7, and day 21; in 100% enzymatically-cleavable hydrogels on day 14 compared to day 1 and day 7, and day 1 compared to day 21; and on day 1 in 0%

enzymatically-cleavable hydrogels compared to 100% enzymatically-cleavable hydrogels (Fig. 4.12B).

PPARγ was not detected in hMSCs except in the 4 sample groups shown in Fig. 4.12C. Comparisons among these groups yielded statistical significance on day 7 between 25% and 100% enzymatically-cleavable samples, on day 14 between 25% and 75% enzymatically-cleavable samples, and in 25% enzymatically cleavable samples on day 14 compared to day 7. PPARγ was not detected in hACL fibroblasts in any samples at any time point.

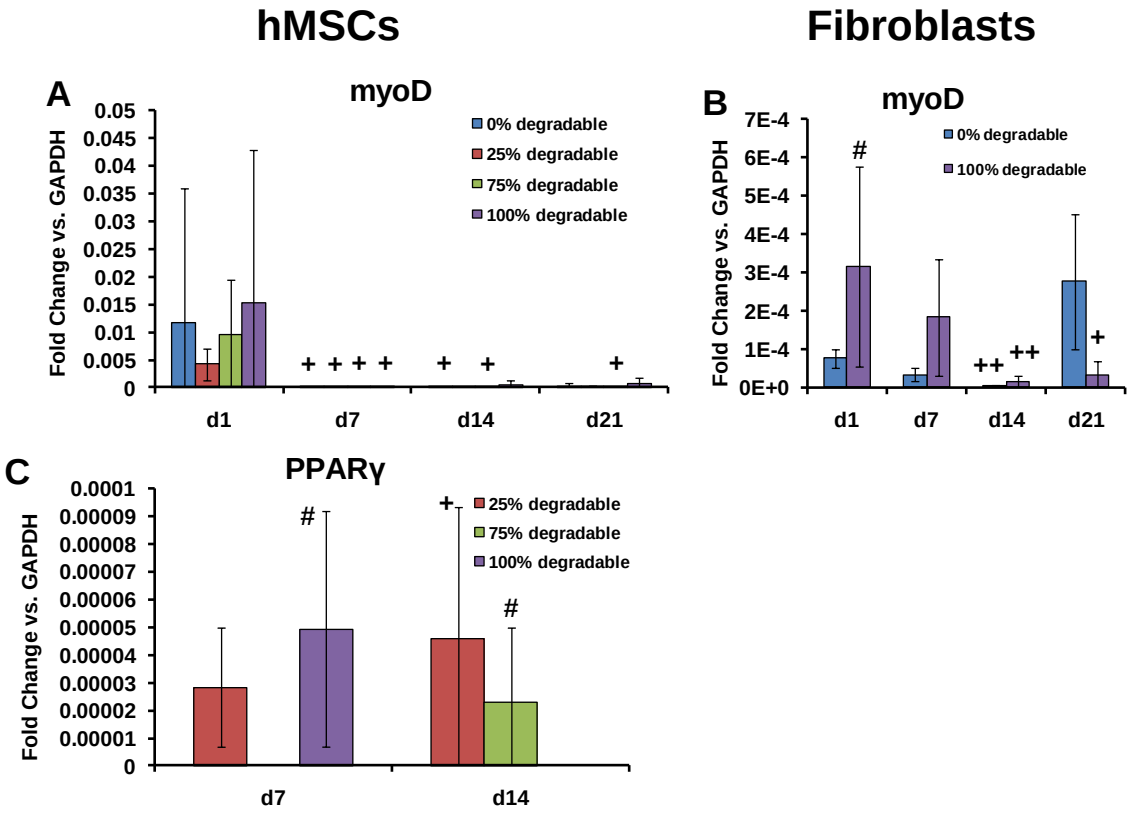


**Figure 4.12. myoD (A, B) and PPARγ (C) gene expression in hMSCs (A, C) or fibroblasts (B) in enzymatically-degradable hydrogels (n≥7 ±SD). PPARγ did not amplify in hMSCs except for the 4 samples displayed in C. PPARγ did not amplify in hACL fibroblasts in any hydrogel type or at any time point. p<0.05 compared to fibroblasts (*) for the given day and hydrogel type. p<0.05 compared to 0% hydrogels(#) for the given time point. p<0.05 compared to d1(+); or d1, d7, and d14(+++); respectively, for the given hydrogel type.**

### 4.3.6 Histology

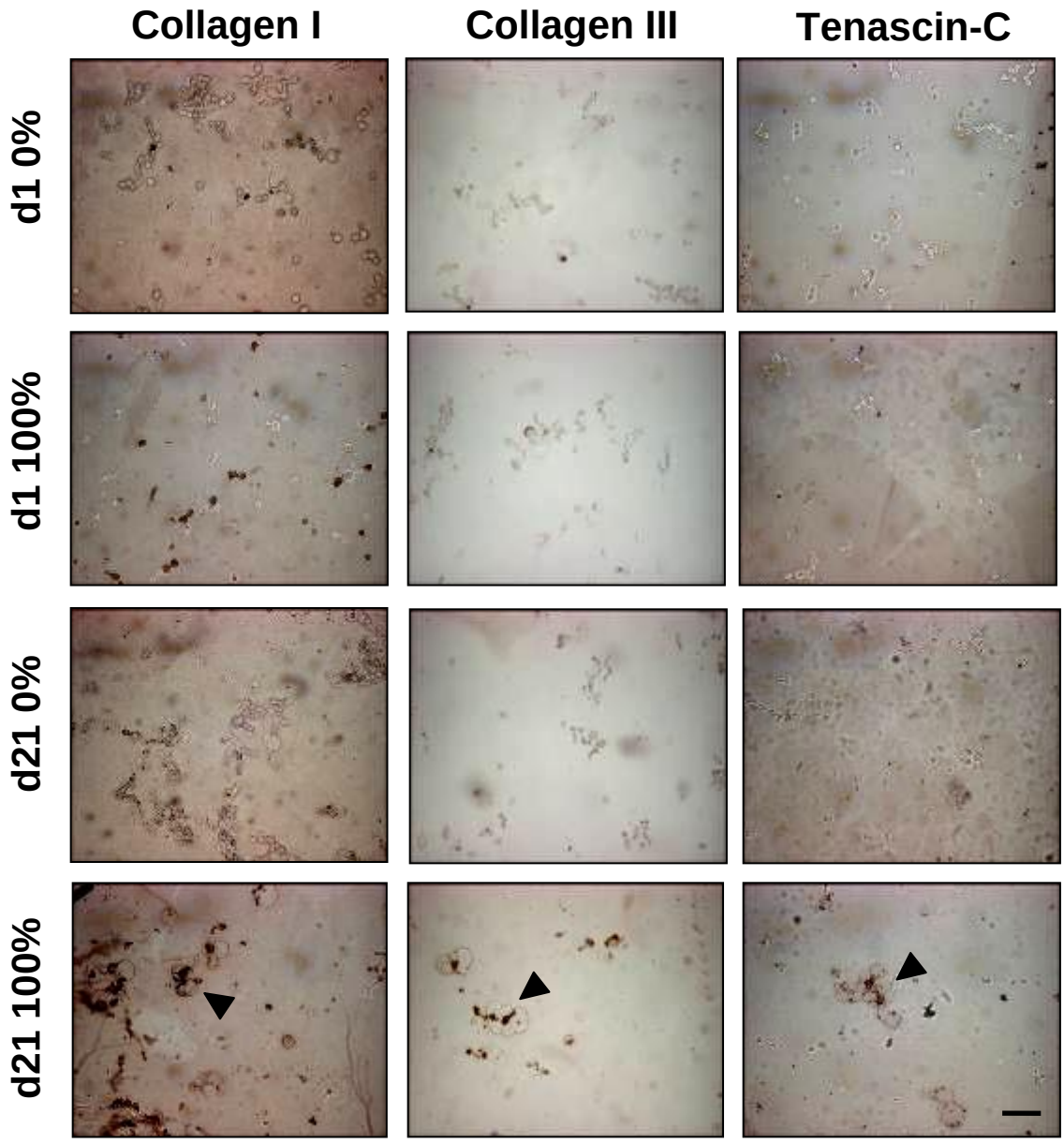


**Figure 4.13. IHC for collagen I, collagen III, or tenascin-C in 0% or 100% enzymatically-degradable hydrogels with hMSCs on day 21 or day 1. Brown color indicates staining for the particular protein. Arrow indicates pericellular staining. Scale bar = 20 µm.**

IHC staining was performed only on samples with hMSCs. This staining indicated the presence of collagen I pericellularly in 100% enzymatically-cleavable hydrogels with hMSCs on day 1 and day 21 (Fig. 4.13). Minimal staining for collagen I

was seen in 0% enzymatically-cleavable hydrogels even by day 21. Staining for collagen III and tenascin-C was seen pericellularly in 100% enzymatically-cleavable hydrogels with hMSCs by 21 (Fig. 4.13). However, little to no staining for collagen III or tenascin-C was seen in 0% hydrogels or on day 1. No staining was seen in control sections with the primary antibody omitted suggesting that neither the secondary antibody nor the Vectastain elite ABC peroxidase kit exhibited significant non-specific binding and that there was minimal endogenous staining from the contrast agent. However it should be noted that no isotype control was used so the possibility of non-specific binding of the primary antibody can not be eliminated.

## 4.4 Discussion

This hydrogel system provides an environment that can take advantage of enzymatic degradation of the biomaterial carrier. The changes in fold swelling that were seen in enzymatically-cleavable hydrogels in collagenase (Fig. 4.3), including complete degradation of some samples, showed that the cleavable LGPA motifs can be targeted for enzyme-mediated degradation, in agreement with previous results.[112,113] In addition, the studies in this chapter showed that the susceptibility of the biomaterial environment to enzyme-mediated degradation can be tailored through changes in the saline content of the hydrogels and through the combination of the LGPA motifs with non-enzymatically-cleavable polymers. Interestingly, enzymatically-cleavable sequences seemed to have a greater affect on fold swelling than mesh size of hydrogels (Fig. 4.4), suggesting that mesh size may not be as sensitive to degradation.

Collagen I, collagen III and tenascin-C mRNA transcripts were found at higher levels in hMSCs in 100% enzymatically-cleavable hydrogels, which possessed the

highest total degradability (Fig. 4.3), compared to samples with lower concentrations of cleavable peptides (Fig. 4.10). The higher transcript levels in hMSCs did not appear to occur in a dose-dependant manner across hydrogel formulations, as there were no significant differences between 0%, 25%, and 75% enzymatically cleavable hydrogels. An upregulation of collagen I, collagen III, and tenascin-C was seen in both hMSCs and hACL fibroblasts for all hydrogel types on day 21 compared to day 1 (Fig. 4.10). hMSCs cultured in collagen-based hydrogels have shown a similar time-dependant upregulation of collagen I and collagen III,[179] suggesting that upregulation of ligament/tendon ECM genes occurs over time in a variety of biomaterial systems. In contrast, changing the cell type seems to promote diverse responses to the enzymatically-cleavable hydrogel environments. Upregulation of ligament fibroblast gene expression was promoted in hMSCs in 100% enzymatically-cleavable hydrogels (Fig. 4.10). Other studies with bovine chondrocytes in enzymatically-degradable hydrogels using a different peptide sequence have shown upregulation of cartilage-related gene expression.[197] The upregulation of ligament fibroblast-related or cartilage-related gene expression depending on cell type suggests that cell responses in enzymatically-degradable hydrogels can be adapted to different applications depending on the cell type used. The particular cleavable sequence employed may also be an important factor to consider and may need to be tailored to the specific application and cell type. In addition, the percentage of the hydrogel that is susceptible to enzymatic degradation may also need to be altered according to the particular application and cell type chosen. This is supported by the upregulation or downregulation of ligament/tendon ECM gene expression seen in

enzymatically cleavable hydrogels compared to non-cleavable samples depending on the cell type used (Fig. 4.10).

In addition to promoting changes in gene expression, the 100% enzymatically-cleavable hydrogels, which possessed the highest total degradability (Fig. 4.3), also seemed to facilitate the production of ECM proteins by hMSCs (Fig. 4.13, IHC was not conducted on hACL fibroblasts), in agreement with previous results using synthetic enzymatically-cleavable hydrogels.[197,198] Hydrogels with lower levels of degradability produced minimal ECM production. Natural scaffolds made of collagen I possess the enzymatically-cleavable motifs that are similar to those used in synthetic enzymatically-cleavable hydrogels so similar patterns of protein production would be expected. While some studies using collagen I scaffolds with hMSCs in static culture have shown collagen III protein production,[100] other studies using collagen I scaffolds with bovine MSCs (bMSCs) have shown minimal collagen III production.[11] As discussed above, responses to enzymatically-degradable environments appear to vary with the cell type used, so the minimal collagen III production by bMSCs may be related to that specific cell type. The matrix production that has been seen in our system and in other studies is likely related to degradation of the scaffold, as increased degradation of hydrogel biomaterials has been linked to greater ECM production.[101] Interestingly, production of collagen I and collagen III ECM by hMSCs has also been seen in synthetic PLLA scaffolds with limited degradability.[193] This matrix production may be explained by the knitted pattern used with the PLLA scaffolds which creates a macroporous structure. This porosity provides the void space required for ECM production without the need of degradation.

MMP-1 did not appear to play a role in hydrogel degradation or the gene expression and protein production changes as this enzyme was not produced at detectable levels in an active form. MMP-13 may play a role in degradation of the hydrogel environment, and thus cellular responses observed, since modest levels of this enzyme in an active form were produced by both hMSCs and hACL fibroblasts (Fig. 4.9). Other MMPs or proteases that were not measured in this study may also play a role in the responses seen.

The higher gene expression levels of collagen I, collagen III, and tenascin-C that were generally seen with hACL fibroblasts compared to hMSCs lends credence to the idea that upregulation of these genes is a sign that hMSCs are developing a phenotype closer to a ligament/tendon fibroblast. However, it should be noted that the hACL fibroblasts used in this study were obtained from a patient undergoing knee surgery. Since these cells were obtained from only one donor, their responses may not be widely applicable. Using cells from multiple donors could strengthen conclusions related to the hACL fibroblasts in this study. In addition, the behavior of the hACL fibroblasts may not be representative of hACL fibroblasts in a healthy tissue environment. Cadaveric tissue or ACL tissue obtained after total knee replacements that do not involve and ACL rupture may be other potential sources of hACL fibroblasts, however the health of the tissue environment in both of these cases is also problematic. Consequently, a perfect source of hACL fibroblasts may not be feasible at this time.

The upregulation of collagen I, collagen III, and tenascin-C expression in hMSCs in 100% enzymatically-cleavable hydrogels compared to other hydrogel formulations (Fig. 4.10), combined with the IHC results, suggests that the enzymatically-cleavable

biomaterial environments facilitated production of ligament/tendon ECM components by hMSCs. While staining of hydrogels containing hMSCS showed the presence of ECM components in ligament/tendon tissues, it can not be specified whether this ECM is similar to hACL fibroblasts in similar hydrogels as IHC was not conducted on those samples. The ECM production that was seen with hMSCs may be due to the susceptibility of the LGPA polymers to cleavage. Cleavage of the LGPA polymers might be achieved by MMPs or other enzymes secreted by encapsulated cells. This would allow for localized degradation of the hydrogel matrix which may facilitate production of ligament/tendon ECM components by providing void space needed for their elaboration. Further confirmation that the enzymatically-cleavable peptides are responsible for the phenomenon seen could be provided through future studies using a scrambled peptide that is not expected to undergo enzymatic degradation, through the use of an MMP inhibitor such as GM6001, or by using an enzymatically-cleavable fluorogenic substrate.[113] If the effects seen in the enzymatically cleavable hydrogels disappear in samples where a scrambled sequence or MMP inhibitor is used, it would suggest that enzymatic-degradation of the biomaterial environment was necessary for the observed responses. An enzymatically-cleavable fluorogenic substrate could also be used to visually confirm that cleavage is occurring in the hydrogel environment.

Cell number (Fig. 4.7) and the morphology (Fig. 4.5) of the hMSCs do not appear to play a role in the changes in ECM production observed seen as these factors are not significantly different between hydrogel types. However, other factors that change across the different biomaterial formulations (Table 4.1) could affect the responses seen. The initial mesh size of the hydrogels is one factor that is different between some of the

biomaterial formulations (Fig. 4.4), but this feature does not appear to be sufficient to explain the changes in gene expression seen with hMSCs. Initial mesh size was not significantly different between 75% and 100% enzymatically-cleavable hydrogel samples (Fig. 4.4). However, there were significant differences in gene expression levels of collagen I, collagen III, and tenascin-C in hMSCs in 100% enzymatically-cleavable hydrogels compared to 75% enzymatically cleavable hydrogels. The 75% and 100% enzymatically-cleavable hydrogels did have different overall levels of susceptibility to enzymatic degradation (Fig. 4.4) which suggests that may be a more important reason why differences were seen between these two sample types.

Another potential factor that may change across hydrogel formulations is the cross-linking of the hydrogels which can be affected by the number of double bonds available for cross-linking and the relative reactivities of the bonds. The increased fold swelling (Fig. 4.3) and mesh size (Fig. 4.4) seen in hydrogels formed from enzymatically-cleavable polymers compared to non-enzymatically cleavable hydrogels suggests that the enzymatically cleavable hydrogels have a lower cross-linking density than non-enzymatically cleavable samples.[186] Changes in the cross-linking density have the potential to affect the elastic modulus of samples which could potentially play a role in cell responses seen.[186,199] However, the differences in mesh size that were seen in these samples are not expected to be large enough to significantly affect mechanical properties, as comparable mesh size changes in other OPF-based hydrogels did not result in significant differences of tensile modulus, fracture strength, or toughness of the samples.[186] Tensile testing of these hydrogels could be useful to provide confirmation

that mechanical properties do not change significantly between the hydrogel formulations used in this study.

Variations in the presentation of the RGD adhesion peptides in these samples also have the potential to play a role in the differences seen between sample types. For example, the efficiency of incorporation of RGD peptides could change across hydrogel formulations and thus affect the presentation of RGD to encapsulated cells. This could occur due to different reactivities of fumarate and acrylate bonds,[200] which are present in different concentrations in the hydrogel formulations used in this study. Changes in the distance between cross-links could also affect the presentation of the adhesion peptides to the cells. However, the cross-link density is not expected to play a major role in the presentation of RGD peptides in these hydrogels as the concentration of double bonds available for cross-linking in all sample types is almost 2 orders of magnitude higher than the number of RGD peptides. In addition, the incorporation of RGD peptides into a variety of hydrogel formulations did not significantly affect the fold swelling of those samples (supplementary Fig. B.3), suggesting that the addition of these sequences has a limited effect on the cross-linking density. Further characterization of the RGD peptide concentration after cross-linking could be achieved through methods such as radiolabeling of the peptide or amino acid analysis. These would provide greater insight into if the efficiency of RGD peptide incorporation varied in different hydrogel formulations.

The upregulation of relevant ligament ECM gene expression seen in hMSCs in enzymatically-degradable hydrogels produced expression levels approaching those observed in hACL fibroblasts (Fig. 4.10) which suggests that an enzymatically-

degradable environment may be an important factor for differentiation of hMSCs toward a ligament/tendon fibroblastic phenotype. The similarities in expression levels do not seem to be related to differences in GAPDH levels as hMSCs and hACL fibroblasts did not have significant differences in GAPDH gene expression except at day 1 (supplementary figure B.2). However, neither cell surface markers that are characteristic of hMSCs nor the differentiation potential of the cells after culture was examined. Further investigation of these factors could further illuminate whether the encapsulated hMSCs are undergoing a differentiation response or are expressing transient modifications of gene expression patterns without terminal differention. It should be noted that even if terminal differentiation is not achieved, the production of ligament/tendon ECM proteins as was seen in enzymatically-degradable hydrogels may be sufficient for tissue engineering applications that seek to replace ligament/tendon ECM.

The differences in the responses between hMSCs and hACL fibroblasts to the enzymatically-cleavable biomaterial carrier suggest that further work is required to produce hMSCs with a ligament fibroblast phenotype. Some of the differences seen between cells types were the generally higher production of MMPs (Fig, 4.7) and higher gene expression levels of collagen I, collagen III, and tenascin-C (Fig. 4.9) in hACL fibroblasts compared to hMSCs. hACL fibroblasts also seemed to demonstrate changes in cellular perimeter in enzymatically-cleavable biomaterial environments (Fig. 4.6) that were not seen with hMSCs (Fig. 4.5). The changes in cell perimeter seen with hACL fibroblasts agree with previous studies showing morphological changes in human foreskin fibroblasts when they were cultured in enzymatically-cleavable hydrogels.[201,202]

However, hMSCs have also been reported to demonstrate spreading in enzymatically-cleavable hydrogels,[203] in contrast to the lack of morphological changes seen with hMSCs in this study. This discrepancy may be related to differences in the biomaterial systems employed including variations between the enzymatically-cleavable sequences used, as sequence differences can affect the degradation kinetics.[204,205]

It is possible that the changes in cell perimeter that were seen in this study with hACL fibroblasts may be related to cell clustering, as previous studies have provided evidence that degradation of the biomaterial environment can lead to cell clustering.[197,206] This would also explain why there were fewer significant differences in hACL fibroblast area and circularity compared to perimeter. Cells in close proximity, similar to what was seen in these hydrogels, can mask changes in circularity, area, and perimeter and thus the analysis used may not show all of the differences that existed between sample types. A single cell spreading and spread cells in close proximity can create offsetting effects in area and circularity readings, compared to a round cell. Perimeter readings would not be expected to have such offsetting effects. Therefore it is expected that measurements of cell perimeter most accurately reflect differences seen in cell morphology/clustering in this system.

Another difference seen between cell types was the apparent decrease in cell number of hACL fibroblasts over time and in 100% enzymatically-cleavable hydrogels compared to 0% enzymatically-cleavable samples, while hMSCs maintained a steady cell number in all sample types (Fig. 4.7). The prevalence of green staining of hACL fibroblasts at all time points, indicating live cells, suggests that changes in cell number are not due to cell death. Alternate explanations include the possibility that hACL

fibroblasts did not adhere to the hydrogels as well as hMSCs and thus a non-adherent population was lost from the hydrogel or that the hACL fibroblasts had a greater propensity to migrate out of the hydrogels than hMSCs. Further, study is needed to examine these possibilities.

Perhaps the most interesting distinction between the hMSCs and hACL fibroblasts was the difference in gene expression responses in different biomaterial environments (Fig. 4.10). While some upregulation of collagen I, collagen III, and tenascin-C was seen with hMSCs in enzymatically-cleavable hydrogels, an opposite trend was seen in hACL fibroblasts with upregulation seen in non-cleavable hydrogels. This data suggests that a biomaterial environment that facilitates stem cell differentiation may be different from the biomaterial environment needed for a terminally differentiated cell. Sophisticated biomaterial carriers that can respond to differentiation of encapsulated cells may be needed to adapt to the changing needs of differentiating cells. Alternately, stem cells differentiated in an enzymatically degradable biomaterial, could be harvested from the hydrogel by digesting it in collagenase. Terminally differentiated cells isolated from their biomaterial carrier could then be encapsulated in a new biomaterial environment that is more conducive to the desired function. In this way, the biomaterial system employed in this study could serve as a means to provide different biomaterial environments to encapsulated stem cells as they differentiate.

Further study with this biomaterial system could include applications that involve harvesting encapsulated cells or the ECM they produce through degradation of the hydrogel in collagenase. The release of cells and ECM molecules facilitates analysis that is not possible while they are encapsulated in the biomaterial carrier, such as

measurement of surface marker expression. It should be noted that harvesting of collagenous ECM components may require modifications of this hydrogel system that make it susceptible to enzymes that do not target collagens.

## 4.5 Conclusions

In addition to providing evidence of promotion of gene regulation and protein production in hMSCs that is indicative of an hACL fibroblast phenotype, the studies described in this chapter provide insight into behavioral differences between hMSCs and hACL fibroblasts in response to the enzymatically-cleavable biomaterial environments used in this study. These studies also highlight the capacity of this model system to adapt to the changing biomaterial requirements needed for stem cell differentiation compared to culture of terminally differentiated cells. Additional work is essential to further elucidate biomaterial factors that stimulate a gene expression and protein production pattern in hMSCs that is characteristic of an hACL fibroblast phenotype. Further study investigating the biomaterial conditions needed for culture at different stages of differentiation is also needed.

Previous studies conducted in our laboratory with non-degradable gels demonstrated hMSC differentiation toward a ligament/tendon fibroblast phenotype under tensile strain.[125] Therefore, the next chapter describes work that uses this well-defined carrier material to better understand how changes to the cell-biomaterial environment that occur over time affect cellular responsiveness to tensile loading, thereby providing basic parameters for next-generation biomaterial/bioreactor combinations to be used in production of tissue-engineered ligament grafts.

# CHAPTER 5

# EFFECTS OF PRECULTURE ON THE EXPRESSION OF KEY LIGAMENT FIBROBLAST ECM GENES IN MSCS UNDER SHORT-TERM TENSILE STRAIN

## 5.1 Introduction

As the predominant cell type in ligament/tendon tissue, fibroblasts are often used for ligament/tendon tissue engineering applications.[4] Unfortunately, the lack of a suitable source of autologous ligament/tendon fibroblasts has limited their usefulness.[10] As a result, tissue engineering techniques for ligament/tendon engineering often use tensile strain to differentiate MSCs toward a ligament fibroblast phenotype.[11,125] Gene upregulation and production of major ligament/tendon matrix components such as collagen I, collagen III, and tenascin-C are often examined as signs of ligament fibroblast phenotypic differentiation.[11,193,195] Previous studies implicating tensile forces in the differentiation of MSCs toward a ligament/tendon fibroblast phenotype have required 14 days or more before upregulation of relevant genes was detected compared to static controls.[11,125] In this time frame upregulation of relevant ligament/tendon ECM gene expression has been seen compared to early time points in static controls.[125] Changes to the extracellular environment of the cells have also occurred due to the production of ligament/tendon ECM proteins over time.[11,100,125] Since gene expression and the ECM environment can change over multiple weeks of culture time, it is not certain whether the mechanical responses measured in MSCs are due to a) a multi-week stimulation response or b) an interaction between shorter amounts of tensile culture and alterations in the cell-

biomaterial system. If the gene expression regulation that arises from multiple weeks of tensile culture is due to interactions with the changing cell-biomaterial system, a period of static preculture combined with short-term loading may be sufficient to achieve responses created with longer-term tensile loading. Further elucidation of these possible interactions could provide insight into how the timing of tensile stimulation can affect MSC differentiation toward a ligament/tendon phenotype. This knowledge could facilitate improvements in future loading protocols for hMSC differentiation, thus aiding in the development of methods to provide an alternate source of autologous ligament/tendon fibroblasts or, eventually, tissue-engineered ligament/tendon grafts.

Therefore, this study was designed to determine whether the response of MSCs to short-term tensile stimulation, as compared to static culture, would be affected by a preculture period. Short-term tensile strains (24 hours) were examined in order to minimize the effect of further alterations in the cell-biomaterial environment such as matrix protein production, gene expression regulation, or biomaterial degradation that may occur during the tensile stimulation period. In particular, in these studies, hMSCs were encapsulated in 100% protease-cleavable hydrogels and precultured for 21 days or used without a preculture period. Non-precultured samples provided a baseline cell-biomaterial environment. Constructs undergoing preculture provided an extracellular environment that was expected to be different from non-preculture baseline samples since changes in the ECM environment over 21 days had been seen in similar constructs cultured statically (Fig. 4.13). Constructs undergoing preculture as well as samples without preculture were exposed to a repeating cyclic tensile strain regimen that was previously used with these hMSCs (Chapter 3) to promote upregulation of

ligament/tendon ECM (collagen I, collagen III, tenascin-C) gene expression.[125] This strain regimen consisted of 10% strain, 1Hz, and 3 hours without stimulation followed by 3 hours of cyclic tensile stimulation. Constructs cultured statically at 0% strain were used as controls. After 24 hours of strain, differences in cell number and gene expression (collagen I, collagen III, tenascin-C) between non-precultured and precultured samples were examined. Baseline values for each of these metrics were also measured before the initiation of mechanical stimuli. Specifically, this study sought to determine whether hMSCs precultured in 100% enzymatically-cleavable hydrogels would demonstrate an upregulation of ligament/tendon fibroblast ECM genes (collagen I, collagen III, tenascin-C) in tensile constructs compared to statically cultured constructs. The particular hypothesis of this study was that preculture in these hydrogels would correlate with upregulation of gene expression of ligament/tendon fibroblast ECM genes (collagen I, collagen III, tenascin-C) in hMSCs in response to short-term tensile strain.

## 5.2 Materials and Methods

### 5.2.1 Peptide Conjugation

To allow presentation of RGD ligands to encapsulated cells, the GRGDS adhesion peptide was conjugated to a 3,400 Da MW acrylated-PEG-succinimidyl valerate spacer according to previous protocols.[108] Briefly, conjugation was achieved by adding the A-PEG-SVA to the GRGDS adhesion peptide dissolved in a sodium bicarbonate buffer solution under gentle stirring over a three hour period. The mixed solution was transferred into 1,000 Da molecular weight cut-off dialysis tubing and dialyzed for two days to remove unreacted peptides. Conjugated peptide was then lyophilized and stored

at -20°C. The same batch of acrylated GRGDS peptide was used in all of these studies. Further details regarding this conjugation are found in appendix A.4.

To provide cellular mediated degradation of the biomaterial environment the enzymatically-degradable peptide, GGGLGPAGGK, was conjugated on both ends to 3,400 Da MW A-PEG-SVA using the peptide conjugation protocol mention above. Briefly, conjugation was achieved by adding A-PEG-SVA to the GGGLGPAGGK peptide dissolved in a sodium bicarbonate buffer solution under gentle stirring over a three hour period. The mixed solution was transferred into 3,500-5,000 Da molecular weight cut-off dialysis tubing and dialyzed for two days to remove unreacted peptides. Conjugated GGGLGPAGGK peptide (LGPA) was then lyophilized and stored at -20°C. All batches of LGPA were subjected to fold swelling measurements to screen out poorly conjugated batches. The exact same set of LGPA batches were used when possible and at least 4 batches of LGPA were used in each group of hydrogels in order to minimize the effects of batch to batch variability. Further details regarding this synthesis are found in appendix A.3.

### 5.2.2 Construct Fabrication

The tensile constructs are fabricated by injecting polymer solutions into a mold between two polyethylene end blocks (75-110 μm pore size). The polymer solution invades the porous end blocks and forms an integrated tensile construct hydrogel after cross-linking. The final tensile construct (Fig. 3.2A, inset) contains a cell-hydrogel section (12.5 mm x 9.5 mm, 1.6 mm) flanked by the porous end blocks. One end block is placed over a stationary peg in the culture wells and the other end block interfaces with the tensile rake of this bioreactor (Fig. 3.2B). The high stiffness of the end blocks

compared to the hydrogel allows a uniform strain field to be imparted across the sample during tensile culture.[169,174]

### 5.2.3 Cell Culture

hMSCs obtained at passage 0 were seeded into tissue culture flasks at 3,333 cells/cm$^2$ and grown in mesenchymal stem cell growth medium. Cells were passaged after reaching approximately 80% confluency using a one to three expansion. At passage 5 (p5), cells were cryopreserved for future use. Culture medium was changed every 2-3 days. hMSCs from four unique donors were pooled in equal numbers at p5 and cultured in Dulbecco's modified Eagle's medium with 4.5 g/L glucose and sodium pyruvate, 10% FBS, 1% non-essential amino acids, and 1% antibiotic/antimycotic. Four different donors (Table 3.1) were used in order to minimize effects that could be due to variation between donors. Medium was changed every 2-3 days (Note: FBS was pre-screened for the highest promotion of cell growth and collagen I, collagen III, and tenascin-C gene expression, with cell growth being the primary criteria). Ascorbic acid (50 µg/ml) was added during feedings to the medium composition described above after cells were encapsulated into constructs.

### 5.2.4 Cell Encapsulation in Constructs

For experiments involving encapsulated hMSCs, constructs were fabricated using low water content (75 wt% PBS) 100% LGPA hydrogels (see Table 4.1) with acrylated-PEG GRGDS adhesion peptide at a concentration of (1 µmol GRGDS)/(g of hydrogel after swelling). After the solutions were filter sterilized using a 0.2 µm filter, hMSCs were added at a concentration of 10 x 10$^6$ cells/ml and the hydrogel solution was cross-linked for 15 min using the same techniques described in section 3.2.4. After fabrication,

the tensile constructs were placed into 6-well plates in culture medium and allowed to swell overnight. After swelling, the time was designated as day 0.

### 5.2.5 Tensile Culture

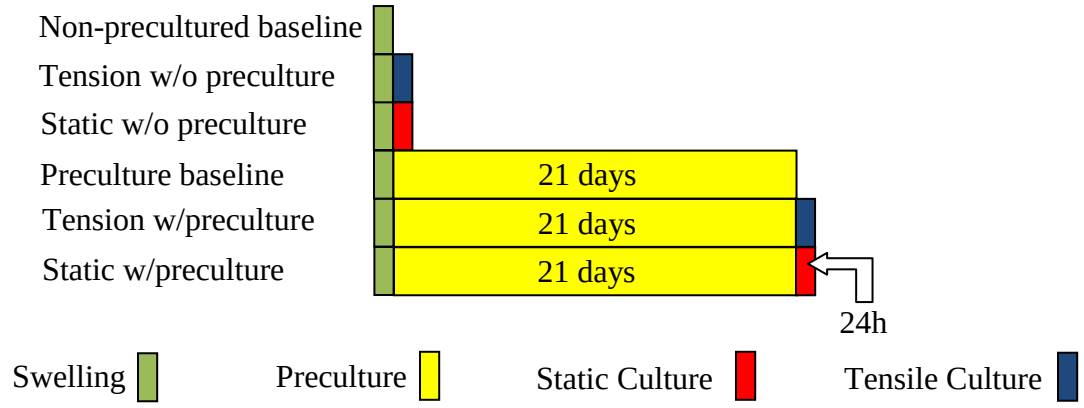


Sample Analysis (Before or After Mechanical Loading)
Cell Number: PicoGreen (n≥5)
Gene Expression: Real time RT-PCR (n≥8)
Protein Production (d0 & d21): IHC (n=2)

**Figure 5.1. Schematic of Tensile Culture Studies**

After equilibrium swelling was achieved, non-precultured constructs were used to produce a baseline cell-biomaterial environment (non-precultured baseline). Constructs precultured for 21 days were used to produce an altered cell-biomaterial environment (precultured baseline). After the preculture period, constructs were loaded into the tensile culture bioreactor for 24 hours of cyclic tensile loading (Fig. 5.1). The cyclic loading regimen for these studies was chosen based on parameters previously used with this system to promote collagen expression and production.[125,171,172] Specifically, constructs were maintained under a sinusoidal cyclic tensile strain regimen of 3 hours at 0% strain followed by 3 hours of 10% strain (5% offset, 5% amplitude) at 1 Hz. This regimen was

maintained for 24 hours. Control hydrogels were loaded into a similar culture system, but held at 0% strain (static culture). Culture medium was replaced every 2-3 days.

### 5.2.6 Histology

Two groups of constructs were analyzed; non-precultured baseline constructs and precultured baseline constructs. This analysis was used to confirm the absence or presence of relevant ECM proteins before mechanical stimulation. After the respective cultures, end blocks were removed and the hydrogel portion of the constructs was cut in half using a scalpel. One half was washed in PBS and the other half was set aside for other assays. After washing in PBS, the hydrogels were fixed in formalin overnight. Samples were put into PBS for 20 minutes to wash out the formalin, then manually dehydrated using the following schedule. 70% dehydration alcohol overnight, 80% dehydration alcohol overnight, 90% dehydration alcohol overnight, 95% dehydration alcohol overnight, 100% dehydration alcohol overnight. After dehydration samples were held under a -20 mmHg vacuum in paraffin for 4 hours to enhance penetration and embedded. Paraffin-embedded hydrogels were cut into 10 μm sections and placed on glass slides. IHC was performed on these sections for collagen I, collagen III, and tenascin-C (n=2). Primary antibody binding to proteins of interest was accomplished using monoclonal IgG mouse anti-human antibodies. Secondary antibody binding to primary antibodies was accomplished using polyclonal goat anti-mouse IgG antibodies conjugated to biotin. Further amplification of signal was achieved using the Vectastain elite ABC peroxidase kit. This amplification is achieved through an avidin conjugated horseradish peroxidase which binds to the biotinylated secondary antibody. Sections

were exposed to DAB chromogen for 5 minutes to elicit a color change. Negative controls included samples immunostained with the primary antibody omitted.

### 5.2.7 Cell Number

Six groups of constructs were analyzed; non-precultured baseline constructs, precultured baseline constructs, non-precultured with cyclic tensile stimulation, precultured with cyclic tensile stimulation, non-precultured with static stimulation, and precultured with static stimulation. After the respective cultures, end blocks were removed and the hydrogel portion of the constructs was cut in half using a scalpel. One half was washed in PBS and the other half was set aside for other assays. After washing, the wet weight of the hydrogel was recorded. Hydrogel portions were mechanically disrupted using a pellet grinder (VWR) and suspended in 750 µl of distilled, deionized water ($ddH_2O$). To disrupt cells and release DNA into solution, samples were subjected to three cycles of freezing at -80°C for 1h, thawing at room temperature for 30 min., and sonicating for 30 min. DNA content, which can be correlated to cell number, was determined ($n \geq 5$) by assaying the resulting supernatant via PicoGreen (Invitrogen) with lambda DNA used for standards (included in kit). The PicoGreen assay uses the Hoescht 33258 fluorophore which binds to double stranded DNA. The fluorescent signal, which is proportional to the amount of double stranded DNA, was measured and compared to standards. The results were normalized to the weight of the hydrogel after culture to account for potential differences in the mass of individual hydrogels. Further details regarding the lab protocol used for this assay are found in appendix A.7.

### 5.2.8 Gene Expression

Six groups of constructs were analyzed; non-precultured baseline constructs, precultured baseline constructs, non-precultured with cyclic tensile stimulation, precultured with cyclic tensile stimulation, non-precultured with static stimulation, and precultured with static stimulation. After the respective cultures, end blocks were removed and the hydrogel portion of the constructs was cut in half using a scalpel. One half was washed in PBS and the other half was set aside for other assays. After washing with PBS, the hydrogels were mechanically disrupted using a pellet grinder. RNA was isolated from the hydrogels with the QiaShredder column (Qiagen). Purification of RNA was achieved using the RNeasy mini kit (Qiagen). cDNA was synthesized with Superscript III RT (Invitrogen) in the presence of a nucleotide mix (Promega, Madison, WI).

Amplification of cDNA through real time RT-PCR was performed using custom designed primers and SYBR Green. The process was conducted and recorded using the StepOnePlus$^{TM}$ Real-Time PCR System. A cycle time (Ct) value for a given gene was determined based on when the amplification curve crossed a threshold value. The threshold was set at the same value for all runs. For statistical analysis, dCt values (cycle time for glyceraldehyde phosphate dehydrogenase (GAPDH) subtracted from the cycle time for the given gene) were used For statistical analysis, the number of transcripts for a given gene normalized to GAPDH was used ($n \geq 8$). Data is represented normalized to GAPDH then to preculture for the given day using the $\Delta\Delta$Ct method. Genes examined included collagen I, collagen III, and tenascin-C as markers for ligament/tendon fibroblast gene expression.[11] Primers were designed as described in previous chapters

(Sections 3.2.10 and 4.2.9). Sequences for the forward and reverse primers used are listed in Table 3.2. Further details regarding the lab protocol used for this assay are found in appendix A.10.

### 5.2.9 Statistics

Results are reported as mean ± standard deviation. A Box-Cox transformation for normality was used on dCt values of gene expression data. Data were analyzed using a two-way ANOVA. If both factors were significant, but interactions were not significant, a Tukey's post hoc test with significance set at $p \leq 0.05$ was used for pairwise comparisons. If only one factor was significant and interactions were not significant one-way ANOVAs were run on the significant factor with each level of the non-significant factor fixed. A Tukey's post hoc test with significance set at $p \leq 0.05$ was used for pairwise comparisons. If interactions were significant, one way ANOVAs were run on the first (or second) factor with each level of the second (or first) factor fixed. A Tukey's post hoc test with significance set at $p \leq 0.05$ was used for pairwise comparisons. For the cell number study and gene expression analysis, the factors were day and mechanical/preculture condition. Statistical analysis was carried out using Systat.

## 5.3 Results

### 5.3.1 Histology

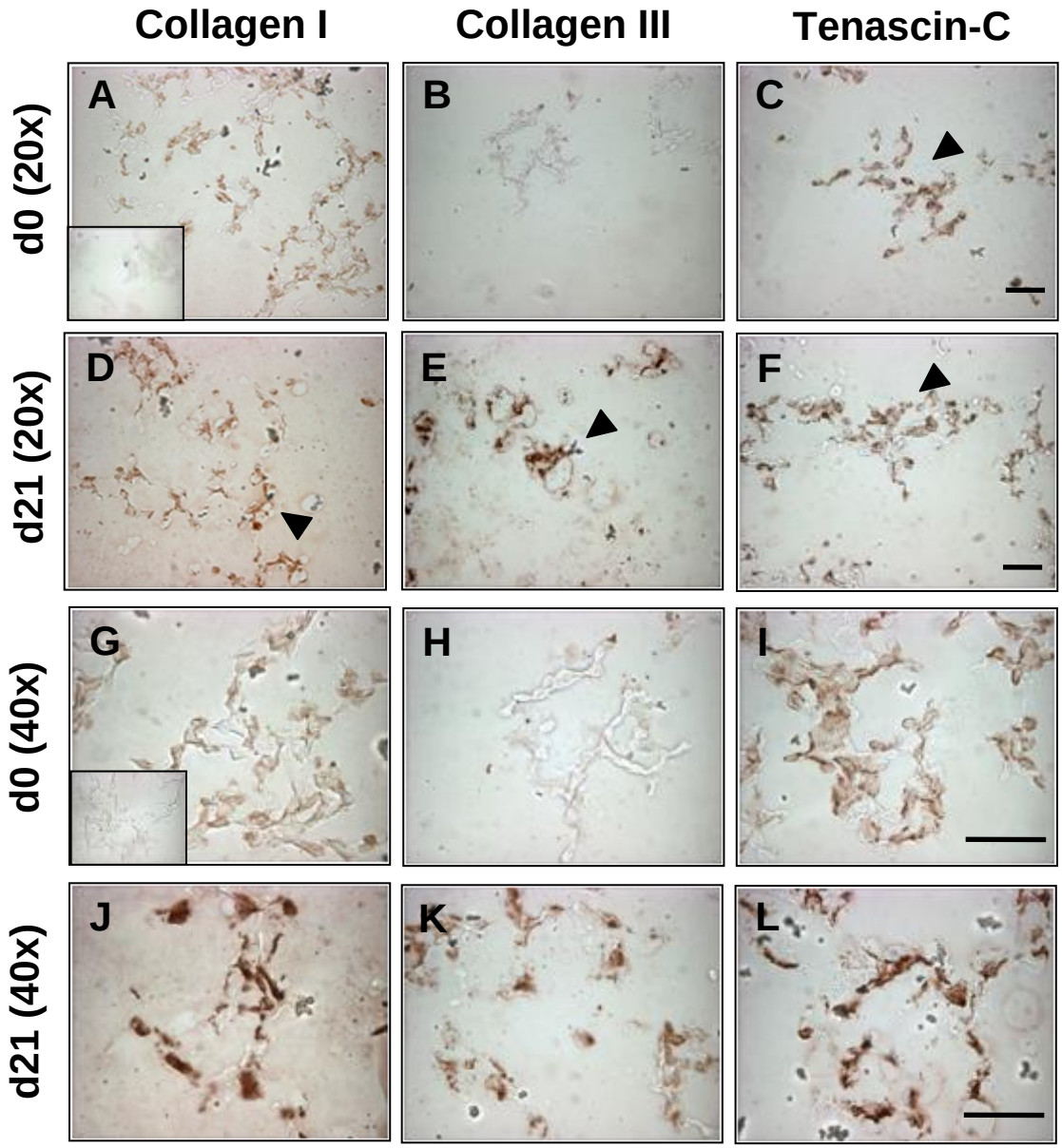


**Figure 5.2. Representative IHC images for collagen I, collagen III, or tenascin-C after no preculture (0d) or with preculture (21d) in 100% enzymatically-degradable hydrogels with hMSCs. Top two rows are at 20x. Bottom two rows are at 40x. Brown color indicates staining for the particular protein. Arrow indicates pericellular staining. Inset of images are control sections where primary antibodies were not used. Scale bars = 20 μm.**

IHC staining indicated the presence of collagen I pericellularly in both non-precultured and precultured constructs (Fig. 5.2A, D, G, J). While, the level of staining for collagen I varied within sections, samples undergoing preculture appeared to stain more strongly for collagen I that non-precultured samples. IHC staining indicated the presence of collagen III pericellularly after preculture (Fig. 5.2E, K), although the level of staining varied within sections. No collagen III was detected without preculture (Fig. 5.2B, H). IHC staining indicated the presence of tenascin-C pericellularly in both non-precultured and precultured constructs (Fig. 5.2C, F, I, L). There did not appear to be a difference in the level of staining for tenascin-C between non-precultured and precultured constructs, although, like the other proteins, the level of staining for tenascin-C varied within sections. Cells in IHC sections generally showed a spread morphology. No staining was detected in negative control sections with the primary antibody omitted (Fig. 5.2 insets), suggesting that neither the secondary antibody nor the Vectastain elite ABC peroxidase kit exhibited significant non-specific binding and that there was minimal endogenous staining from the contrast agent. However it should be noted that no isotype control was used so the possibility of non-specific binding of the primary antibody can not be eliminated.

### 5.3.2 Cell Number

No differences in DNA content/sample weight (an indicator of cell number) were seen between static constructs, tensile constructs, and baseline constructs under either preculture condition (Fig. 5.3). However, a significant decrease in DNA content/sample weight was seen on day 21 for all culture conditions.

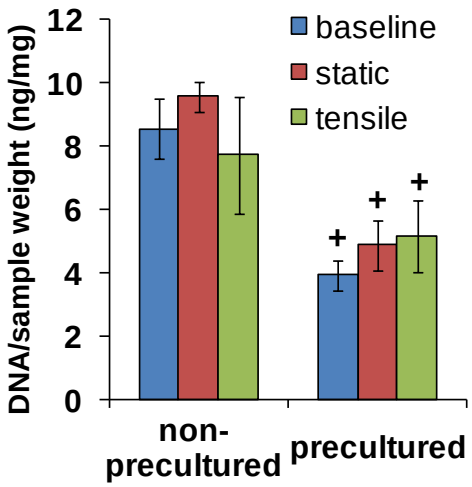


**Figure 5.3. DNA content of hMSCs normalized to sample weight of 100% enzymatically-cleavable hydrogels after preculture or 24h of static or tensile stimulation (n≥5 ±SD). p<0.05 compared to d0 hydrogels(+).**

### 5.3.3 Gene Expression

Collagen I, collagen III, and tenascin-C gene expression was upregulated (Fig. 5.4) in hMSCs in all precultured hydrogels compared to non-precultured samples. Collagen I gene expression levels were higher in static hydrogels after preculture compared to baseline samples while collagen I gene expression levels were lower in static and cyclic hydrogels without preculture compared to baseline samples. Collagen III gene expression levels were significantly different in static hydrogels compared to baseline samples both before and after preculture. Collagen III gene expression was also significantly different before preculture in static hydrogels compared to cyclic samples. Tenascin-C gene expression levels in static samples before preculture were significantly different compared to both baseline and tensile gene expression levels. Tenascin-C gene expression was also significantly different after preculture in static and cyclic hydrogels compared to baseline samples.

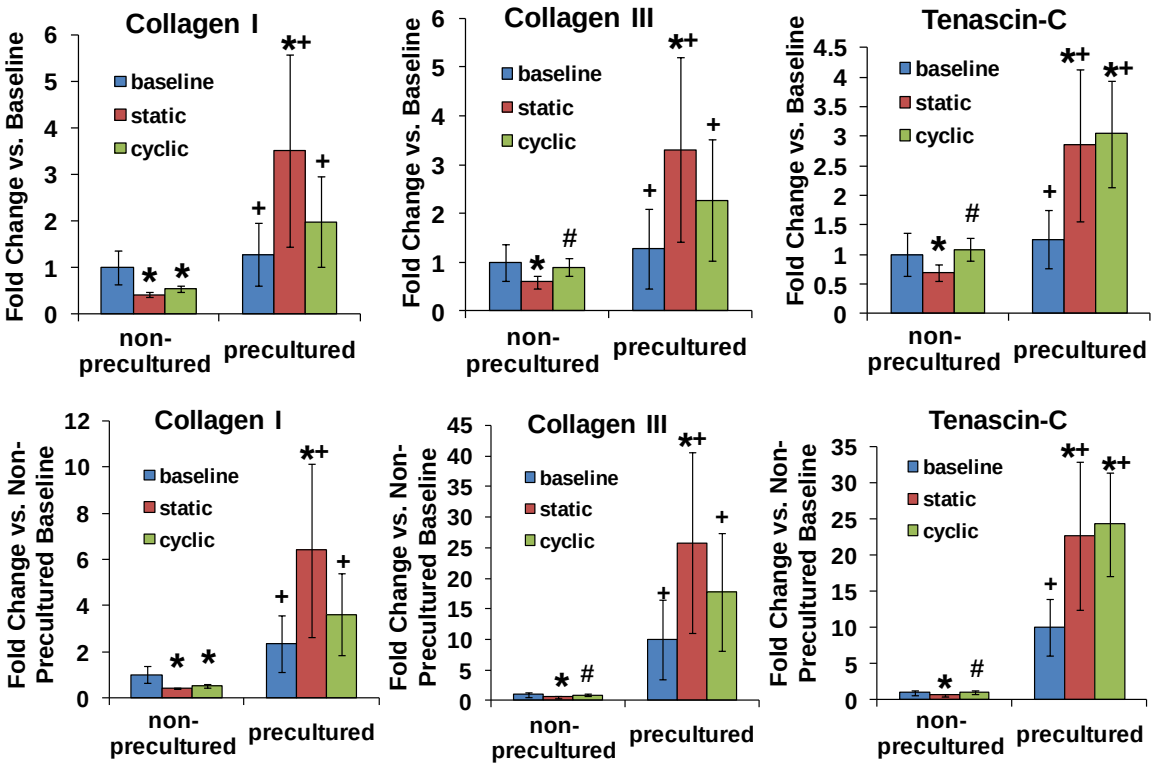


**Figure 5.4. Collagen I, collagen III, and tenascin-C gene expression in hMSCs in 100% enzymatically-degradable hydrogels before mechanical stimulation (baseline) or after 24h of static or tensile culture at the given time point (n≥8 ±SD). Top row: gene expression normalized to baseline of that group (non-precultured or precultured). Bottom row: gene expression normalized to baseline values in the non-precultured group. $p<0.05$ compared to non-precultured hydrogels(+). $p<0.05$ compared to baseline hydrogels(*). $p<0.05$ compared to static hydrogels(#).**

## 5.4 Discussion

The enzymatically-degradable hydrogel system employed in this study provided a model system for elucidation of the effect of preculture on cellular responses to tensile stimuli. The preculture period was successful in producing changes in the baseline ECM environment (Fig. 5.2) and the baseline gene expression response (Fig. 5.4) compared to non-precultured samples. Interestingly, preculture was insufficient to produce upregulation of the examined genes after 24 hours of tensile culture compared to static controls, despite the changes in the cell-biomaterial environment. This is in agreement

with previous studies without preculture periods that have similarly shown no change in collagen I or collagen III gene expression or protein production after 1d of cyclic tensile strain.[179,207]

While no difference was seen in gene expression of precultured samples in this study after 24 hours of tensile stimulation compared to static culture, MSC gene expression and protein production has been shown to be responsive to short-term cyclic loading in other studies using this tensile culture system. Bovine MSCs under tensile strain after a preculture period have demonstrated upregulation of collagen II, aggrecan, sox-9, and collagen I gene expression after 3 hours of stimulation along with proteoglycan synthesis after 24 hours of stimulation.[208] The upregulation of gene expression with this study, in contrast with results presented in this chapter, may be related to the different cell types, biomaterial environments, preculture periods, and genes examined.

Other studies without preculture have shown modest collagen I and collagen III protein production and upregulation of collagen I, collagen III, and tenascin-C gene expression in hMSCs after 1 day of cyclic tensile strain.[209,210] However, it should be noted that these studies strained cells in a 2D environment which may explain the differences in cell responses, as ligament/tendon gene expression can have diverse regulation patterns in 2D compared to 3D environments.[179] The ECM environment, especially collagen, has been found to play an important role in the gene expression of mesenchymal cell types[211] and their differentiation responses.[212] The gene expression of MSCs under cyclic tensile strain has also been affected depending on whether the cells were cultured on a collagen substrate or an elastin substrate[209] which suggests that

changes in the ECM environment can influence cellular responses to mechanical loading. A well-defined biomaterial environment, such as the one employed in this study, could facilitate the controlled studies required to further elucidate the interaction of the diverse effects of differences in biomaterial biochemistry and substrate material properties on cellular differentiation in 3D.

Similarly, further studies are required to determine whether a period of tensile stimulation that is longer than 24 hours, but shorter than the multi-week stimulation normally required for upregulation, can facilitate upregulation of relevant gene expression after a static preculture period in 3D constructs such as those used in these studies. These studies could provide further insight into possible interactions between changes in the extracellular environment and tensile stimulation. However, conclusions drawn from such studies may need to be limited as there are a number of potential changes in the cell-biomaterial environment that can occur during preculture including differentiation of cells, changes in gene expression regulation, degradation of the biomaterial carrier, and changes in cell shape over time. These factors provide a complex network of stimuli that have the potential to influence cellular responses in diverse ways. As a result, if an interaction between preculture and mechanical stimulation is discovered, further characterization of the changes that occur in the extracellular environment during preculture may be required to understand the mechanism behind this interaction.

When developing outcome measures for future studies, scleraxis may be an important gene to consider evaluating. Scleraxis is a transcription factor involved in ligament development that has been upregulated in hMSCs after 1d of cyclic strain while collagen I and collagen III upregulation occurred at later time points.[179] The early

upregulation of scleraxis compared to other relevant ligament/tendon genes suggests that it may respond to differentiation stimuli before other markers of a ligament/tendon fibroblast phenotype and thus may be an important gene to examine in future short-term loading experiments.

The production of collagen III seen (Fig. 5.2) was a confirmation of findings in previous studies (Fig. 4.11) that showed the presence of collagen III on day 21 in 100% enzymatically-cleavable hydrogels, but no staining for collagen III by day 1. In contrast to collagen III, tenascin-C showed similar matrix production at both time points in this study. Cell spreading seen in IHC sections contrasted with the generally round morphology seen in previous studies (Fig. 3.5 and 4.11). The contrast in cell shape seen in this work compared to previous work may be related to a) the use of enzymatically-degradable hydrogels in this study facilitating the creation of space for cells to spread (compared to chapter 3) and b) the use of larger hydrogel constructs (compared to chapter 4) which may have reduced the kinetics of diffusion of cell-produced MMPs or other enzymes out of the gel and therefore facilitated localized degradation. More work is needed to rigorously examine these possibilities.

That lack of changes in DNA content (Fig. 5.3) in response to culture conditions confirm that the short-term strain regimens used in this study do not affect cell number, in agreement with previous results.[133,207] However, a decrease in cell number was seen due to culture time. The high viability seen at day 21 in similar constructs (Fig. 3.3 and 4.7) suggests that the decrease in cell number is not due to cell death. An alternative explanation is that cells are migrating from the hydrogels (either the surface or interior) and are preferentially adhering to the surrounding tissue culture wells by day 21. The

presence of adherent cells in tissue culture wells containing hydrogel samples has been seen at earlier time points, but not at later time points (visual observation) which provides support of this possibility. The absence of changes in cell number in similar hydrogels over time (Fig. 4.7) may be due to the relative size differences between the constructs. Smaller hydrogels (such as samples in chapter 4) will have proportionately greater surface areas than larger samples. The lower height of small constructs along with the relatively larger surface area may provide greater opportunity for cells to leave the surface of small hydrogels and thus facilitate a faster migration of cells to the tissue culture surfaces. However, the possible migration of cells the hydrogels was not measured so the reason for the decreased cell number seen in larger constructs can not be confirmed.

## 5.5 Conclusions

This study provides one of the first examinations of responses to tensile stimuli in relation to preculture for ligament/tendon tissue engineering applications. Evidence was provided suggesting that a 21 day preculture period was not sufficient to promote upregulation of ligament/tendon matrix protein gene expression in hMSCs after short-term, 24 hour tensile stimulation. Tensile stimulation periods longer than 24 hours appear to be required for ligament/tendon tissue engineering strategies that seek to promote upregulation of relevant ligament/tendon fibroblast gene expression in hMSCs. Questions still remain as to whether preculture can promote ligament/tendon fibroblast phenotypic upregulation in hMSCs in conjunction with longer periods of tensile strain. If tensile strain does interact with preculture to promote changes in gene expression,

additional work will be required to further characterize changes that occur during the preculture period and investigate the possible roles of those factors.

# CHAPTER 6

# CONCLUSIONS AND RECOMMENDATIONS

## 6.1 Summary

Ligament/tendon tissue engineering has the potential to provide therapies that overcome the limitations of incomplete natural healing responses and inadequate graft materials. Finding a suitable cell type and biomaterial environment for current tissue engineering strategies are some of the challenges that still remain to be resolved. While ligament/tendon fibroblasts are an obvious choice of cell type for these applications, difficulties associated with the availability of cell sources have limited their utility. MSCs are seen as a viable alternative since they can be harvested through routine medical procedures and can be differentiated toward a ligament/tendon fibroblast lineage. Tensile stimulation is one common method employed to differentiate MSCs toward a ligament/tendon fibroblast phenotype. However, further study is needed to create a biomaterial/mechanical environment for ligament/tendon fibroblastic differentiation. The overall goal of this dissertation was to improve the understanding of the role that biomechanical stimulation and the biomaterial environment play, both independently and combined, on hMSC differentiation toward a ligament/tendon fibroblast phenotype. Specifically, the effects of cyclic tensile stimuli were studied in a biomaterial environment that provided controlled presentation of biological moieties. The influence of an enzymatically-degradable biomaterial environment on hMSC differentiation was investigated by creating hydrogels containing enzymatically-cleavable moieties. The role that preculture may play in tensile responses of hMSCs was also explored. Together, these studies provided insights into the contributions of the biomaterial environment and

the biomechanical environment to hMSC differentiation toward a ligament/tendon fibroblast phenotype.

The studies presented in chapter 3 investigated the effects of cyclic tensile loading on hMSCs in an OPF-based biomaterial. The OPF biomaterial provided a hydrogel environment with well controlled presentation of bioactive moieties. In response to cyclic tensile strain, upregulation in gene expression of major ligament/tendon ECM proteins was seen. Specifically, upregulation of collagen III and tenascin-C gene expression was observed by day 21 and upregulation of collagen I was detected by day 7. In addition, the production of collagen I and tenascin-C matrix proteins were detected with greater staining for tenascin-C seen in cyclically strained constructs on day 21. These results indicated that ligament fibroblast phenotypic changes were induced in hMSCs due to cyclic tensile strain. Interestingly, upregulation of these genes was also seen in static constructs over time, which suggested that medium conditions and the biomaterial environment could promote some degree of phenotypic change even in the absence of tensile strain. No staining for collagen III was detected in either cyclically strained constructs or static samples, which suggested that additional cues were needed to facilitate hMSC differentiation. Additional tensile experiments on laminated hydrogel scaffolds provided a proof-of-concept for possible future side-by-side co-culture studies involving tensile stimulation.

The studies in chapter 4 explored the effects of an enzymatically-cleavable biomaterial environment on hMSCs. Enzymatically-cleavable sequences that are believed to be susceptible to MMPs were introduced into the biomaterial system and provided the bioactive motifs needed to facilitate local cleavage of bioactive sequences.

hACL fibroblasts served as controls to provide an estimate of the degree to which hMSCs had achieved a ligament fibroblast phenotype. Upregulation of gene expression levels of collagen I, collagen III, and tenascin-C along with protein production in hydrogels with enzymatically-cleavable motifs suggested that the enzymatically-cleavable biomaterial carriers facilitated the development of a ligament/tendon fibroblast phenotype in hMSCs. However, gene expression in hMSCs did not reach the levels seen in hACL fibroblasts, suggesting that the biomaterial cues were not sufficient to fully differentiate hMSCs over 21 days of culture. Characterization of cell surface markers of hMSCs before and after experimentation may be important for further confirmation of their differentiation state. Perhaps the most interesting finding in chapter 4 was that hMSCs and hACL fibroblasts responded differently to the enzymatically-cleavable hydrogels. hMSCs generally showed upregulation and hACL fibroblasts generally showed downregulation of relevant gene expression in the presence of enzymatically-cleavable peptides compared to non-enzymatically cleavable sequences. This data provided evidence that the biomaterial environment needed for hMSC differentiation may be different from the biomaterial environment needed for culture of hACL fibroblasts.

The studies in chapter 5 examined the effect of a 21 day preculture period on the response of encapsulated hMSCs to short-term tensile strain (24 hours). hMSCs were encapsulated in enzymatically-cleavable hydrogels and either precultured for 21 days or were not precultured. Baseline changes in the extracellular environment that were observed in precultured compared to non-precultured samples included changes in gene expression of collagen I, collagen III, and tenascin-C and differences in ECM proteins produced. Despite these changes in the extracellular environment after preculture, gene

expression levels of hMSCs in hydrogels under 24 hours of cyclic tensile strain remained similar to static constructs. The results of this study suggested that preculture does not influence the response of encapsulated hMSCs to short-term tensile strains. Overall the findings in this dissertation provided a significant elucidation of the roles that biomechanical cues and the extracellular environment play in the promotion of a characteristic ligament/tendon fibroblast gene expression and protein production profile in hMSCs.

## 6.2 Conclusions

In addition to confirming the responsiveness of hMSCs to tensile loading, the studies in this dissertation demonstrated the feasibility of this novel system for examination of cellular differentiation under tensile loading in response to controlled physicochemical changes in the extracellular environment. In chapter 3, the upregulation of collagen I, collagen III, and tenascin-C gene expression in cyclic constructs compared to static samples by day 21 suggested that, under the loading conditions chosen, cyclic strain promoted a ligament/tendon fibroblastic phenotype in hMSCs by 21 days. This was in agreement with previous studies that have employed three-dimensional constructs.[11,100,213] While, an enzymatically-cleavable biomaterial environment also appeared to promote a ligament fibroblast phenotypic response in hMSCs (Fig. 4.9), tensile strain appears to be the more potent stimulus.

Collagen I gene expression generally correlated with pericellular matrix deposition in enzymatically-cleavable hydrogels (Fig. 4.11, 5.2) with enzymatically-cleavable sequences correlating with an apparent increase in the levels of collagen I proteins produced by hMSCs. In cyclically cultured hydrogels little collagen III staining

was observed at day 21, despite upregulation of collagen III expression levels. This lack of collagen III protein production may be related to the non-degradable biomaterial environment used in chapter 3 studies, as work in chapter 4 showed collagen III protein production in statically cultured enzymatically-degradable hydrogels at day 21 even without tensile strain (Fig. 4.11). Similar to the results seen in chapter 3, no collagen III protein production was detected in non-degradable hydrogels or at day 1 for any hydrogel type (Fig. 4.11). Taken together, these results suggest that the biomaterial environment had a significant role in the ability of hMSCs to produce collagen III even in the absence of tensile strain stimuli. Specifically, it appears that a hydrogel system that is responsive to cell-mediated degradation (such as our enzymatically-cleavable hydrogels) can facilitate the production of collagen III ECM. Previous reports demonstrated collagen III production in response to cyclic strains when MSCs were cultured in collagen I gels,[11,100] providing further evidence of the ability of the biomaterial environment to affect collagen III production. These studies provided insights into the importance of both cyclic strain and the biomaterial environment in gene expression and protein production. Since collagen is the largest component of the ligament/tendon ECM,[1,12,15] systems the promote upregulation of collagen gene expression and protein production, similar to the ones used in these studies, may be important for production of tissue engineered ligaments and tendons. Early collagen III production may be especially important for strategies that seek to mimic a natural healing response, as collagen III is initially deposited during normal healing.[33]

Tenascin-C is another important protein to examine in ligament/tendon tissue engineering. This protein is often expressed in organogenesis, but generally disappears

or decreases in prevalence in fully developed organs,[214] although it maintains a high expression at insertion sites of ligaments and tendons to bone.[192] Tenascin-C is generally regarded as an anti-adhesive protein as it prevents the adhesion of cells, including fibroblasts, to fibronectin.[215] However, tenascin-C interacts with different cell types in diverse ways and can actually promote adhesion in some cell types.[214] In this work, tenascin-C generally appeared to be localized pericellularly, similar to developmental expression patterns.[192] Biomaterial and biomechanical environments both appeared to affect tenascin-C production. Cyclic culture increased the production of tenascin-C compared to static controls (Fig. 3.5B and 3.5E). In addition, enzymatically-cleavable hydrogels allowed tenascin-C production by day 21 in static culture, whereas this was not found in non-cleavable hydrogels (Fig. 4.11). Taken together these results suggest that tensile culture and enzymatically-degradable environments both improve the production of tenascin-C by encapsulated hMSCs. Since tenascin-C is mainly present at insertion sites of ligament/tendon,[192] approaches that target tenascin-C expression to well-defined areas of a biomaterial construct may be needed to produce fibrous ligament tissues and their insertion sites. The laminated constructs described in chapter 3 of this dissertation are a hydrogel system that can provide regional differences in biomaterial properties in one unified construct. Thus, these laminated hydrogel biomaterials could provide a valuable system to facilitate production of tissue engineering ligaments/tendons that are well integrated with their insertion sites. Overall, culture methods that encourage upregulation of gene expression and protein production of collagen I, collagen III and tenascin-C, similar to our system, show promise as techniques for tissue engineering of ligaments and tendons.

Chapter 4 investigated the effect of cell-mediated degradation through the use of a biomaterial environment containing enzymatically-cleavable peptides. In addition to promoting changes in gene expression, enzymatically-cleavable hydrogels also seemed to facilitate the production of ECM proteins (Fig. 4.13), in agreement with previous results using synthetic enzymatically-cleavable hydrogels.[197,198] Natural scaffolds made of collagen I possess the enzymatically-cleavable motifs that are used in synthetic enzymatically-cleavable hydrogels so similar patterns of protein production would be expected. While some studies with collagen I scaffolds with hMSCs in static culture have shown collagen III protein production,[100] other studies using collagen I scaffolds with bMSCs have shown minimal collagen III production.[11] Since responses to enzymatically-degradable environments appear to vary with the cell type used, the minimal collagen III production by bMSCs may be related to that specific cell type. The matrix production that has been seen in our system and in other studies is likely related to degradation of the scaffold, as increased degradation of hydrogel biomaterials has been linked to greater ECM production,[101] although other factors could also play a role. Collagen I and collagen III ECM has also been produced by hMSCs in synthetic PLLA scaffolds.[193] While the PLLA scaffolds have limited degradability, void space in the constructs is made available by the knitted pattern which creates a macroporous structure. This void space may facilitate ECM production even in the absence of degradation. Overall, this data suggested that ECM production could be facilitated though the use of enzymatically degradable sequences in the biomaterial carrier.

The data presented in chapter 5 suggested that preculture does not influence the response of encapsulated hMSCs to short-term tensile strains in our hydrogel system.

The presence of preculture (0 days vs. 21 days preculture) did not appear to have an effect on cellular responses to tensile strain as hMSCs in constructs under tensile strain for 24 hours showed similar gene expression levels of collagen I, collagen III, and tenascin-C compared to static samples (Fig. 5.4). While 24 hours of tensile culture was insufficient to produce upregulation of the examined genes, it is possible that a longer period of stimulation could produce upregulation in conjunction with a preculture period. hMSCs generally showed upregulation of collagen I, collagen III, and tenascin-C at day 21 compared to day 1, confirming that static culture alone can produce upregulation of relevant ligament/tendon ECM gene expression over 21 days in this biomaterial system although not at the same levels as tensile strain.

An unexpected finding that arose out of comparisons in chapter 4 between hMSCs and hACL fibroblasts was the difference in gene expression across enzymatically-cleavable biomaterial environments (Fig. 4.9). While some upregulation of collagen I, collagen III, and tenascin-C was seen with hMSCs in enzymatically-cleavable hydrogels, an opposite trend was seen in hACL fibroblasts with upregulation seen in non-cleavable hydrogels. This data suggested that the ideal biomaterial environment for hMSC differentiation toward an hACL fibroblastic phenotype may be different from the biomaterial environment needed to promote matrix production by hACL fibroblasts. Further analysis of the ECM produced by both cell types after culture in these gels will be needed to confirm this. The enzymatically-cleavable hydrogels employed in this dissertation have great potential to take advantage of this information by adapting the biomaterial environment to the changing needs of differentiating cells – i.e. by harvesting

cells from a degraded enzymatically-cleavable hydrogel and re-encapsulating in a new biomaterial environment.

### 6.3 Future Directions

The findings in this dissertation elucidated the roles that biomechanical stimulation and extracellular cues play, both independently and combined, on hMSC differentiation toward a ligament/tendon fibroblast phenotype. Significant study is still required to provide further understanding of how these types of factors interact to affect hMSC differentiation responses.

While preculture did not influence cellular responses to short-term (24 hours) cyclic tensile strains, it remains unclear whether hMSC responses to longer periods of strain may be influenced by preculture. No upregulation of relevant gene expression was seen due to short-term tensile strains, but work in chapter 3 showed that up to 21 days of cyclic tensile strain can be required to promote gene expression responses in hMSCs. Therefore, encapsulated cells may require periods of strain longer than 24 hours to provoke changes in gene expression in response to a preculture period. Similar experiments involving static preculture periods that expose encapsulated hMSCs to longer (~7d-14d) tensile strain periods would provide a significant advancement in the understanding of the impact of the timing and duration of cyclic tension stimulation on hMSCs.

In addition to the cell-produced ECM environment, studies that investigate whether "priming" of hMSC gene expression plays a role in responses to tensile strain could also prove instructive. As shown in chapter 3 and chapter 4, over time encapsulated hMSCs can upregulate collagen I, collagen III, and tenascin-C gene

expression in constructs that are cultured without tensile strain. While this upregulation did not reach the same levels seen with tensile stimulation it did attain statistical significance. Since 21 days of culture were required before cyclic tensile strain promoted changes in collagen III and tenascin-C gene expression, it is possible that early weeks of tensile culture did not produce any effects, but allowed a temporal upregulation of relevant gene expression. Once gene expression reached a sufficient level it may have become more susceptible to tensile strain stimuli and manifested this sensitivity with upregulation of gene expression in response to biomechanical perturbations. Studies that employ various preculture periods to produce different levels of gene expression for relevant genes could elucidate the role of already present gene expression patterns in tensile strain responses. One complicating factor is that different ECM environments would also be produced during this preculture time. The effects of these two influences could be decoupled by culturing cells in enzymatically-degradable hydrogels and harvesting the cells from degraded hydrogels after preculture. In this way, cells whose gene expression profiles were "primed" with different lengths of preculture could be reintroduced into new biomaterial environments without cell-produced ECM proteins. Future studies that create different gene expression patterns and reintroduce the cells into new biomaterial environments exposed to tensile culture would be valuable in elucidating the role that these patterns play on responses to biomechanical perturbations.

While the production of a certain external environment may be needed before hMSCs can respond to tensile stimulation, an alternative hypothesis is that tensile stimulation directly influences cell responses during the entire tensile period, but that phenotypic changes measured in these studies are downstream effects that take weeks to

manifest. It is known that cells respond to mechanical strains through a number of mechanisms including stretch induced ion channels, integrin-dependant signaling, and cytoskeletal tensegrity.[216] Mechanical regulation can also occur through signal transduction pathways such as those mediated by Rho kinase, ERK1/2, and MAP kinase cascades.[217] It is probable that known mechanisms of mechanotransduction are important in the cellular responses seen in these studies. Interference with these signaling mechanisms could potentially block the phenotypic changes that were observed. Disruption of these pathways during the first week of tensile stimulation would be expected to prolong the time needed to manifest phenotypic changes only if tensile strain at the early time periods were an important part of cell responses at later time periods. Gadolinium and streptomycin, cytochalasin and phallotoxin, and Y-27632 are potential agents for that could be used for inhibition of mechanotransduction pathways. These inhibitors block stretch activated ion channels, actin cytoskeletal assembly and disassembly, and Rho kinase activity, resepectively.[216,218] Use of these inhibitors in future studies that disrupt known mechanotransduction pathways at early time points could help to elucidate the necessity of tensile strain in early phases of culture. In addition, these inhibitors could aid in the understanding of the role of mechanotransduction through these specific pathways in hMSC responses to tensile stimulation.

Transcript levels of collagen I, collagen III, and tenascin-C gene expression seen in hMSCs in cyclically strained constructs (chapter 3), reached the same levels measured in hACL fibroblasts in static culture in similar biomaterial environments (chapter 4). Increases in transcript levels were also seen with hMSCs in response to enzymatically-

cleavable biomaterial environments, although they did not reach the levels achieved through tensile stimulation. It is unclear whether these gene expression responses are facilitated by differentiation of hMSCs to a ligament fibroblast cell type or if upregulation is achieved through mechanical stimulation without a differentiation response. Probing of cell surface markers associated with MSCs along with examination of adipogenic, osteogenic, and chodrogenic potential, according to established protocols,[219,220] could help elucidate the level of differentiation of MSCs in response to extracellular cues and biomechanical stimuli. Probing for cell surface markers associated with ligament/tendon fibroblast cells would also be valuable, although further study is required to establish cell surface markers for this cell type. In addition, probing for surface markers associated with non-ligament/tendon fibroblast mesenchymal cell lineages could provide indirect evidence of levels of ligament/tendon fibroblastic differentiation. These studies would be facilitated by the ability to harvest cells after encapsulation in enzymatically-cleavable biomaterials, such as the ones used in this dissertation, by using collagenase to degrade the biomaterial matrix.

Results obtained through the studies in chapter 4 suggested that the optimal biomaterial environment for differentiation of hMSCs may be different from the optimal biomaterial environment for culture of hACL fibroblasts. The enzymatically-degradable hydrogels employed in those studies provide a valuable system that can be used to adapt the biomaterial environment in response to these differences. After differentiation of hMSCs is achieved in an enzymatically-degradable biomaterial environment, the cells can be harvested by degrading the hydrogel in collagenase. The differentiated cells can then be cultured in a new biomaterial environment. Thus, the enzymatically-degradable

hydrogel system may be a useful tool in future studies that adapt the biomaterial environment to the changing needs of encapsulated stem cells as they differentiate.

In addition to applications that involve the harvesting of encapsulated cells, an enzymatically-degradable hydrogel system, similar to the one used in this dissertation, may be a useful tool in studies that harvest ECM proteins produced by encapsulated cells. It should be noted that for harvesting of collagenous ECM environments, such as those produced by MSCs and ligament/tendon fibroblasts, a degradable hydrogel system susceptible to enzymes that don't target collagenous matrix proteins would need to be used. One possible application would involve growing hMSCs in an ECM environment produced by encapsulated ligament/tendon fibroblasts. An ECM microenvironment produced by ligament/tendon fibroblasts has the potential to provide differentiation cues for hMSC induction toward a ligament/tendon fibroblast phenotype. This ECM microenvironment could be produced by culturing the ligament/tendon fibroblasts in enzymatically-degradable hydrogels. After production of relevant proteins was accomplished, the ECM could be harvested by degrading the hydrogels, thus releasing the encapsulated proteins. hMSCs would then be encapsulated in new hydrogels with the harvested proteins. Thus, the enzymatically-degradable hydrogel system may be a valuable tool in future studies that seek to explore hMSC differentiation through exposure to a ligament/tendon fibroblast-produced ECM environment.

The biomaterial/biomechanical system employed in this dissertation provides a versatile scaffold-bioreactor system for the study of the effects of the local ECM environment and mechanical loading on cellular differentiation. The ability to incorporate specific ECM moieties makes this an attractive system for controlled studies

to tease out the independent effects of various key ECM components in cellular responses to tensile strain. Enzymatically-degradable peptides are useful tools for a variety of applications and can be employed to create a biomaterial environment that can be targeted for cell-mediated degradation, or, depending on the exact sequence, can allow for harvest of cells post-culture using exogenous enzymes. Future studies similar to the experiments presented in this work could provide significant advances in the understanding of the interrelationship between biomaterial and biomechanical stimuli on hMSC differentiation.

# APPENDIX A

# LABORATORY PROTOCOLS

## A.1 OPF Synthesis

**Fumaryl Chloride (FuCl) Distillation (if necessary)**

Warning: Fumaryl chloride has a very pungent odor. Work only in the fume hood with the sash down as far as possible. Double glove, and leave jars, glassware, used gloves in the hood overnight to air out.

1. Wash and dry:

   2 x 500 ml round-bottom flasks,

   1 x joint for thermometer,

   1 x thermometer to fit joint (~160°C),

   1 x large condenser,

   1 x glass elbow,

   1 x joint for desiccators,

   1 x glass stopper,

   1 x glass funnel,

   1 x egg-shaped FuCl stir bar.

2. Set up the distillation apparatus as shown, without the FuCl flask and collection flask:

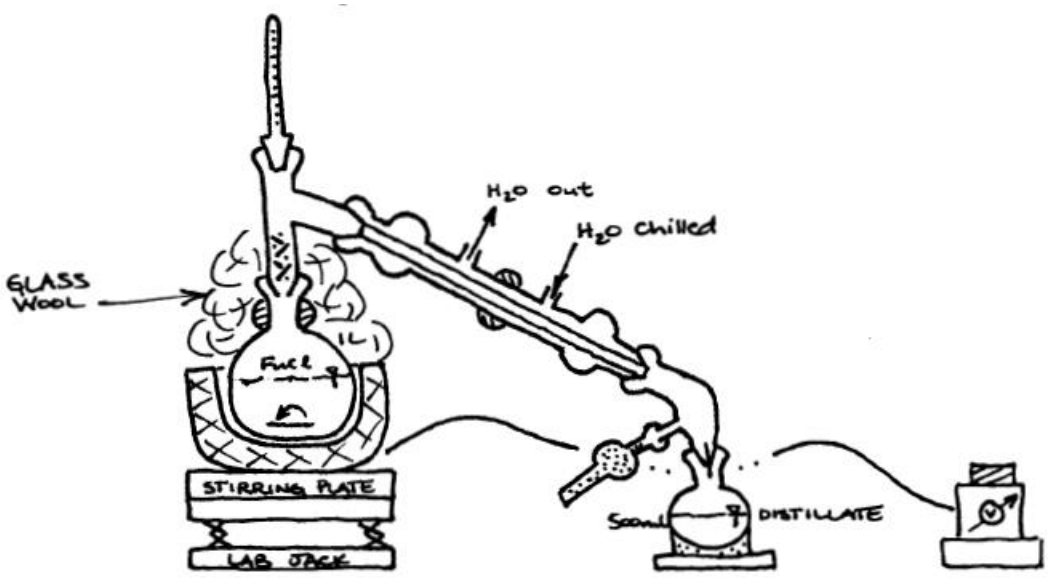


3. Replace the 500 ml collection flask with a 100 ml round bottom flask to collect the first 30 ml of distillate.
4. Clamp the apparatus to the scaffolding in the back of the fume hood.
5. Vacuum grease and clamp all connections.
6. Run cold, ice water UP the condenser tube using the circulation pump. This allows any bubbles to flow up and out of the condenser. Make sure that the circulation pump is not actively heating the water by turning the temperature control all the way down to -20°C.
7. Tie a KimWipe around the bottom of the condenser to catch external condensation.
8. Use the funnel to pour 150 ml (100 g) of FuCl into a 500 ml round-bottom flask.
9. Add the FuCl stir bar into the FuCl flask.
10. Vacuum grease the FuCl flask, and connect the flask to apparatus.
11. Place the flask in heating mantle with magnetic stirring at ~3.

12. Insulate the flask and neck with glass wool all the way up to the condensing tube to promote boiling and prevent condensation.
13. Start the transformer at 40 units.
14. Increase the transformer by 10 units, every 5 minutes.
15. Increase the transformer until the vapor temperature is 160°C (~80 units on transformer).
16. Dispose of the first ~30 ml of distillate by turning the neck up, removing the 1$^{st}$ 100 ml collection flask, and quickly replacing it with a clean 500 ml round-bottom flask.
17. FuCl distillate should be a light amber color.
18. The solution in the heated FuCl flask will become darker and more viscous.
19. When ~50-75 ml remains the heated FuCl flask and the solution is dark brown, turn off the transformer, remove the glass wool, turn the condenser off, and replace the heating mantle with a cork ring.
20. Stopper the FuCl distillate, parafilm the stopper, cover the flask with aluminum foil, and label it.
21. Store the distillate in the 4°C explosion-proof refrigerator.
22. Dilute the FuCl waste with tap water, and leave it in the hood overnight. Be careful of HCl production in the reaction with water, and pour the water in SLOWLY.
23. On the next day, use a spatula to break up the FuCl waste, retrieve the stir bar, and disposed of the waste in the aqueous waste container.
24. Glassware can be cleaned with acetone and the base bath.

**Methylene Chloride (MeCl) Distillation**

Warning: Use nitrile or silver-shield gloves when handling MeCl.

1. Wash and dry:

   1 x 1000 ml round-bottom flask,

   1 x joint for thermometer,

   1 x thermometer to fit joint (~40°C),

   1 x large condenser,

   1 x glass elbow,

   1 x joint for desiccators,

   1 x glass stopper,

   1 x glass funnel.

2. Set up the distillation apparatus as shown, without the MeCl flask and collection flask:

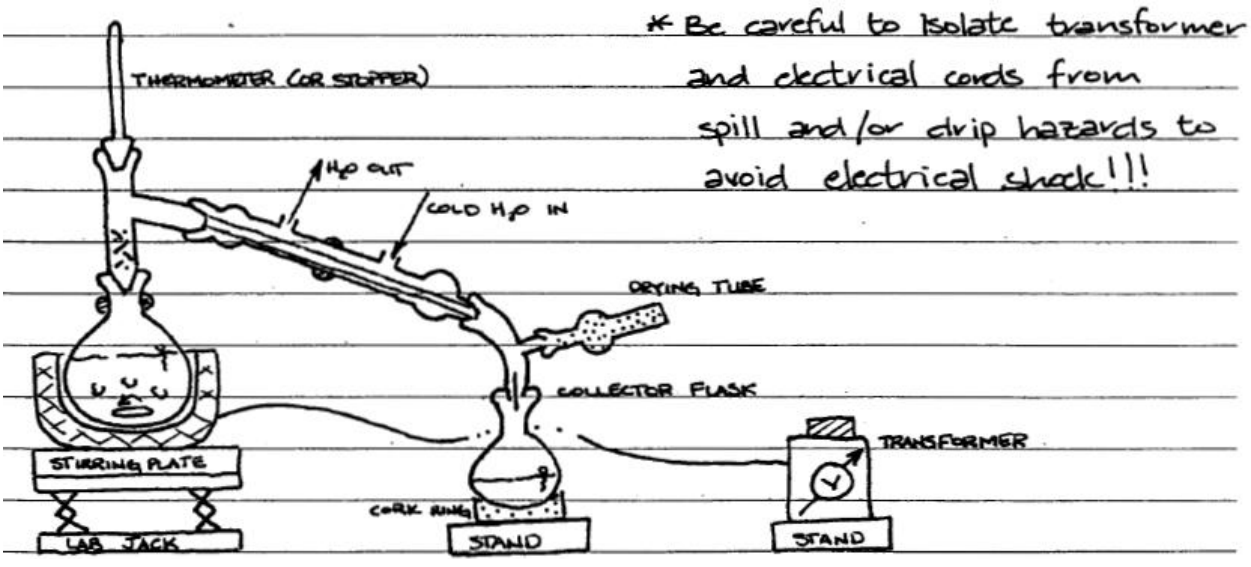

3. Replace the 500 ml collection flask with a 100 ml round bottom flask to collect the first 30 ml of distillate. Clamp the apparatus to the scaffolding in the back of the fume hood.
4. Vacuum grease and clamp all connections.
5. Run cold, ice water UP the condenser tube using the circulation pump. This allows any bubbles to flow up and out of the condenser. Make sure that the circulation pump is not actively heating the water by turning the temperature control all the way down to -20°C.
6. Tie a KimWipe around the bottom of the condenser to catch external condensation.
7. Use funnel to add 750 ml of MeCl and calcium hydride ($CaH_2$, if needed) into the existing MeCl + $CaH_2$ flask.
8. Vacuum grease the MeCl flask, and connect the flask to apparatus.
9. The MeCl + $CaH_2$ flask already contains a stir bar. Place the flask in heating mantle with magnetic stirring at ~4.
10. Insulate the flask and neck with glass wool all the way up to the condensing tube to promote boiling and prevent condensation.
11. Set the transformer to 35 units.
12. Vapor temperature should increase to ~40°C.
13. Dispose of the first ~30 ml of distillate by turning the neck up, removing the 1$^{st}$ collection flask, and quickly replacing it with a clean 1000 ml round-bottom flask.
14. When ~150-200 ml remains in the heated MeCl flask, turn off the transformer, remove the glass wool, turn the condenser off, and replace the heating mantle

with a cork ring. You should have ~500 ml MeCl distillate in your collection flask (need 340-380 ml for remaining steps).

15. Vacuum grease the glass stopper, and stopper the MeCl distillate, and label it.
16. Store the anhydrous MeCl distillate in the hood overnight. Do not parafilm the stopper.
17. Vacuum grease the original MeCl + $CaH_2$ stopper, stopper the undistilled MeCl + $CaH_2$, and store it in the back of the hood.
18. Dispose of the MeCl waste in the chlorinated organic solvents waste container.
19. Glassware can be dried in the hood, and then cleaned normally.

**Azeotropic Distillation of PEG**

Warning: Use nitrile or silver-shield gloves when handling toluene.

1. Wash and dry:

   1 x 500 ml or 1000 ml round-bottom flask,

   1 x Dean stalk,

   1 x condenser,

   1 x glass stopper,

   1 x Kontes #2 glass valve with LARGE hole,

   1 x egg-shaped stir bar,

   1 x glass funnel,

   1 x 250 ml glass graduated cylinder.

2. Set up the distillation apparatus as shown, without the PEG/toluene flask:

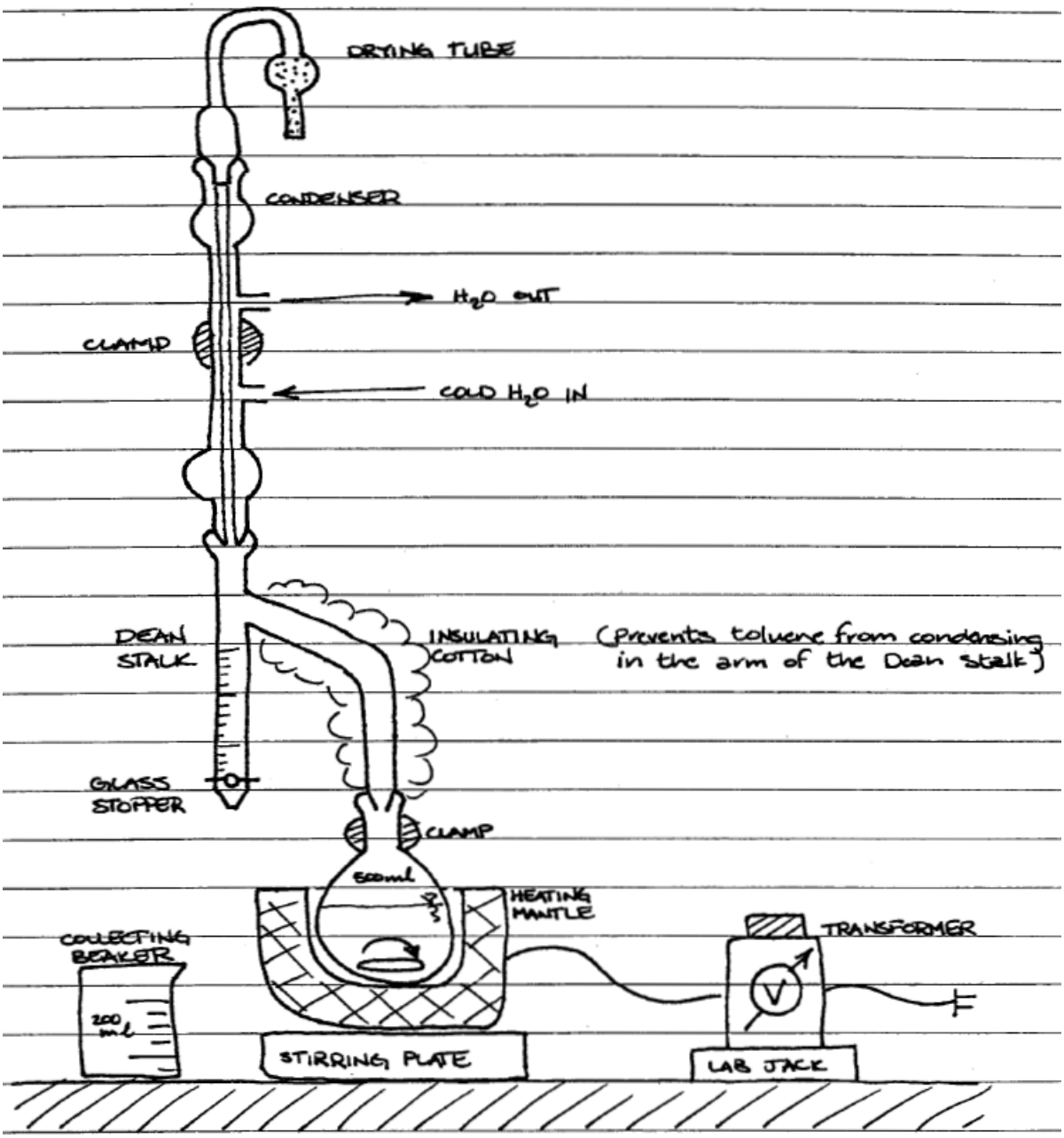


3. Clamp the apparatus to the scaffolding in the back of the fume hood.
4. Vacuum grease and clamp all connections.
5. Run cold, ice water UP the condenser tube using the circulation pump. This allows any bubbles to flow up and out of the condenser. Make sure that the circulation pump is not actively heating the water by turning the temperature control all the way down to -20°C.

6. Tie a KimWipe around the bottom of the condenser to catch external condensation.
7. Weigh 50 g PEG 3.4K or 10K in the 500 ml round-bottom flask.
8. Use the graduated cylinder and funnel to add 200 ml of toluene to the PEG in the 500 ml flask.
9. Add the stir bar to the flask, vacuum grease the flask, and connect the flask to apparatus.
10. Place the flask in heating mantle with magnetic stirring at ~5. The PEG will dissolve with stirring and heating.
11. Insulate the flask and neck with glass wool all the way up to the condensing tube to promote boiling and prevent condensation.
12. Set the transformer to 65 units.
13. When the Dean stalk fills to 20 ml, dispose of the toluene by draining the solution from the Dean stalk into a 250 ml waste beaker. The first few batches of waste may be partially cloudy, while others should be clear.
14. Repeat step 13 seven more times, removing 20 ml toluene at a time until ~160-180 ml toluene has been removed.
15. Turn off the transformer, remove the glass wool, turn the condenser off, and replace the heating mantle with a cork ring. 2-5 ml extra toluene waste may condense as you do this.
16. Allow the distilled PEG and toluene to cool, and then vacuum grease the glass stopper and stopper the distilled PEG. Parafilm the stopper, and label the flask.
17. Store the distilled PEG in the hood overnight. The PEG will solidify as it cools.

18. Dispose of the toluene waste in the nonchlorinated organic solvent waste container.
19. Glassware can be dried in the hood, and cleaned normally.

**OPF Reaction**

Warning: Use nitrile or silver-shield gloves when handling MeCl.

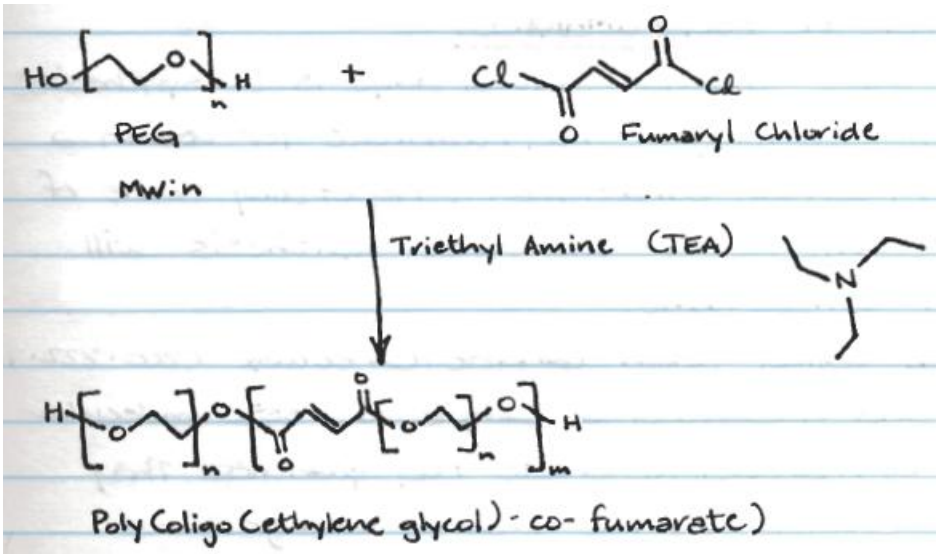


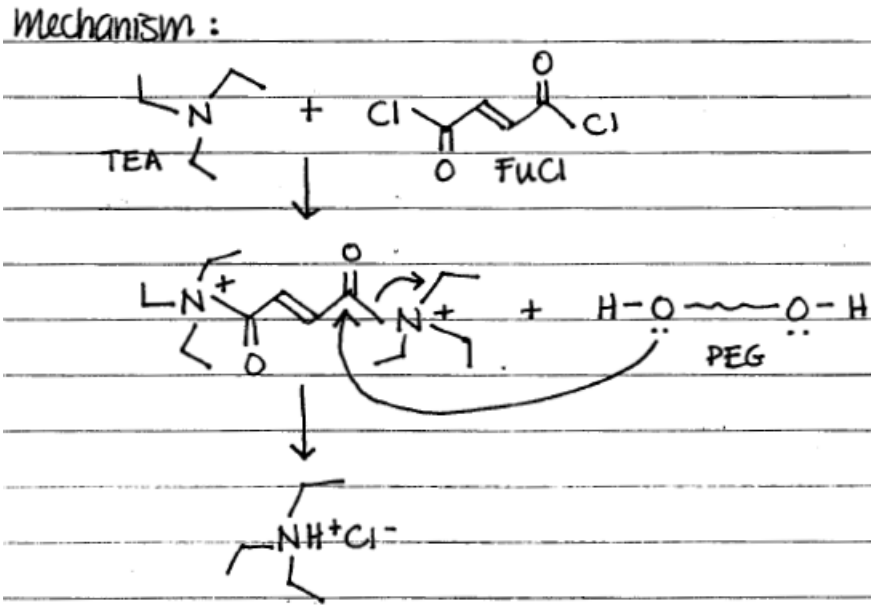


**3.4K Calculations:**

PEG MW = 3,400 Da

50 g PEG = 0.01471 mol PEG

1 PEG : 0.9 FuCl → 10% molar excess for PEG addition to ends of FuCl

(0.9 mol FuCl / mol PEG) * (0.01471 mol PEG) = 0.01324 mol FuCl

FuCl MW = 153 g/mol

(0.01324 mol) * (153 g/mol) = 2.025 g FuCl

FuCl density = 1.415 g/ml

(2.0235 g) / (1.415 g/ml) = **1.431 ml FuCl**

1 FuCl : 2 TEA → TEA removes Cl from ends of FuCl, 2 Cl per FuCl → Twice as much TEA as FuCl

(2 mol TEA / mol FuCl) * (0.01324 mol FuCl) = 0.02648 mol TEA

TEA MW = 101.2 g/mol

(0.02648 mol) * (101.2 g/mol) = 2.6798 g TEA

TEA density = 0.726 g/ml

(2.6798 g) / ( 0.726 g/ml) = **3.6912 ml TEA**

**10K Calculations:**

PEG MW = 10,000 Da

50 g PEG = 0.005 mol PEG

1 PEG : 0.9 FuCl → 10% molar excess for PEG addition to ends of FuCl

(0.9 mol FuCl / mol PEG) * (0.005 mol PEG) = 0.0045 mol FuCl

FuCl MW = 153 g/mol

(0.01324 mol) * (153 g/mol) = 0.6885 g FuCl

Density FuCl = 1.415 g/ml

(0.6885 g) / (1.415 g/ml) = **0.4866 ml FuCl**

1 FuCl : 2 TEA → TEA removes Cl from ends of FuCl, 2 Cl per FuCl → Twice as much TEA as FuCl

(2 mol TEA / mol FuCl) * (0.0045 mol FuCl) = 0.009 mol TEA

TEA MW = 101.2 g/mol

(0.009 mol) * (101.2 g/mol) = 0.9108 g TEA

TEA density = 0.726 g/ml

(0.9108 g) / ( 0.726 g/ml) = **1.2545 ml TEA**

1. Wash and dry:

   1 x 1000 ml 3-arm round-bottom flask,

   2 x 60 ml dropping funnels,

   1 x joint for the $N_2$ balloon,

   1 x PTFE valve for the $N_2$ balloon,

   2 x Kontes #2 glass valves with LARGE holes,

   2 x glass stoppers,

   1 x 250 ml or 1000 ml glass graduated cylinder.

2. Use the funnel and graduated cylinder to add 320 ml MeCl to the distilled PEG/toluene. Dissolve PEG with stirring.
3. Use the funnel to pour the PEG/MeCl into the 3-arm flask. The PEG distillation stir bar can be reused in this step.
4. Set up the reaction apparatus as shown, without the glass stoppers and $N_2$ balloon:

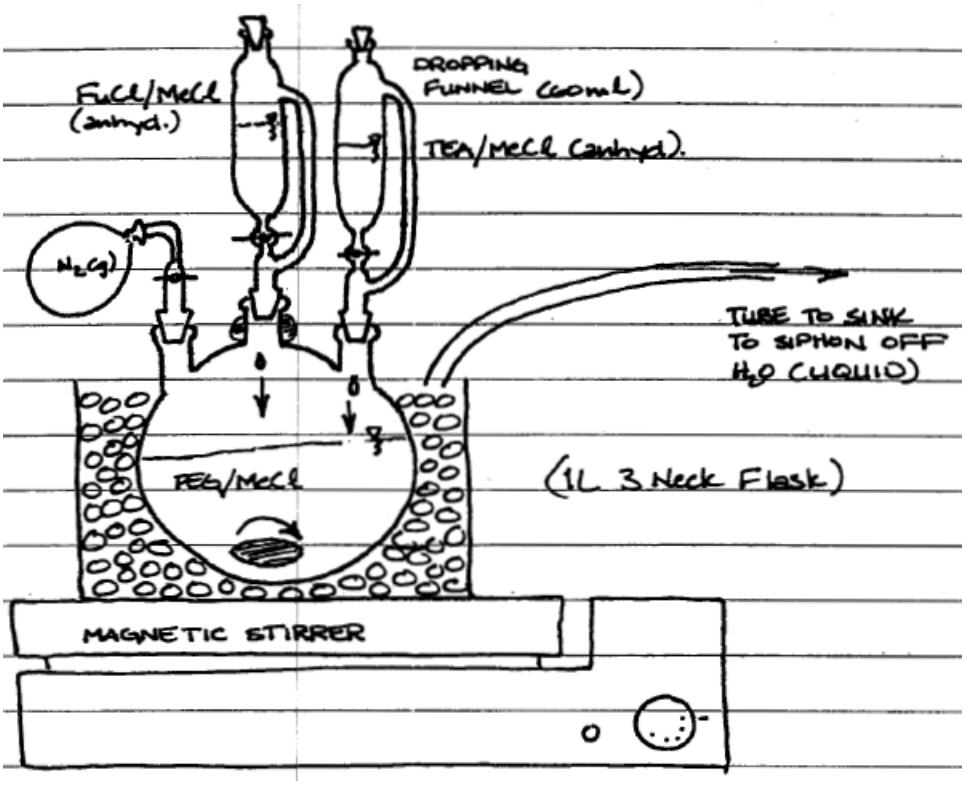


5. Clamp the apparatus to the scaffolding in the back of the fume hood.
6. Vacuum grease and clamp all connections. Be careful not to vacuum grease over the holes in the valves, or else the FuCl and TEA will not flow through. Also the PTFE valve for the $N_2$ balloon does not require vacuum grease.
7. Place the 3-arm flask in a small autoclave bin, filled with ice on a large stir plate. Optional: Add salt to the ice to keep the ice from melting.
8. For PEG 3.4K, use glass pipettes to add 30 ml MeCl to volumes of FuCl and TEA calculated above (3.4K: 1.431 ml FuCl and 3.6912 ml TEA). Add MeCl to dropping funnels first, then FuCl and TEA. MeCl removes the markings from glass pipettes, so exercise care when transferring MeCl.

9. For PEG 10K, use glass pipettes to add 10 ml MeCl to volumes of FuCl and TEA calculated above (10K: 0.4866 ml FuCl and 1.2545 ml TEA). Add MeCl to dropping funnels first, then FuCl and TEA. MeCl removes the markings from glass pipettes, so exercise care when transferring MeCl.
10. Flush system with $N_2$ gas, using the $N_2$ tank and hose and the $N_2$ filled balloon. Lift the glass stoppers from the dropping funnels slightly to purge excess air. Make sure the $N_2$ valve remains open.
11. Stir PEG solution on the stir plate at ~5.
12. Start reaction by dropping the FuCl and TEA at the same rate of 1 drop per ~3-4 seconds. A slower drop rate will result in a more efficient reaction.
13. Reaction will turn dark brown.
14. When necessary, siphon melted water from the ice bin, and replace the ice.
15. When dropping is complete, allow the reaction to continue on ice for the rest of the day.
16. When necessary, siphon melted water from the ice bin, and replace the ice.
17. At the end of the day, remove the ice bin, remove the dropping funnels, and replace the funnels with glass stoppers.
18. Allow the reaction to continue at room temperature with stirring on a cork ring for at least 2 days.
19. Check the $N_2$ balloon over the next 2 days, and refill the balloon if necessary (close valve when refilling the balloon).
20. Glassware can be dried in the hood, and cleaned with acetone and the base bath.

**Rotovaporing of MeCl**

Warning: Use nitrile or silver-shield gloves when handling MeCl.

1. Wash and dry:

   1 x 1000 ml round-bottom flask,

   1 x glass funnel.
2. Turn on Rotovapor by switching Vacuum Controller V-800, Rotovapor R-200, and Vacuum V-500 on.
3. Fill the water bath with distilled H2O, and heat to 40°C.
4. Use the circulating pump to flow cold, ice water through the condensing tube.
5. Use the funnel to pour the OPF solution into a 1000 ml round-bottom flask.
6. Clamp and vacuum grease the flask to the Rotovapor.
7. Lower the flask into the water bath, so the OPF solution and water levels are the same.
8. Slowly rotate the flask in the water bath.
9. Turn on the vacuum on at 850 mbar ("Set" → Up or down → "Run").
10. Gradually decrease the vacuum as necessary to maintain a steady drip of condensation into the collecting flask. Vacuum can be decreased as low as 700 mbar.
11. When OPF/MeCl solution is thick and "stew-like" consistency, remove OPF from Rotovapor.
12. Dispose of the MeCl waste in the chlorinated organic solvents waste container.
13. Glassware can be dried in the hood, and cleaned normally.

**Wash in Ethyl Acetate**

Warning: Use nitrile or silver-shield gloves when handling ethyl acetate.

1. Wash and dry:

   2 x 2 L aspiration flasks,

   1-2 x 2 L Erlenmeyer flasks,

   1-2 x 2 L beakers,

   2 x Buchner funnels,

   1-2 x glass funnels,

   1 x stir bar,

   2 x spatulas.
2. Add ethyl acetate (EA) to the OPF solution until the flask is ~2/3 full.
3. Stir the solution while heating with the heatgun (low speed, med heat) for 15-20 min, rotating every 5 minutes.
4. Solution will become less viscous and salts become visible at the surface. Ethyl acetate is a solvent for the OPF, but not for the salts produced in the TEA reaction.
5. Connect the vacuum and filter the solution through a Buchner funnel with #1 Whatman filter paper (11 µm pores) into a 2 L aspiration flask.
6. The salts will be filtered out of the solution by the filter paper. Discard these salts.
7. Add EA to the OPF to a total volume of 1500-1700 ml.
8. Stopper the flask with a #9 rubber stopper and parafilm the stopper and aspiration neck, and place the flask into the -20°C explosion-proof freezer for at least 2 hours or overnight if necessary.
9. If necessary, clean glassware for the next step.

10. After cooling, remove the OPF/EA from the freezer. The decreased temperature alters the solubility of the OPF, causing the OPF to precipitate out.
11. Connect the vacuum and filter the solution through a Buchner funnel with #1 Whatman filter paper, capturing the OPF in the filter paper and pulling the EA into an aspiration flask.
12. While filtering, stir the solution, allowing the EA to be pulled through the filter paper. Discard the EA.
13. When nearly dry, transfer the OPF from the filter paper to a beaker.
14. Add 1 L ethyl acetate to the solution.
15. Stir the solution while heating with the heat gun to redissolve the OPF in the EA. Solution goes from light brown to dark brown and becomes less viscous.
16. Use a clean glass funnel to transfer the OPF and EA to a 2 L Erlenmeyer flask and add EA to a total volume of 1500-1700 ml.
17. Stopper the flask with a #10 rubber stopper, and recrystallize the OPF/EA solution in a 2 L aspiration flask at -20°C for 1.5 hours or overnight.
18. Dispose of the EA waste in the nonchlorinated organic solvent waste container.
19. After cooling, filter the solution through a clean Buchner funnel with #4 Whatman filter paper (20-25 µm pores), capturing the OPF in the filter paper and pulling the EA into an aspiration flask.
20. The second filtering step may proceed much more slowly than the first. If EA/OPF is solid after removing from the freezer, add more EA to the solution. Tape 2 spatulas together to scoop product from the bottom of the flask.
21. Dispose of the EA waste in the nonchlorinated organic solvent waste container.

22. Optional: Repeat steps 13-19 for a third filtering step. This may be necessary if OPF appears too dark.
23. Dispose of the EA waste in the nonchlorinated organic solvent waste container.
24. Glassware can be dried in the hood, and cleaned normally.

**Wash in Ethyl Ether**

Warning: Use nitrile or silver-shield gloves when handling ethyl acetate and/or ethyl ether.

1. Wash and dry:

   1 x 2 L beaker,

   1 x stir bar,

   1 x Buchner funnel,

   2 x PTFE coated jars.
2. When OPF is nearly dry and EA is mostly gone, add 1 L ethyl ether (EE) directly to the funnel to remove the EA.
3. Once mostly dry, transfer the OPF from the funnel and filter paper to a 2 L beaker.
4. Add 1 L ethyl ether (EE) to the OPF for a second wash with stirring.
5. Filter the solution through a Buchner funnel with #4 Whatman filter paper (20-25 µm pores), capturing the OPF in the filter paper and pulling the EE into an aspiration flask.
6. Optional: Add EE to the OPF for a third wash.

7. As the EE filters through and the OPF dries, use a spatula to break up any clumps of OPF.
8. By the end, you should have a fine powder that is mostly dry.
9. Scoop the OPF powder evenly into 2 Teflon-coated jars with the spatula.
10. Leave the OPF in the hood overnight with the lid on loosely.
11. Dispose of the EE waste in the nonchlorinated organic solvent waste container.
12. Glassware can be dried in the hood, and cleaned normally.

**Vacuum Dry OPF**

1. Clamp a lyophilizer tube to the scaffolding in the back of the fume hood as shown:

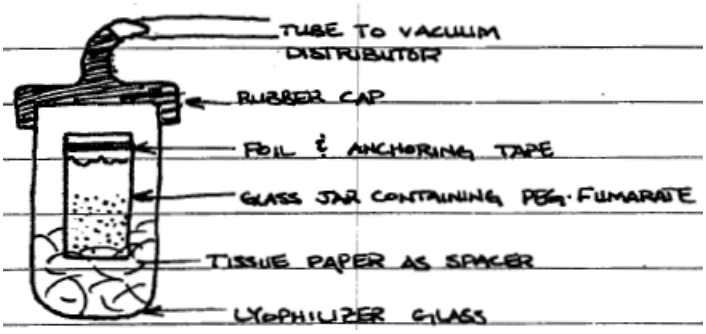


2. Tape aluminum foil to the top of the OPF jars and poke holes in the foil with a small gauge needle.
3. Add liquid nitrogen to the solvent trap.
4. Connect the vacuum to the solvent trap.
5. Close the valves to the samples ($3^{rd}$ and $4^{th}$ from the top). Open the valve to the manometer (bottom).
6. The top 2 valves are open to the atmosphere and should remain closed.
7. Turn on manometer, and then the vacuum pump.

8. Once a vacuum is established, gradually open the valves to the samples. Open the valve to the first sample until a vacuum is established, then close that valve. Then open the valve to the second sample until a vacuum is established. Now you can reopen the first sample.
9. Pressure should be less than 10 mbar (preferably 1-2 mbar).
10. Check the pressure and the liquid nitrogen level every 30-45 minutes.
11. Refill the liquid nitrogen if necessary.
12. When OPF is dry and you cannot smell any EE in the powder, open the valve to break the vacuum and turn off the pump.
13. Dispose of solvent from the solvent trap.
14. Parafilm OPF and store it at -20°C.

**Verify Product**

1. A lighter brown color is preferred.
2. Polymerize a 100% OPF hydrogel with thermal and photo-initiation to test crosslinking.
3. Run GPC on the OPF in chloroform to verify molecular weight.

## A.2 PEG-DA Synthesis

Reaction Calculations

*Reaction Calculations*

1) Begin with **24 g PEG, MW 3400**.

2) React with 100% excess acryloyl chloride (AcCl; 2 AcCl:1 PEG).

24 g PEG / (3400 g/mol PEG) = 7.06 mmol PEG

7.06 mmol PEG * 2 end groups * 2 (100% excess) = 28.24 mmol AcCl

0.02824 mol AcCl * 90.51 g/mol / (1.114 g/mL) = **2.294 mL AcCl**

3) React with 1:1 AcCl:triethylamine (TEA)

0.00706 mmol PEG * 2 end groups = 0.0141 mol TEA

0.0141 mol TEA * 101.9 g/mol / (.726 g/mL) = **1.982 mL TEA**

4) Workup with anhydrous potassium carbonate ($K_2CO_3$)

0.02824 mol AcCl * 2 mol $K_2CO_3$/mol AcCl / 2 M $K_2CO_3$ = **28.2 mL 2M $\mathbf{K_2CO_3}$** (aq)

138.205 g/mol = 276.41 g in 1L = 27.641 g in 100 mL = 8.2923 g $K_2CO_3$ in 30 mL dd$H_2O$

Day 1 – Methylene Chloride Distillation

Distill MeCl following the instructions in the OPF synthesis protocol. Keep in mind that you only need approximately 100 mL. Distillation is necessary to remove aqueous contamination (make MeCl anhydrous) that might generate unwanted side reactions in Day 2.

Day 2 – Reaction

*What's going on?* PEG is being acrylated. TEA acts as a catalyst by sequestering HCl to allow the reaction to proceed to completion. MeCl is the solvent used for this reaction.

**Caution**: AcCl doesn't smell as bad as FuCl, but it is worse for you (eye, throat irritant)!

1. Set up 3-arm round bottom flask in the fume hood on a stir plate. Weigh and add PEG to the flask. Add stir bar.

| | |
|---|---|
| *Equipment:*<br>1x 500 mL 3-arm round bottom flask<br>1x dropping funnel<br>1x PTFE gas valve<br>3x glass stoppers<br>1x glass stopcock<br>1x PTFE stopcock<br><br>1x stirbar<br>1x glass funnel<br>1x graduated cylinder | 1x balloon<br>Glass pipettes<br>1x stir plate<br>1x clamp<br>6x green clamps<br><br>*Chemicals:*<br>MeCl (anhydrous)<br>PEG<br>TEA<br>AcCl |

2. Attach one dropping funnel, with a glass stopper, and a PTFE valve for $N_2$ gas flow. Vacuum grease glass-glass connections for the dropping funnel (excluding glass stopper) and the PTFE valve. Do not grease the PTFE valve itself.
3. Hook up $N_2$ tubing to the valve. Continually purge the whole system as you add 40 mL MeCl to the round bottom flask through the ungreased arm using a glass funnel. Stir. Gently float a glass stopper in the arm on the air being pushed out.
4. When dissolved, use a glass pipette to add TEA. Vacuum grease a glass stopper and gently float the dropping funnel's glass stopper as before. Let stir for 5 min.
5. Use a glass pipette to add 20 mL MeCl and the appropriate amount of AcCl to the dropping funnel. Be aware that MeCl (and its fumes) will remove markings from glass pipettes. Vacuum grease and stopper the funnel while you are adding and turn off $N_2$ flow.
6. Remove the $N_2$ hose and attach an $N_2$ balloon.
7. Drip the AcCl/MeCl mixture into the round bottom flask (about 1 drop every 3-4 seconds). Drip AcCl in MeCl very slowly (about 1 drop every 4 seconds).
8. After dripping is complete, you can replace the funnels with stopcocks.
9. Let stir overnight.

<u>Day 3 – Workup</u>

*What's going on?* To remove TEA-HCl, we first react the mixture with potassium carbonate to produce KCl, which will transfer to the aqueous phase. Some TEA will remain in the organic phase for Day 3 filtration.

*Equipment:*
1x 250 mL separatory funnel
1x glass stopper
1x glass funnel
1x glass stopcock
1x ring clamp

*Chemicals:*
$K_2CO_3$, anhydrous

1. Use a glass funnel to transfer the mixture from the

round bottom flask to a separatory funnel with a greased stopcock. (Don't forget to close the stopcock prior to transfer. Also, remember to wipe vacuum grease from connections before pouring.)

*Equipment:*
2x 250 mL beakers
1x 1L aspiration beaker
1x 2-3L beaker
2x stir bars
2x Buchner funnels
Filter paper (fine pores, 42)

*Chemicals:*
$MgSO_4$, MeCl
Ethyl ether

2. Add appropriate amount of 2M $K_2CO_3$ to the separatory funnel.
3. Stopper funnel, hold vertically, and give it a quick shake or two. Immediately open the stopper to release $CO_2$. Repeat a few times.
4. Hold the separatory funnel horizontally, but with the tip tilted higher. One hand should hold the glass stopper, the other holding the stopcock knob up. Rotate vigorously, and open the stopcock periodically to release $CO_2$. Repeat until all gas is released. Solution should have the consistency of a milky-white emulsion.
5. Leave overnight. Place a beaker underneath to capture any leaked product.

Day 4 – Filtration and Drying

*What's going on?* We isolate the mixture from KCl in the aqueous phase, add $MgSO_4$ to remove any additional aqueous solution, and precipitate PEG-DA in ethyl ether. TEA should remain in solution.

1. Drain the two organic phases into a 250 mL beaker on a stir plate with stir bar.
2. While stirring, add MgSO4 until the mixture goes from a lumpy consistency to a well dispersed mixture of powder and organic solvent. It should appear as opaque milk – if it doesn't look like milk, add more MgSO4. Add ~20-40 mL MeCl to keep the PEG-DA in solution (may help to have a smaller bottle or beaker with

MeCl). The goal here is to add as little MeCl as possible to keep the solution saturated with PEG-DA. But, if you add too much, no sweat.

3. Prepare a Buchner funnel with aspiration flask and filter paper and pre-wet the filter paper with MeCl.
4. Pour the mixture into the filter and a clear liquid should be collected (containing PEG-DA). If the liquid is cloudy, filtration should be performed again. The vacuum will also begin to evaporate MeCl. Thus, you can elect to evaporate MeCl if necessary.
5. Prepare a 2L beaker with 1.7L ethyl ether and a stir bar. Pour in the PEG-DA solution and wait 10 min to precipitate PEG-DA.
6. Prepare another Buchner funnel with two filter paper sheets, and pre-wet with ethyl ether.
7. Filter to separate PEG-DA. If the filtrate is not clear, re-filter. Pound into bits. See an older grad student to measure your performance.
8. Dry under vacuum until no ether can be smelled (at least 5 hours). At least some of this vacuum drying must be performed immediately after filtration.
9. Store at -20ºC. Expected recovery is approximately 75%.

Note: If necessary, you may need to dialyze the resulting product to remove impurities. Use a 1000 MWCO dialysis membrane at 0.2 g/mL and lyophilize after dialysis.

### A.3 LGPA Synthesis

**Purpose:** To attach PEG-acrylate to each end of an enzymatically-cleavable peptide.

**Materials:**

Plastic conical vial, 200-250 mL beaker, 2-3L beaker, stir plate

Acrl-PEG-NHS (SVA) [MW: 3400 Da]; GGGLGPAGGK peptide [MW: 769.86 Da]

Dialysis tubing (3500-5000 Da MWCO; Spectrapor 131201/131204) and clips

**Preparation:**

1) Wash glassware and dialysis clips (Alconox, water, $dH_2O$)
2) Make a 50mM sodium bicarbonate buffer solution and pH to 8.5. For reacting 100 mg peptide, this means 420 mg sodium bicarbonate in 100 mL $ddH_2O$ in the 200-250 mL beaker. Shield your beaker from light.
3) Calculate amounts of Acrl-PEG-NHS (2.2:1 moles of NHS to peptide) needed for cleavable peptide. For 100 mg peptide, you need 971.6 mg Acrl-PEG-SVA.

**Reaction:**

4) Dissolve the peptide in 20% of your buffer in a 15 or 50 mL conical (100 mg in 20 mL).
5) Dissolve the Acrl-PEG-NHS in the buffer that's left in your beaker (971.6 mg in 80 mL). The beaker should be shielded from light.
6) Immediately add peptide solution to your beaker, stir (~6) and cover with parafilm.
7) Allow to stir for >3 hours at room temperature.
8) Prepare tubing for dialysis. One (super-wide, 131204) strip should be used for every 10 mL solution. 100 mg peptide = 100 mL buffer = 10 tubes.
9) Rinse dialysis tubing 4x in a 2L beaker, 15 min between each rinse, to remove sodium azide.
10) Close one end of each dialysis strip with a weighted closure. Due to potential leakage, fold over the tubing before sealing with the closure.

11) Use a transfer pipette to add the solution to each tube. Close the open end of the tubing with a non-weighted closure.
12) Dialyze to remove byproducts for 2 overnights. If starting on the morning of the first day change the water the morning and night of the second day. Keep from light.

**Lyophilization:**

13) Weigh empty scintillation vials and record the weight.
14) Transfer solution from tubes to vials. Two scintillation vials should be used for each tube of dialysis product.
15) Remove the caps from the scintillation vials and place aluminum foil over the tops and tape this foil down. Poke holes in the top of the foil with a needle to let air escape.
16) Freeze vials in liquid nitrogen and lyophilize the product for 2 overnights.
17) Reweigh the scintillation vials so that the mass of the product inside the vial can be determined.
18) Parafilm and store the resulting product at -20°C.

## A.4 RGD Conjugation

Purpose: To attach the acrylated PEG spacer arm to the desired peptide.

Materials:

2-3L beaker x2 (1 to wash tubing, 1 to do purification)

100 ml beaker

Peptide (GRGDS) [MW: 490.47] (generally 25mg)

Spacer arm (A-PEG-NHS): (346.7 mg/25mg RGD)

Sodium bicarbonate

Dialysis tubing (need about 3, MWCO 1000)

Dialysis clips (need 2/tubings or about 6/25 mg RGD)

Teflon tape

Stir plate

Stir bar x2

Days: Prepare day 1, refresh water day 2, freeze dry days 3-5.

Preparation:

1. Wash glassware (water, $dH_2O$, acetone)
2. Wash dialysis clips (water, $dH_2O$, ethanol)
3. Wash stir bars (water, $dH_2O$, ethanol)
4. Make sodium bicarbonate buffer (pH 8.1 – 8.3)
   Use 10 mL $ddH_2O$ per 0.02 g of sodium bicarbonate. The total amount of the buffer should be 1 ml of buffer per 1 mg peptide that will be used.
5. Calculate amounts of peptide and A-PEG-NHS (1:2 molar ratio)
   10 mg A-PEG-NHS: $2.94 \times 10^{-6}$ mol

Reaction:

6. Pour the peptide into the buffer and mix. In order to get all of the peptide from the vial add 1 ml of the buffer solution to the vial. Close the vial and shake. Pour the remaining contents into the buffer solution. Dissolve peptide into the buffer

solution at room temperature.

7. Add A-PEG-NHS (approximately 50 – 100 mg every 15 min) to the peptide solution with stirring (stirrer ~ 6). Put paraffin over the top of the beaker while stirring.
8. Maintain reaction for 2.5 hour at room temperature
9. Cut the dialysis tubing into strips a little shorter than the beaker that will be used for dialysis.
10. Since the dialysis tubing is stored in sodium azide it needs to be rinsed. To do this put the dialysis tubing in a beaker with about 1L of $dH_2O$ and mix. Refresh the $dH_2O$ every 15 minutes (3x) in order to thoroughly rinse the tubing.
11. After the tubing is thoroughly rinsed remove it from the beaker and close one end of the dialysis tubing with a weighted closure. After the reaction in step 7 is complete, use a transfer pipette to add the mixture to the tubing until the tubing is about half full. Close the open end of the tubing with a non-weighted closure and place into beaker of distilled water.
12. Dialyze to remove by-products for 2 overnights. If starting on the morning of the first day change the water the morning and night of the second day.

Freeze dry the product:

13. Weigh the empty scintillation vials and record the weight.
14. Carefully remove the dialyzed products from the water and remove the clip at the top of one of the membranes.
15. Two scintillation vials will be used for each tube of dialysis products. Use a

transfer pipette to relocate about half of the dialysis products from one tube to a scintillation vial. Pour the rest into the same vial.

16. Pour about half of the dialyzed product in the scintillation vial into a second scintillation vial. Each of the vials should have about half of the products from the dialysis tubing.
17. Repeat steps 15-17 for each dialysis membrane.
18. Fill a styrofoam container with liquid nitrogen to a height that is about one half to three fourths the height of the scintillation vials.
19. Remove the caps from the scintillation vials and place aluminum foil over the tops and tape this foil down. Poke holes in the top of the foil with a needle to let air escape.
20. Using long tweezers carefully place the scintillation vials in the liquid nitrogen. They should be sitting on the bottom of the container and surrounded by liquid nitrogen, but not completely covered by it.
21. Leave the vials in the liquid nitrogen for 2-3 min. until the product becomes frozen.
22. Lyophilize the product overnight twice.
23. Reweigh the scintillation vials so that the mass of the product inside the vial can be determined.
24. Store the resulting product at -20°C in a scintillation vial that has been sealed with paraffin.

### A.5 Ligament Fibroblast Isolation Protocol

Purpose: Ligament was digested to remove matrix (i.e. collagen) and isolate the fibroblasts for use in experiments.

Procedure for Cell Isolation

1. Prepare DMEM+ a.k.a. Arnold (overnight antiobiotics for tissue samples)
    a. Use sterile high glucose DMEM. Add 10 ml/L PSN (stock @ 100x), 10 ml/L kanamycin (stock @ 100x), 1 ml/L gentamicin (stock @ 1000x), and 1 ml/L fungizone (stock @ 1000x).
2. Prepare 0.4% collagenase digest solution
    a. In DMEM+ (see above) add 0.4% collagenase. Make enough for 10 ml digest solution per 1 gram tissue + extra volume.
    b. CALCULATION: [total mass of tissue]*10 ml/g tissue * 0.004 = ___ g of collagenase.
    c. Sterile filter collagenase solution using 60 ml syringe and 0.2 µm filter.
3. Dice the tissue into roughly 1-3 $mm^3$ cubes.
4. Record weight of empty Petri dish. Aspirate excess PBS and weigh tissue in Petri dish to get tissue only weight.
5. Place tissue into T-75 flasks so that there is about 2-3 grams of tissue per flask.
6. Add 10 ml of 0.4% collagenase digest solution per 1 gram of tissue to each T-flask. T-flasks should be placed on their sides and secured firmly to the shaker plate. The whole assembly is then placed into the incubator for 12-48 hours. Agitate at 3-5 Hz.

*After digestion (~48 hr)*

7. When fully digested, filter cell suspension by pipetting suspension into a 60 ml syringe attached to a metal cell strainer with 74µm mesh. Strain cell solution into a 50 ml conical. Dilute the suspension 1:1 with warm PBS to decrease the viscosity of the collagenase solution.
8. Centrifuge all samples at 1300 rpm for 10 minutes. For ligament and tendon the solution above the pellet may appear murky due to cells that did not completely separate out during the centrifugation. If this occurs leave at least 5 ml of solution above the pellet when aspirating. Then, dilute and repeat centrifugation to get the maximum number of cells to pellet down.
9. Aspirate off collagenase solution and resuspend cells in 10 ml sterile PBS w/o IONS or DMEM. Recombine and repeat if necessary.
10. Count cells to determine how much mediumto later add for the desired cell density.
11. Spin the cells at 1000 rpm for 10 min. Aspirate off the PBS.
12. Add an appropriate amount of mediumwith 10% FBS and 10% DMSO. Use the auto to pipette up and down to mix cells thoroughly throughout the solution.
13. Add 1 ml of cell solution to each tube you will be freezing down.
14. Place the cell vials in the appropriate cooling container and place them in a -80°C freezer.
15. After enough time has passed put the now cold vials into the liquid nitrogen for long-term storage.

### A.6 Cell Encapsulation

Purpose: Encaspulate cells in hydrogels

Materials:

Medium(prepared day before)

Sterile PBS

6 Scintillation vials

Weigh paper

2(3) 15 ml falcon tubes

1(2) 50 ml falcon tubes

5(7) 1 ml syringes

2(4) 18G needle

2(3) Filter caps

2 Racks

4(6) 6 well plates

2(4) 12 well plates

12 (18) Micro-centrifuge tube caps, sterilized (molds)

Spatulas, sterilized

Tweezers, sterilized

Protocol:

1. Add polymers to a scintillation vial in appropriate amounts for the experiment. If desired vials containing polymers can be stored overnight at 4°C or for longer periods at -20°C. If the vials are stored they should be parafilmed and covered in

aluminum foil. Note: ~400-700 μl of the original solution is lost during filter sterilization.

Day of encapsulation

1. If necessary, remove vials from the freezer/refrigerator and warm to room temperature.
2. Add appropriate amount of PBS to polymers, vortex, and place the vial in the incubator at 37 °C for about one hour or until bubbles have left the solution.
3. Create 0.3 M stock solutions of APS and TEMED (10 ml will be made).
    a. APS: 0.684 g/ 10 mL PBS
    b. TEMED: 0.348 g/ 10 mL PBS
4. Filter sterilize the APS and TEMED solutions. Make sure to cover the vials with aluminum foil to prevent photoinitiation.
5. Remove the polymer solutions from the incubator and allow to cool at room temperature
6. Filter sterilize the polymer solution. Aliquot it out into individual 15 ml tubes as appropriate for each cross-linking step that is needed.
7. Cells needed for encapsulation should have been plated for at least 3 days before using them. Wash, trypsinize, and resuspend cells at the required concentration (typically $50x10^6$ cells/ml) according to established lab protocols.

*Crosslinking/encapsulation*

8. Add appropriate amount of APS and vortex at low speed for about 5 seconds.

9. Add the appropriate amount of the cell solution and quickly mix with pipette. The concentrated cell solution typically is used at a concentration of $50x10^6$ cells/ml with the resultant concentration being $10x10^6$ cells/ml.
10. Similarly, add the appropriate amount of TEMED and quickly mix with pipette.
11. Pipette the appropriate amount of the solution (typically 30 µl for small hydrogels and 350 µl for tensile constructs) into the mold that is being used.
12. Cover mold and place it in the incubator.
13. Heat the molds at 37 °C for 10 min.
14. Remove from the heat and put the gels into well plates with mediumas appropriate.

    Note: Only ~14 30 µl hydrogels and 3-4 tensile construct hydrogels can be created at one time before the solution cross-links with the APS and TEMED. In addition, only a limited number of plates can be trypsinized effectively at one time. Therefore, the trypsinization process may need to be repeated on different sets of plates and the cross-linking process may also need to be repeats as appropriate.

### A.7 Cell Number/PicoGreen

Purpose: The Pico Green assay quantifies the amount of DNA present which is an indirect measure of the number of cells.

Materials:

12 well plates

Sterile PBS

Spatulas, sterilized

Tweezers, sterilized

96 well plates

*For Hydrogels*

1. Remove media.
2. Add 2ml iPBS.
3. Remove iPBS.
4. Add 2-4ml iPBS (covering sample).
5. Place in incubator for 30 min to an hour. Leave in incubator until gels are no longer the color of the mediumand have become clear.
6. Transfer the gels between pieces of weigh paper to remove excess water and weigh the gels. Then put the gels in 1.5 ml eppendorf tubes.
7. Homogenize the gels with a pellet grinder in the tubes. Be careful not to loose any of the gel.
8. When the gel is well ground add $ddH_2O$ to the tube depending on the size of the gel (750 µl for those cast in the caps). Some of the $ddH_2O$ can be used to wash the pellet grinder tip into the tube and to wash the side of the tube. This will maximize the amount of gel that is available for the bioassay.
9. Let sit at room temperature for 30 min.
10. Store at -20 °C if needed.

*Lysing the cells*

11. Freeze the cells at -80 °C for a minimum of 1 hour.
12. Thaw at room temperature for 30 minutes.

13. Sonicate for 30 min. to lyse the cells.

    *Note:* The sonicator will heat up after each usage. Ice should be added to the water in order to cool the sonicator down. If this is not done the DNA in the sample could break down.

    *Safety note:* The sonicator is meant to lyse the cells. Do not put fingers into the water bath while the sonicator is on or cells in your fingers will be lysed.

14. Repeat steps 11-13 two additional times.

15. If the samples are being stored before the assay is done freeze them at -80°C .

*For Plated Cells in a well plate*

1. Aspirate liquid from the wells of the plate
2. Add 2 ml PBS to rinse.
3. Repeat steps 1-2.
4. Add 1 ml distilled, deionized water ($ddH_2O$).
5. Let sit at room temperature for 30 min.
6. Store at -20 °C if needed.

*Lysing the cells*

7. Freeze the cells at -80 °C for a minimum of 1 hour.
8. Thaw at room temperature for 30 minutes.
9. Sonicate for 30 min. to lyse the cells.

    *Note:* The sonicator will heat up after each usage. Ice should be added to the water in order to cool the sonicator down. If this is not done the DNA in the sample could break down.

*Safety note:* The sonicator is meant to lyse the cells. Do not put fingers into the water bath while the sonicator is on or cells in your fingers will be lysed.

10. Repeat steps 7-9 two additional times.

*Making the plates*

Standards

1. Make sure to thaw out samples and PicoGreen reagents for about 20 minutes before doing the assay.
2. Make up buffer solution and PicoGreen according to the PicoGreen calculator. Vortex both solutions to make sure they are mixed thoroughly.

   *Note*: When creating the buffer solution make sure to take the volume in the DNA standards into account. Also, cover the PicoGreen solution in aluminum foil to protect it from light.
3. Make up DNA standards according to the table below.

| Conc. (ug/ml) | DNA (ul) | Buffer Solution |
|---|---|---|
| 5 | 25 | 475 |
| 3 | 15 | 485 |
| 1 | 5 | 495 |
| 0.5 | 50 of 5 ug/ml | 450 |
| 0.3 | 50 of 3 ug/ml | 450 |
| 0.1 | 50 of 1 ug/ml | 450 |
| 0.05 | 50 of 0.5 ug/ml | 450 |
| 0.03 | 50 of 0.3 ug/ml | 450 |
| 0.01 | 50 of 0.1 ug/ml | 450 |
| 0 | 0 | 1000 |

4. Add 43 µl of your sample solutions into the appropriate wells of a 96 well plate. Make sure to change tips between samples.
5. Add 107 µl of the buffer solution into the wells.
6. Add 150 of the PicoGreen Solution to the wells.
7. Read in a plate reader: ex 485, em 528.

## A.8 Live/Dead Assay

Purpose: This assay uses calcein and ethidium homodimer-1 to stain cells so that live cells vs. dead cell can be differentiated via fluorescence. Calcein (494/517 nm) is permeable in the cell membrane of living cells and is cleaved in the cytosol to fluoresce green indicating healthy cells. This cleavage occurs when the cells is undergoing its normal metabolic processes. Ethidium (528/617 nm) can not permeate the cell's membrane so it only enters cells whose membrane has been ruptured. Ethidium binds to DNA to fluoresce red, indicating dead cells.

Materials:

Sterile PBS

12 well plates

Spatulas, sterilized

Tweezers, sterilized

Live/Dead stain

Protocol:

1. Remove mediumfrom well plate with hydrogels or transfer hyrogels to well plates as appropriate.
2. Add 1 ml of 1X PBS to rinse the wells, then remove the PBS.
3. Add PBS to the wells and place them in the incubator for at least 30 min or until gels are no longer the color of the mediumand have become clear. This serves to

rinse out mediumwhich would otherwise autofluoresce in the Live/Dead assay and cause imaging interference.

4. Create live/dead solution using the amounts below (scale to your number of samples). Cover the tube with the solution in aluminum foil to prevent photobleaching of the live dead solution.

**Dye Amounts:**

For 6 samples (1 ml dye/sample, makes 6.75 ml staining solution):

6.8 µl @ 1 mM or 1.70 µL calcein @ 4 mM (1 mM ≈ 1 mg/ml)

3.38 µL eth.

6.75 ml PBS

5. Wait about 45 min – 1hr before imaging. Remove PBS and add 1 ml of dye. Cover these wells in foil to prevent photobleaching and place in incubator for 45 min – 1hr.
6. Move gels to new wells and add 2 ml of fresh PBS to rinse out excess dye. To prevent the gels from drying out leave the gels in PBS until you are ready to image them.
7. Move gels to the cell chamber and image using an inverted fluorescence microscope or confocal microscope. Be careful to avoid photobleaching during imaging.

## A.9 MMP Production

### A.9.1 Protocol for Measurement of MMP-1

A human MMP-1 flurokine kit (RND systems, F1M00) was used.

1. Reconstitute MMP-1 standard in calibrator diluents RD5-25 solution to produce a stock solution of 25 ng/ml. Allow standard solution to sit for a minimum of 15 minutes with gentle agitation before making dilutions.
2. Prepare standards according to table below.

| Conc. (ng/ml) | MMP (ul) | Calibrator diluent RD5-25 (ul) |
|---|---|---|
| 12.5 | 500 | 500 |
| 6.25 | 500 of 12.5 ng/ml | 500 |
| 3.12 | 500 of 6.25 ng/ml | 500 |
| 1.56 | 500 of 3.12 ng/ml | 500 |
| 0.78 | 500 of 1.56 ng/ml | 500 |
| 0.39 | 500 of 0.78 ng/ml | 500 |
| 0 | 0 | 500 |

3. Remove excess black strips from plate and return to pouch. Reseal pouch and store.
4. Add 100 µl of RD1-64 to wells.
5. Add 150 µl of your sample solutions into the appropriate wells of a 96 well plate. Make sure to change tips between samples. Cover with an adhesive strip.
6. Incubate 3h on a shaker table (450-550 rpm) at RT.
7. Prepare wash buffer.

| # of Wells | Wash buffer | dH2O | Total buffer |
|---|---|---|---|
| 32 | 4.2 ml | 105 ml | 109.2 ml |
| 64 | 8 ml | 200 ml | 208 ml |
| 96 | 10 ml | 250 ml | 260 ml |

8. Aspirate solution from wells, add 400 µl wash buffer.
9. Repeat previous step three times.
10. Prepare APMA solution within 15 minutes of use.

| # of Wells | APMA stock | Reagent diluent 2 | Total APMA |
|---|---|---|---|
| 32 | 42 ul | 6.96 ml | 7 ml |
| 64 | 83 ul | 13.92 ml | 14 ml |
| 96 | 135 ul | 22.5 ml | 22.64 ml |

11. Aspirate solution from wells.
12. Invert plate and blot against a clean paper towel.
13. Add 200 µl APMA to standards and desired wells. Add 200 ul of Reagent iluents 2 to other wells. Make sure to change tips between samples. Cover with an adhesive strip. APMA activates any MMPs present so do not add if you are measuring endogenous active MMPs. Always add APMA to standards.
14. Incubate for exactly 2h at 37 °C in humid environment.
15. Aspirate solution from wells, add 400 µl wash buffer.
16. Repeat previous step three times.
17. Prepare substrate solution within 15 minutes of use.

| # of Wells | Substrate stock | Reagent diluent 2 | Total Substrate |
|---|---|---|---|
| 32 | 109 ul | 6.89 ml | 7 ml |
| 64 | 219 ul | 13.78 ml | 14 ml |
| 96 | 360 ul | 22.5 ml | 22.88 ml |

18. Aspirate solution from wells.
19. Add 200 µl of substrate to each well. Cover with a new adhesive strip. Incubate for 17-20h at 37 °C in dark, humid environment.
20. Read at ex 320 nm, em 405 nm.

### A.9.2 Protocol for Measurement of MMP-13

A human MMP-13 flurokine kit (RND systems, F13M00) was used.\

1. Reconstitute MMP standard in distilled water to produce a stock solution of 32 ng/ml. Allow standard solution to sit for a minimum of 15 minutes with gentle agitation before making dilutions.
2. Prepare standards according to table below.

| Conc. (ng/ml) | MMP (ul) | Calibrator diluent RD5-25 (ul) |
|---|---|---|
| 16 | 700 | 700 |
| 8 | 700 of 16 ng/ml | 700 |
| 4 | 700 of 8 ng/ml | 700 |
| 2 | 700 of 4 ng/ml | 700 |
| 1 | 700 of 2 ng/ml | 700 |
| 0.5 | 700 of 1 ng/ml | 700 |
| 0.25 | 700 of 0.5 ng/ml | 700 |
| 0 | 0 | 700 |

3. Remove excess black strips from plate and return to pouch. Reseal pouch and store.
4. Add 200 µl of your sample solutions into the appropriate wells of a 96 well plate. Make sure to change tips between samples. Cover with an adhesive strip.
5. Incubate 3h on a shaker table (450-550 rpm) at RT.
6. Prepare wash buffer.

| # of Wells | Wash buffer | dH2O | Total buffer |
|---|---|---|---|
| 32 | 4.2 ml | 105 ml | 109.2 ml |
| 64 | 8 ml | 200 ml | 208 ml |
| 96 | 10 ml | 250 ml | 260 ml |

7. Aspirate solution from wells, add 400 µl wash buffer.
8. Repeat previous step three times.
9. Prepare APMA solution within 15 minutes of use.

| # of Wells | APMA stock | Reagent diluent 2 | Total APMA |
|---|---|---|---|
| 32 | 42 ul | 6.96 ml | 7 ml |
| 64 | 83 ul | 13.92 ml | 14 ml |
| 96 | 135 ul | 22.5 ml | 22.64 ml |

10. Aspirate solution from wells.
11. Invert plate and blot against a clean paper towel.
12. Add 200 µl APMA to standards and desired wells. Add 200 ul of Reagent diluent 2 to other wells. Make sure to change tips between samples. Cover with an

adhesive strip. APMA activates any MMPs present so do not add if you are measuring endogenous active MMPs. Always add APMA to standards.

13. Incubate for exactly 1h at 37 °C in humid environment.
14. Aspirate solution from wells, add 400 µl wash buffer.
15. Repeat previous step three times.
16. Prepare substrate solution within 15 minutes of use.

| # of Wells | Substrate stock | Reagent diluent 2 | Total Substrate |
|---|---|---|---|
| 32 | 115 ul | 6.89 ml | 7 ml |
| 64 | 230 ul | 13.78 ml | 14 ml |
| 96 | 375 ul | 22.5 ml | 22.88 ml |

17. Aspirate solution from wells.
18. Add 200 µl of substrate to each well. Cover with a new adhesive strip. Incubate for 17-20h at 37 °C in dark, humid environment.
19. Read at ex 320 nm, em 405 nm.

## A.10 Real Time RT-PCR

**RNA Extraction**

**Extract RNA using Qiagen RNeasy Mini Kit**

**(Consult the RNeasy kit manual for more specific protocols depending on your cell/tissue source)**

*Materials*

Molecular BioProducts RNase Away Spray (VWR 17810-491; 475 ml)

Aerosol Filter Pipette Tips for Rainin LTS, 20 µl (VWR 83009-688; pack of 960)

Aerosol Filter Pipette Tips for Rainin LTS, 200 µl (VWR 82003-196; pack of 960)

Aerosol Filter Pipette Tips for Rainin LTS, 1000 µl (VWR 82003-198; pack of 576)

QIAshredder (Qiagen 79654 or 79656; 50 or 250 runs)

RNeasy Mini Kit (Qiagen 74104 or 74106; 50 or 250 runs)

Optional Alternative: RNeasy Protect Mini Kit (Qiagen 74124 or 74126; 50 or 250 runs)

EMD 2-Mercaptoethanol (VWR EM-6010; 100 ml)

RNAse-free DNase Set (Qiagen 79254; 50 runs)

*Protocol*

For plated cells

I. Trypsinize cells and centrifuge (10 min, 1000 rpm).

II. Aspirate supernatant, resuspend pellet in media, and centrifuge (10 min, 1000 rpm).

III. Aspirate supernatant, rinse pellet with PBS, and centrifuge again (10 min, 1000 rpm), aspirate PBS.

For gels

I. Soak gels in PBS for ~ 1h to remove media.

II. Transfer the gel to an RNase free, DNase free microcentrifuge tube.

III. Break the gel into small pieces using a pellet grinder.

1. Lyse cell pellet or cells in gel in **350 µl Buffer RLT with β-mercaptoethanol** (add 10 µl BME per 1 ml Buffer RLT).
2. Put solution in **purple QIAshredder column** and centrifuge **(2 min, 14000 rpm)**.
3. Discard filter and add **350 µl 70% ethanol** to eluted substance.
4. Transfer suspension to **pink RNeasy column** and centrifuge **(15 sec, 14000 rpm)**.

5. Discard eluted substance and put filter back on. (Do NOT mix Buffer RLT or RW1 with bleach when discarding. Contact with acids forms highly reactive guanidine salts and liberates very toxic gas)
6. Add **350 µl Buffer RW1** to column and centrifuge **(15 sec, 14000 rpm)**.
7. Discard eluted substance and put filter back on.
8. Add **10 µl DNase I** (lyophilized DNase I is resuspended in 550 µl RNase-free water) to **70 µl Buffer RDD** for each sample.
9. Add **80 µl of DNase/RDD solution** directly onto RNeasy membrane and incubate at **room temperature for 15 min**.
10. Add **350 µl Buffer RW1** to column and centrifuge **(15 sec, 14000 rpm)**.
11. Discard eluted substance and put filter back on.
12. Add **500 µl Buffer RPE** (add 44 ml of 96-100% ethanol to starting 11 ml of Buffer RPE concentrate before first time use) to column and centrifuge **(15 sec, 14000 rpm)**.
13. Discard eluted substance and put filter back on.
14. Add **500 µl Buffer RPE** to column and centrifuge **(2 min, 14000 rpm)**.
15. Discard eluted substance and transfer column to new 2 ml collection tube.
16. Centrifuge **(1 min, 14000 rpm)**.
17. Discard 2 ml collection tube, and transfer column to new 1.5 ml collection tube with cap.
18. Add **30-50 µl RNase-free water** and centrifuge **(1 min, 14000 rpm)**.
19. The water elutes the RNA into the collection tube – cap the tube and store RNA at -80˚C.

**Quantify and check purity of RNA**

*Materials*

MP Biomedicals RNase, DNase-free water (VWR IC821739; 500 ml)

Corning UV Transparent 96-well plate (Fisher 07-200-623; pack of 25)

*Protocol*

1. In a UV-transparent 96-well plate, add 2 µl of extracted RNA and 98 µl RNase-free water to 3 wells (dilution factor = 50).
2. In 3 more wells, add 100 µl RNase-free water.
3. Take absorbance readings at 260 nm and 280 nm light.
4. Quantity of RNA can be calculated using the following equations:
    - Corrected $A_{260}$ = average sample $A_{260}$ – average blank $A_{260}$
    - Concentation in µg/ml = (corrected $A_{260}$) * (44 µg/ml) * (dilution factor)

      (using above protocol, dilution factor = 50)
    - Total mass in µg = (µg/ml concentration value) * (µl volume) / 1000

      (volume of RNA extraction sample; using above extraction protocol, volume = 30-50 µl)
    - Volume in µl needed for 1 µg RNA = (1 µg RNA) * 1000 / (µg/ml concentration value)

      (1 ng to 5 µg RNA can be used for Reverse Transcription)
    - Volume of water in µl needed = 10 µl total volume – RNA volume determined above
5. Purity of RNA can be calculated using the following equation:

- Purity = $A_{260}$ / $A_{280}$
- This value should be between 1.5 and 1.9.

**Reverse Transcription**

**Reverse Transcription with SuperScript III Reverse Transcriptase**

*Materials*

Oligo(dT)$_{15}$ Primer (Promega C1101; 20 µg)

PCR Nucleotide Mix, 10 mM (Promega C1141; 200 µl)

SuperScript III Reverse Transcriptase (Invitrogen 18080-093 or 18080-044; 2000 or 10000 units)

Invitrogen RNaseOUT RNase Inhibitor, 40 units/ml (Invitrogen 10777-019; 5000 units)

*Protocol*

1. Add the following components to a nuclease-free PCR tube:
   - **1 ng to 5 µg total RNA: 10 µl**
   - **Oligo(dT)$_{15}$ (500 µg/ml): 1 µl**
   - **dNTP Mix (10 mM each): 1 µl**
   - **RNase, DNase-free water: to 12 µl final volume**
2. Heat mixture to 65˚C for 5 min and chill on ice for at least 1 min. Collect the contents of the tube by brief centrifugation and add:
   - **5X First-Strand Buffer (250 mM Tris-HCl, 375 mM KCl, 15 mM $MgCl_2$)**: **4 µl**

- **0.1 M DTT**: **1 µl**
- **RNaseOUT (40 units/µl)**: **1 µl**

3. Mix contents of the tube gently. Incubate at 42˚C for 2 min.
4. Add **1 µl (200 units) of SuperScript III RT** and mix by pipetting gently up and down.
5. Incubate at 50˚C for 30-60 min.
6. Inactivate the reaction by heating at 70˚C for 15 min.
7. Store cDNA at -20˚C.
8. Amplification of PCR targets (>1 kb) may require the removal of RNA complementary to the cDNA. To remove RNA complementary to the cDNA, add 1 µl (2 units) of *E. coli* RNase H and incubate at 37˚C for 20 min.

**Primer Preparation**

**Reconstitute primers (100 µM)**

*Materials*

Custom Primers/Oligonucleotides, desalted (Invitrogen; 25 nmol)

*Protocol*

1. Find the total nmoles from the information sheet that came with the primer.
2. The volume of DNase-free water needed to create a 100 µM stock can be calculated using the following equation:
   - Volume of DNase-free water in µl = (nmoles of primer) *1000 / (100 µM)

**Make 10 µM aliquots**

*Protocol*

1. Briefly spin the primers and add the needed amount of water for a 10-fold dilution.
2. Make a 10-fold dilution (1 part primer: 9 parts DNase-free water) to obtain a 10 µM aliquot.

**Polymerase Chain Reaction**

**Run PCR**

*Materials*

SYBR Green Master Mix (Applied Biosystems 4309155; 5 ml)

Applied Biosystems StepOnePlus Real-Time PCR System and Materials

- MicroAmp Fast 96-Well Reaction Plates, 0.1 ml (Applied Biosystems 4346906; 20 plates)
- MicroAmp Optical Adhesive Films (Applied Biosystems 4360954; 25 films)

OR

- MicroAmp Fast 8-Tube Strips, 0.1 ml (Applied Biosystems 4358293; 125 strips)
- MicroAmp Optical 8-Cap Strips (Applied Biosystems 4323032; 300 strips)
- MicroAmp 96-Well Trays for Veriflex Blocks (Applied Biosystems 4379983; 10 trays)

*Protocol*

1. Thaw the following components on ice:
    - SYBR Green mix
    - 10 µM forward primer of interest
    - 10 µM reverse primer of interest
    - Sample cDNA
2. To make **Master Mix**, count the number of wells needed for each primer, add 2, and multiply this number by the following to obtain enough Master Mix for all wells of the primer:
    - **12.5 µl SYBR Green mix**
    - **10.5 µl DNase-free water**
    - **0.5 µl 10 µM forward primer**
    - **0.5 µl 10 µM reverse primer**
3. Load PCR wells:
    - Load **24 µl of Master Mix** into each well for that primer (target sequence of interest).
    - Add **1 µl of sample cDNA** into the well with Master Mix and mix by pipetting up and down.

      (change pipette tips between each well)
4. After all wells are loaded, cover with optical tape or caps, and put entire plate on ice until ready to run PCR.
5. Load plate into StepOnePlus system:
    - Load plate into machine (A1 in upper-left, H12 in lower-right).
    - Open “StepOne Software v2.0” program.

- Click “Advanced Setup” button.
- Under “Experiment Properties,” enter an Experiment Name, select “StepOnePlus Instrument (96 Wells)” for the instrument, select “Quantitation – Comparative $C_T$ ($\Delta\Delta C_T$)” for the experiment, select “SYBR Green Reagents” for the reagent (melt curve is optional), and select “Standard” for the ramp speed.
- Under “Plate Setup,” add your targets and samples under “Define Targets and Samples,” changing the Reporter to “SYBR” and the Quencher to “None.” Under “Assign Targets and Samples,” assign the appropriate targets and samples to each well, selecting your control sample as the reference sample, GAPDH as the endogenous control, and “ROX” as the “dye to use as a passive reference.”
- Under “Run Method,” change the reaction volume to 25 µl and set the method to the following:
    - Hold at 95˚C for 10 min (100% ramp).
    - Cycle 40 times at 95˚C for 15 sec and 60˚C for 1 min, collecting data at 60˚C.
    - Optional melt curve: 95˚C for 15 sec, 60˚C for 1 min, and +0.3˚C ramp, ending at 95˚C for 15 sec and collecting data during the +0.3˚C ramp.
- Save the file.

  (Templates can be saved to reduce setup time.)
- Select “Start Run.”

- After the run, click “Analyze” (settings can be modified under “Analysis Settings”) and resave the file.
- Export results to Excel by clicking “Export…” and export “Results” as “One File” with “.xls” file type.

6. Analyze data using the following $\Delta\Delta C_T$ equation:
   - $\Delta C_{T,\ sample} = C_{T,\ sample,\ target} - C_{T,\ sample,\ GAPDH}$
   - $\Delta C_{T,\ reference} = C_{T,\ reference,\ target} - C_{T,\ reference,\ GAPDH}$
   - $\Delta\Delta C_T = \Delta C_{T,\ sample} - \Delta C_{T,\ reference}$
   - Fold regulation $= 2^{-\Delta\Delta CT}$

     $= 2^{-(\Delta CT,\ sample\ -\ \Delta CT,\ reference)}$

     $= 2^{-\Delta CT,\ sample} / 2^{-\Delta CT,\ reference}$

     $\mathbf{= 2^{-(CT,\ sample,\ target\ -\ CT,\ sample,\ GAPDH)} / 2^{-(CT,\ reference,\ target\ -\ CT,\ reference,\ GAPDH)}}$

     $= 2^{(CT,\ sample,\ GAPDH\ -\ CT,\ sample,\ target)} / 2^{(CT,\ reference,\ GAPDH\ -\ CT,\ reference,\ target)}$

     $= 2^{(CT,\ sample,\ GAPDH\ -\ CT,\ sample,\ target)\ -\ (CT,\ reference,\ GAPDH\ -\ CT,\ reference,\ target)}$

## A.11 Histology

1. Section samples at 10 um.
2. Deparaffinize using the autostainer.
3. Draw a circle around the samples using the PAP pen.
4. Wash by adding PBS to sections, remove PBS, repeat.

5. **Antigen Retrieval:** Add trypsin for 10 min at 37°C.
6. Wash by adding PBS to sections, remove PBS, repeat.
7. **Peroxidase Blocking:** Incubate sections in 0.3% H2O2 in Methanol solution for 15 minutes at room temperature.
    a. 10 ml methanol
    b. 100 µl $H_2O_2$.
8. Wash by adding PBS to sections, remove PBS, repeat.
9. **Serum Blocking:** incubate sections in normal serum (20 min) – species same as secondary antibody.
    **a. Normal Goat Serum Block Solution (3ml):**
        i. (2.6 ml of this solution) 1%BSA (stabilizer)
        ii. (60 ul) 2% goat serum (blocking)
        iii. (300 ul 1% gelatin) 0.1% cold fish skin gelatin (blocking) – do not use if staining for collagen
        iv. (30 ul) 0.1% Triton X-100 (penetration enhancer)
        v. (15 mg) 0.05% sodium azide (preservative)
        vi. Mix and store at 4 ºC.
10. Prepare the **working dilution of the primary** antibody in 1% BSA in 1X PBS (if using Ab for the first time you will need to run a series of dilutions to determine the optimal working concentration).
11. Blot off the blocking solution.
12. Use a 10 ul pipette to apply **primary antibody** to just the parts of the section with your specimen.

13. Incubate sections in a humid chamber **overnight**.
14. Wash by adding PBS to sections, remove PBS, repeat.
15. **Secondary Antibody:** incubate sections in **secondary antibody** conjugated to biotin in PBS for 30 minutes at room temperature – try a range of concentrations.
16. Wash by adding PBS to sections, remove PBS, repeat.
17. Add ABC reagent for 30 min.
    a. 5 ml PBS
    b. 2 drops A
    c. 2 drops B
    d. Let sit for 30 min before use
18. Wash by adding PBS to sections, remove PBS, repeat.
19. **Chromagen/Substrate:** incubate sections in peroxidase substrate solution (DAB) for 5-10 min (generally 5 min - prepare solution just before use).
    a. 1 ml substrate
    b. 20 ul chromogen
20. Wash by adding PBS to sections, remove PBS, repeat.
21. Coverslip.

# APPENDIX B

# SUPPLEMENTARY FIGURES

## B.1 Adhesion Studies

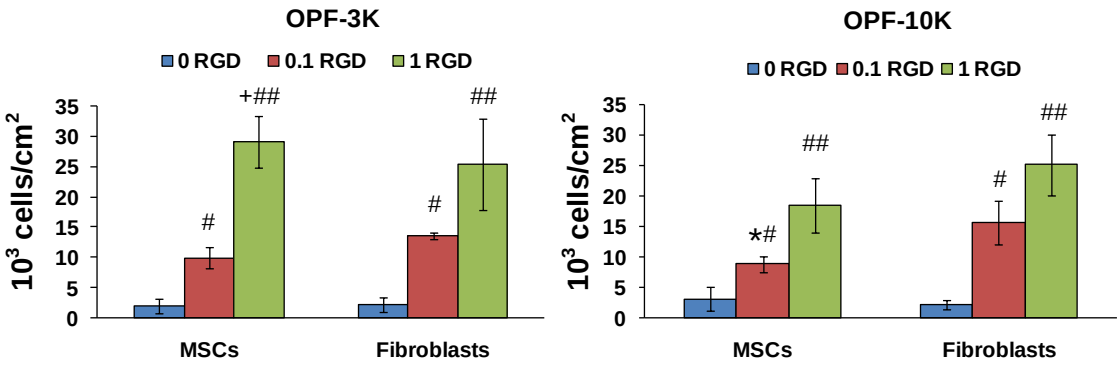


**Figure B.1. Number of adherent cells after 24h on OPF-3K hydrogels (left) or OPF-10K hydrogels (right) (n=4 ± std. dev.). p<0.05 compared to fibroblasts(*). p<0.05 compared to OPF-10K(+). p<0.05 compared to 0 RGD(#) or 0.1 RGD(#).**

OPF-3k or OPF-10k and PEG-DA were combined in a 1:1 wt/wt ratio and suspended in saline (75 wt% liquid). Polymer solutions were cross-linked in thin (0.7 mm) disc-shaped (14 mm radius) molds (10 min at 37 °C) using APS and TEMED thermal radial initiators (0.018 M). Hydrogels were fabricated with 0, 0.1, or 1 μmol RGD/g swollen hydrogel. Bovine ligament fibroblasts or bovine MSCs were seeded (39,750 cells/cm$^2$) on top of the thin or thick hydrogels in an area confined by stainless steel annuli (19 mm long, ID: 9.8 mm, OD: 15.5 mm). At 24 hours hydrogels were rinsed with saline to remove non-adherent cells and at least four representative phase contrast images per sample were taken. For quantification, the number of cells per image was counted and cell numbers from multiple hydrogels in a particular group were averaged (n≥4). These averages were divided by the area of the image to obtain the

cellular density in cells/cm$^2$. Data from studies was analyzed for significance using ANOVA followed by Tukey's Multiple Comparison Test ($p<0.05$).

### B.2 GAPDH Gene Expression for Chapter 4 Samples.

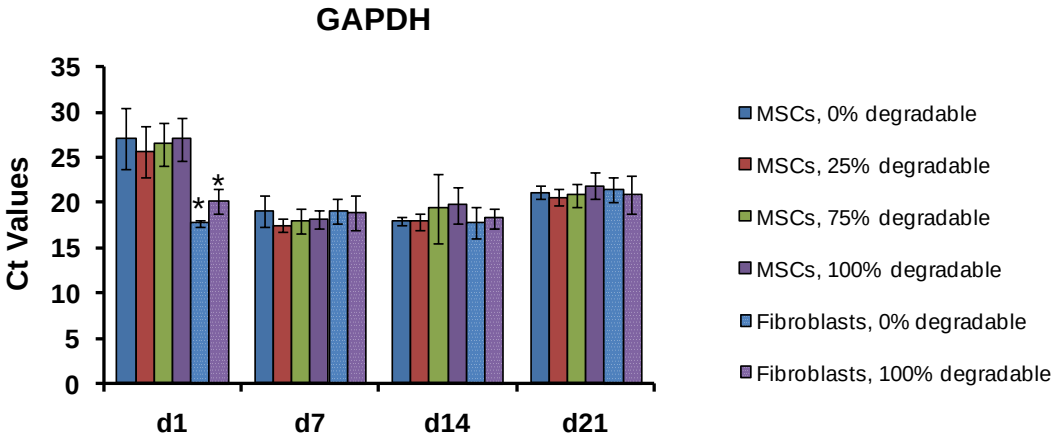


**Figure B.2. GAPDH gene expression in hMSCs or hACL fibroblasts over 21 days of culture in a range of enzymatically-cleavable hydrogels (n≥6 ±SD). GAPDH levels were similar in all sample types at a given time point except for day 1. $p<0.05$ compared to hMSCs in 0%, 25%, 75%, and 100% enzymatically-degradable hydrogels(*).**

### B.3 Fold Swelling With or Without RGD.

OPF-3k or OPF-10k and PEG-DA were combined in a 60:40 or 50:50 wt/wt ratio and suspended in saline (75 wt% liquid). Polymer solutions were cross-linked in thin (0.5 mm) disc-shaped (12 mm radius) molds (10 min at 37 °C) using APS and TEMED thermal radial initiators (0.018 M). Hydrogels were fabricated with 0 or 1 μmol RGD/g swollen hydrogel. After 7 days of culture, samples were removed (n≥4). Fold swelling was calculated by $W_w/W_d$ where $W_w$ is the weight of the hydrogel after culture and before drying, and $W_d$ is the weight of the hydrogel after vacuum-drying. Data between samples with RGD peptides and samples without RGD peptides were analyzed for

significance using two-tailed, homoscedasctic, t-tests ($p<0.05$). No significant differences were seen in fold swelling after the addition of the RGD peptide sequences.

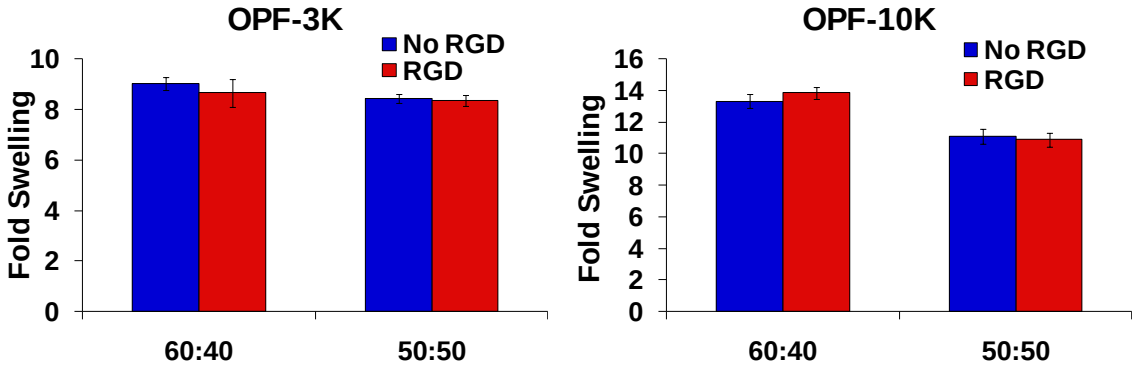


**Figure B.3. Fold swelling of hydrogels fabricated without any RGD or with 1 µmol RGD/g swollen hydrogel (n≥4 ±SD). No significant differences were found between samples with RGD peptides and samples without these sequences. 60:40 and 50:50 represent the ratio of OPF:PEG-DA (wt/wt) used to fabricate the hydrogels.**

# REFERENCES


1. Khatod, M., Amiel D. Ligament biochemistry and physiology. In: Pedowitz R.A., O'Connor J., Akeson W., eds. Daniel's knee injuries. Philadelphia: Lippincott Williams and Wilkins, 2003, pp. 31-42.

2. Butler, D.L., Dressler M, Awad H. Functional tissue engineering: Assessment of function in tendon and ligament repair. In: Guilak F., Butler D., Goldstein S., Mooney D., eds. Functional tissue engineering. New York: Springer, 2003, pp. 213-226.

3. Khatod, M., Akeson, W., Amiel, D. Ligament injury and repair. In: Pedowitz R., O'Connor J., Akeson W., eds. Daniel's knee injuries. Philadelphia: Lippincott Williams and Wilkins, 2003, pp. 185-201.

4. Louie, L., Yannas, I.V., Spector, M. Tissue engineered tendon. In: Patrick Jr. C.W., Mikos A.G., McIntire L.V., eds. Frontiers in Tissue Engineering. New York, NY: Elsevier Science Inc., 1998, pp. 412-442.

5. Kim, C.W., Pedowitz RA. Part A: Graft choices and the biology of graft healing. In: Pedowitz R.A., O'Connor J., Akeson W., eds. Daniel's knee injuries. Philadelphia: Lippincott Williams & Wilkins, 2003, pp. 435-491.

6. Nemzek, J., Arnoczky, S., Swenson, C. Retroviral transmission by the transplantation of connective-tissue allografts. An experimental study. J Bone Joint Surg Am **76**, 1036-1047, 1994.

7. O'Brien, S., Warren, R., Pavlov, H., Panariello, R., Wickiewicz, T. Reconstruction of the chronically insufficient anterior cruciate ligament with the central third of the patellar ligament. J Bone Joint Surg Am **73**, 218-96, 1991.

8. Cooper, J., Bailey, L., Carter, J., Castiglioni, C., Kofron, M., Ko, F., Laurencin, C. Evaluation of the anterior cruciate ligament, medial collateral ligament, Achilles tendon and patellar tendon as cell sources for tissue-engineered ligament. Biomaterials **27**, 2747-54, 2006.

9. Freedman, K.B., D'Amato, M.J., Nedeff, D.D., Kaz, A., Bach, B.R., Jr. Arthroscopic anterior cruciate ligament reconstruction: a metaanalysis comparing patellar tendon and hamstring tendon autografts. Am J Sports Med **31**, 2-11, 2003.

10. Vunjak-Novakovic, G., Altman, G., Horan, R., Kaplan, D.L. Tissue engineering of ligaments. Annu Rev Biomed Eng **6**, 131-56, 2004.

11. Altman, G.H., Horan, R.L., Martin, I., Farhadi, J., Stark, P.R., Volloch, V., Richmond, J.C., Vunjak-Novakovic, G., Kaplan, D.L. Cell differentiation by mechanical stress. FASEB J **16**, 270-2, 2002.

12. Martin, R., Burr, D., Sharkey, N. Mechanical properties of ligament and tendon. In: Skeletal tissue mechanics. New York: Springer, 1998, pp. 309-46.

13. Wang , J. Mechanobiology of tendon. J Biomech **39**, 1563-82, 2006.

14. Lin, T.W., Cardenas, L., Soslowsky, L.J. Biomechanics of tendon injury and repair. J Biomech **37**, 865-77, 2004.

15. Thomopoulos, S., Williams, G.R., Gimbel, J.A., Favata, M., Soslowsky, L.J. Variation of biomechanical, structural, and compositional properties along the tendon to bone insertion site. J Orthop Res **21**, 413-9, 2003.

16. Persikov, A., Brodsky, B. Unstable molecules form stable tissues. PNAS **99**, 1101-1103, 2002.

17. Scott-Burden, T. Extracellular matrix: The cellular environment. NIPS **9**, 110-115, 1994.

18. Amiel, D., Frank, C., Harwood, F., Fronek, J., Akeson, W. Tendons and ligaments: a morphological and biochemical comparison. J Orthop Res **1**, 257-65, 1984.

19. Derwin, K.A., Soslowsky, L.J., Kimura, J.H., Plaas, A.H. Proteoglycans and glycosaminoglycan fine structure in the mouse tail tendon fascicle. J Orthop Res **19**, 269-77, 2001.

20. Yoon, J., Halper, J. Tendon proteoglycans: biochemistry and function. J Musculoskelet Neuronal Interact **5**, 22-34, 2005.

21. Viidik, A. Interdependence between structure and function in collagenous tissues. In: Viidik A., Vuust J., eds. Biology of collagen. London: Academic Press, 1980, pp. 257-280.

22. Kuhn, K. The classical collagens: types I, II, and III. In: Mayne R., Burgeson R., eds. Structure and function of collagen types. Orlando: Academic Press, 1987, pp. 1-42.

23. Tanzer, M. Cross-linking. In: Ramachandran G., Reddi A., eds. Biochemistry of collagen. New York: Plenum Press, 1976, pp. 137-162.

24. Light, N., Bailey, A. Molecular structure and stabilization of the collagen fibre. In: Viidik A., Vuust J., eds. Biology of collagen. London: Academic Press, 1980, pp. 15-38.

25. Harwood, F.L., Amiel, D. Differential metabolic responses of periarticular ligaments and tendon to joint immobilization. J Appl Physiol **72**, 1687-91, 1992.

26. Hanson, D., Eyre, D. Molecular site specificity of pyridinoline and pyrrole cross-links in type I collagen of human bone. J Biol Chem **271**, 26508-16, 1996.

27. Knott, L., Bailey, A. Collagen biochemistry of avian bone: comparison of bone type and skeletal site. Br Poult Sci **40**, 371-9, 1999.

28. Vogel, K. What happens when tendons bend and twist? Proteoglycans. J Musculosklet Neuronal Interact **4**, 202-203, 2004.

29. Vogel, K., Meyers, A. Proteins in the tensile region of adult bovine deep flexor tendon. Clin Orthop Relat Res **367S**, S344-S355, 1999.

30. Danielson, K.G., Baribault, H., Holmes, D.F., Graham, H., Kadler, K.E., Iozzo, R.V. Targeted disruption of decorin leads to abnormal collagen fibril morphology and skin fragility. J Cell Biol **136**, 729-43, 1997.

31. Bradshaw, A., Sage, E. Regulation of cell behavior by matricellular proteins. In: Lanza R., Langer R., Vacanti J., eds. Principles of tissue engineering. San Diego: Academic Press, 2000, pp. 119-127.

32. Probstmeier, R., Pesheva, P. Tenascin-C inhibits beta-1 integrin-dependent cell adhesion and neurite outgrowth on fibronectin by a disialoganglioside-mediated signaling mechanism. Glycobiology **9**, 101-114, 1999.

33. Sharma, P., Maffulli, N. Biology of tendon injury: healing, modeling and remodeling. J Musculoskelet Neuronal Interact **6**, 181-90, 2006.

34. Lim, J.J., Temenoff, J.S. Tendon and ligament tissue engineering: Restoring tendon/ligament and its interfaces. In: Meyer U., Handschel J., Meyer T., Wiesmann H.P., eds. Fundamentals of Tissue Engineering and Regenerative Medecine. Berlin: Springer, 2009.

35. Tallon, C., Maffulli, N., Ewen, S.W. Ruptured Achilles tendons are significantly more degenerated than tendinopathic tendons. Med Sci Sports Exerc **33**, 1983-90, 2001.

36. Cerullo, G., Puddu, G., Cipolla, M., Selvanetti, A. Results of arthroscopic treatment of degenerative meniscal tears (meniscosis). Ital J Orthop Traumatol **17**, 513-22, 1991.

37. Arndt, A.N., Komi, P.V., Bruggemann, G.P., Lukkariniemi, J. Individual muscle contributions to the in vivo achilles tendon force. Clin Biomech (Bristol, Avon) **13**, 532-541, 1998.

38. Sheng, P., Jamsen, E., Lehto, M., Pajamaki, J., Halonen, P., Konttinen, Y. Revision total knee arthroplasty with the total condylar III system: a comparative analysis of 71 consecutive cases of osteoarthritis or inflammatory arthritis. Acta Orthop **77**, 512-8, 2006.

39. Covey, D., Sapega, A. Anatomy and function of the posterior cruciate ligament. Clin Sports Med **13**, 509-516, 1994.

40. Monto, R., Cameron-Donaldson, M., Close, M., Ho, C., Hawkins, R. Magnetic resonance imaging in the evaluation of tibial eminence fractures in adults. J Knee Surg **19**, 187-90, 2006.

41. Nakasa, T., Fukuhara, K., Adachi, N., Ochi, M. Evaluation of anterior talofibular ligament lesion using 3-dimensional computed tomography. J Comput Assist Tomogr **30**, 543-7, 2006.

42. Heller, J., Bernt, R., Seeger, T., Weissenback, A., Tuchler, H., Resnik, D. MR-imaging of anterior tibiotalar impingement syndrome: agreement, sensitivity and specificity of MR-imaging and indirect MR-arthography. Eur J Radiol **58**, 450-60, 2006.

43. Yadao, M., Savoie, F., Field, L. Posterolateral rotary instability of the elbow. Instr Course Lect **53**, 607-14, 2004.

44. Arvind, C., Hargreaves, D. Table top relocation test--New clinical test for posterolateral rotary instability of the elbow. J Shoulder Elbow Surg **15**, 500-1, 2006.

45. Ebrahim, F., DeMaeseneer, M., Jager, T., Marcelis, S., Jamadar, D., Jacobson, J. US diagnosis of UCL tears of the thumb and Stener lesions: technique, pattern-based approach, and differential diagnosis. Radiographics **26**, 1007-20, 2006.

46. Milz, S., Aktas, T., Putz, R., Benjamin, M. Expression of extracellular matrix molecules typical of articular cartilage in the human scapholunate interosseous ligament. J Anat **208**, 671-9, 2006.

47. Lin, W., Wu, C., Su, C., Fan, K., Tseng, I., Chiu, Y. Surgical treatment of acute complete acromioclavicular dislocation: comparison of coracoclavicular screw fixation supplemented with tension band wiring of ligament transfer. Chang Gung Med J **29**, 182-9, 2006.

48. Jin, C.Z., Kim, H., Min, B. Surgical treatment for distal clavicle fracture associated with coracoclavicular ligament rupture using a cannulated screw fixation technique. J Trauma **60**, 1358-61, 2006.

49. Homsi, C., Bordalo-Rodrigues, M., daSilva, J., Stump, X. Ultrasound in adhesive capsulitis of the shoulder: is assessment of the coracohumeral ligament a valuable diagnostic tool? Skeletal Radiol **35**, 673-8, 2006.

50. Cormier, G., Berthelot, J., Maugars, Y. Gluteus tendon rupture is underrecognized by French orthopedic surgeons: results of a mail survey. Joint Bone Spine **73**, 411-3, 2006.

51. Dahlgren, L.A., Mohammed, H.O., Nixon, A.J. Temporal expression of growth factors and matrix molecules in healing tendon lesions. J Orthop Res **23**, 84-92, 2005.

52. Galatz, L.M., Sandell, L.J., Rothermich, S.Y., Das, R., Mastny, A., Havlioglu, N., Silva, M.J., Thomopoulos, S. Characteristics of the rat supraspinatus tendon during tendon-to-bone healing after acute injury. J Orthop Res **24**, 541-50, 2006.

53. Woo, S.L., Watanabe, N., Hildebrand, K. Tissue engineering of ligament healing. In: Huard J., Fu F.H., eds. Gene therapy and tissue engineering in orthopaedic and sports medicine. Boston: Birkhauser, 2000.

54. Riley, G.P., Curry, V., DeGroot, J., van El, B., Verzijl, N., Hazleman, B.L., Bank, R.A. Matrix metalloproteinase activities and their relationship with collagen remodelling in tendon pathology. Matrix Biol **21**, 185-95, 2002.

55. Woo, S.L., Abramowitch, S.D., Kilger, R., Liang, R. Biomechanics of knee ligaments: injury, healing, and repair. J Biomech **39**, 1-20, 2006.

56. Petrigliano, F.A., McAllister, D.R., Wu, B.M. Tissue engineering for anterior cruciate ligament reconstruction: a review of current strategies. Arthroscopy **22**, 441-51, 2006.

57. Guidoin, M.F., Marois, Y., Bejui, J., Poddevin, N., King, M.W., Guidoin, R. Analysis of retrieved polymer fiber based replacements for the ACL. Biomaterials **21**, 2461-74, 2000.

58. Nau, T., Lavoie, P., Duval, N. A new generation of artificial ligaments in reconstruction of the anterior cruciate ligament. Two-year follow-up of a randomised trial. J Bone Joint Surg Br **84**, 356-60, 2002.

59. Legnani, C., Ventura, A., Terzaghi, C., Borgo, E., Albisetti, W. Anterior cruciate ligament reconstruction with synthetic grafts. A review of literature. Int Orthop **34**, 465-71, 2010.

60. Goulet, F., Rancourt, D., Cloutier, R., Germain, L., Poole, A., Auger, F. Tendons and ligaments. In: Lanze R., Langer R., Vacanti J., eds. Principles of tissue engineering. San Diego: Academic Press, 2000, pp. 711-22.

61. Cooper, J.A., Bailey, L.O., Carter, J.N., Castiglioni, C.E., Kofron, M.D., Ko, F.K., Laurencin, C.T. Evaluation of the anterior cruciate ligament, medial collateral ligament, Achilles tendon and patellar tendon as cell sources for tissue-engineered ligament. Biomaterials **27**, 2747-2754, 2006.

62. Funakoshi, T., Majima, T., Iwasaki, N., Yamane, S., Masuko, T., Minami, A., Harada, K., Tamura, H., Tokura, S., Nishimura, S.-I. Novel chitosan-based hyaluronan hybrid polymer fibers as a scaffold in ligament tissue engineering. J Biomed Mater Res A **74A**, 338-346, 2005.

63. Majima, T., Funakosi, T., Iwasaki, N., Yamane, S.-T., Harada, K., Nonaka, S., Minami, A., Nishimura, S.-I. Alginate and chitosan polyion complex hybrid fibers for scaffolds in ligament and tendon tissue engineering. J Orthop Sci **10**, 302-307, 2005.

64. Altman, G.H., Horan, R.L., Lu, H.H., Moreau, J., Martin, I., Richmond, J.C., Kaplan, D.L. Silk matrix for tissue engineered anterior cruciate ligaments. Biomaterials **23**, 4131-4141, 2002.

65. Lu, H.H., Cooper, J.A., Manuel, S., Freeman, J.W., Attawia, M.A., Ko, F.K., Laurencin, C.T. Anterior cruciate ligament regeneration using braided biodegradable scaffolds: in vitro optimization studies. Biomaterials **26**, 4805-4816, 2005.

66. Drury, J.L., Mooney, D.J. Hydrogels for tissue engineering: scaffold design variables and applications. Biomaterials **24**, 4337-51, 2003.

67. Butler, D.L., Awad, H.A. Perspectives on cell and collagen composites for tendon repair. Clin Orthop Relat Res, S324-32, 1999.

68. Awad, H.A., Butler, D.L., Harris, M.T., Ibrahim, R.E., Wu, Y., Young, R.G., Kadiyala, S., Boivin, G.P. In vitro characterization of mesenchymal stem cell-seeded collagen scaffolds for tendon repair: effects of initial seeding density on contraction kinetics. J Biomed Mater Res **51**, 233-240, 2000.

69. Awad, H.A., Boivin, G.P., Dressler, M.R., Smith, F.N.L., Young, R.G., Butler, D.L. Repair of patellar tendon injuries using a cell-collagen composite. J Orthop Res **21**, 420-431, 2003.

70. Gentleman, E., Lay, A.N., Dickerson, D.A., Nauman, E.A., Livesay, G.A., Dee, K.C. Mechanical characterization of collagen fibers and scaffolds for tissue engineering. Biomaterials **24**, 3805-3813, 2003.

71. Ide, A., Sakane, M., Chen, G., Shimojo, H., Ushida, T., Tateishi, T., Wadano, Y., Miyanaga, Y. Collagen hybridization with poly(l-lactic acid) braid promotes ligament cell migration. Mater Sci Eng C **C17**, 95-99, 2001.

72. Torres, D.S., Freyman, T.M., Yannas, I.V., Spector, M. Tendon cell contraction of collagen-GAG matrices in vitro: effect of cross-linking. Biomaterials **21**, 1607-19, 2000.

73. Murray, M.M., Spector, M. The migration of cells from the ruptured human anterior cruciate ligament into collagen-glycosaminoglycan regeneration templates in vitro. Biomaterials **22**, 2393-402, 2001.

74. Laurencin, C.T., Ambrosio, A.M.A., Borden, M.D., Cooper Jr., J.A. Tissue engineering: orthopedic applications. Ann Rev of Biomed Eng **1**, 19-46, 1999.

75. Koob, T.J. Biomimetic approaches to tendon repair. Comp Biochem Physiol A Mol Integr Physiol **133**, 1171-92, 2002.

76. Cornwell, K.G., Downing, B.R., Pins, G.D. Characterizing fibroblast migration on discrete collagen threads for applications in tissue regeneration. J Biomed Mater Res A **71**, 55-62, 2004.

77. Gentleman, E., Livesay, G.A., Dee, K.C., Nauman, E.A. Development of ligament-like structural organization and properties in cell-seeded collagen scaffolds in vitro. Ann Biomed Eng **34**, 726-36, 2006.

78. Meaney Murray, M., Rice, K., Wright, R.J., Spector, M. The effect of selected growth factors on human anterior cruciate ligament cell interactions with a three-dimensional collagen-GAG scaffold. J Orthop Res **21**, 238-44, 2003.

79. Murray, M., Forsythe, B., Chen, F., Lee, S., Yoo, J., Atala, A., Steinert, A. The effect of thrombin on ACL fibroblast interactions with collagen hydrogels. J Orthop Res **24**, 508-15, 2006.

80. Henshaw, D., Attia, E., Bhargava, E., Hannafin, J. Canine ACL fibroblast integrin expression and cell alignment in response to cyclic tensile strain in three-dimensional collagen gels. J Orthop Res **24**, 481-90, 2006.

81. Musahl, V., Abramowitch, S., Gilbert, T., Tsuda, E., Wang , J., Badylak, S., Woo, S. The use of porcine small intestinal submucosa to enhance the healing of the medial collateral ligament--a functional tissue engineering study in rabbits. J Orthop Res **22**, 214-20, 2004.

82. Dejardin, L.M., Arnoczky, S.P., Ewers, B.J., Haut, R.C., Clarke, R.B. Tissue-engineered rotator cuff tendon using porcine small intestine submucosa: Histologic and mechanical evaluation in dogs. Am J Sports Med **29**, 175-84, 2001.

83. Derwin, K., Androjna, C., Spencer, E., Safran, O., Bauer, T.W., Hunt, T., Caplan, A., Iannotti, J. Porcine small intestine submucosa as a flexor tendon graft. Clin Orthop Relat Res **423**, 245-52, 2004.

84. Rodeo, S.A., Maher, S.A., Hidaka, C. What's new in orthopaedic research. J Bone Joint Surg Am **86A**, 2085-95, 2004.

85. Funakoshi, T., Majima, T., Iwasaki, N., Suenaga, N., Sawaguchi, N., Shimode, K., Minami, A., Harada, K., Nishimura, S. Application of tissue engineering techniques for rotator cuff regeneration using a chitosan-based hyaluronan hybrid fiber scaffold. Am J Sports Med **33**, 1193-201, 2005.

86. Chen, J., Altman, G.H., Karageorgiou, V., Horan, R., Collette, A., Volloch, V., Colabro, T., Kaplan, D.L. Human bone marrow stromal cell and ligament fibroblast responses on RGD-modified silk fibers. J Biomed Mater Res A **67**, 559-70, 2003.

87. Altman, G.H., Diaz, F., Jakuba, C., Calabro, T., Horan, R.L., Chen, J., Lu, H., Richmond, J., Kaplan, D. Silk-based biomaterials. Biomaterials **24**, 401-16, 2003.

88. Martinek, V., Latterman, C., Usas, A., Abramowitch, S., Woo, S.L., Fu, F.H., Huard, J. Enhancement of tendon-bone integration of anterior cruciate ligament grafts with bone morphogenetic protein-2 gene transfer: a histological and biomechanical study. J Bone Joint Surg Am **84-A**, 1123-31, 2002.

89. Ahmed, Z., Underwood, S., Brown, R.A. Low concentrations of fibrinogen increase cell migration speed on fibronectin/fibrinogen composite cables. Cell Motil Cytoskeleton **46**, 6-16, 2000.

90. Zustiak, S.P., Leach, J.B. Hydrolytically degradable poly(ethylene glycol) hydrogel scaffolds with tunable degradation and mechanical properties. Biomacromolecules **11**, 1348-57, 2010.

91. Altman , G.H., Lu, H., Horan, R.L., Calabro, T., Ryder, D., Kaplan, D., Stark, P., Martin, I., Richmond John, C., Vunjak-Novakovic, G. Advanced bioreactor with controlled application of multi-dimensional strain for tissue engineering. J Biomech Eng **124**, 742-9, 2002.

92. Laurencin, C.T., Freeman, J.W. Ligament tissue engineering: An evolutionary materials science approach. Biomaterials **26**, 7530-7536, 2005.

93. Ouyang, H.W., Toh, S.L., Goh, J., Tay, T.E., Moe, K. Assembly of bone marrow stromal cell sheets with knitted poly (L-lactide) scaffold for engineering ligament analogs. J Biomed Mater Res B Appl Biomater **75B**, 264-271, 2005.

94. Cooper, J.A., Lu, H.H., Ko, F.K., Freeman, J.W., Laurencin, C.T. Fiber-based tissue-engineered scaffold for ligament replacement: design considerations and in vitro evaluation. Biomaterials **26**, 1523-1532, 2004.

95. Qin, T.W., Yang, Z.M., Wu, Z.Z., Xie, H.Q., Qin, J., Cai, S.X. Adhesion strength of human tenocytes to extracellular matrix component-modified poly(DL-lactide-co-glycolide) substrates. Biomaterials **26**, 6635-42, 2005.

96. Ge, Z., Yang, F., Goh, J.C., Ramakrishna, S., Lee, E.H. Biomaterials and scaffolds for ligament tissue engineering. J Biomed Mater Res A **77**, 639-52, 2006.

97. Murray, A.W., Macnicol, M.F. 10-16 year results of Leeds-Keio anterior cruciate ligament reconstruction. Knee **11**, 9-14, 2004.

98. van Heerwaarden, R.J., Stellinga, D., Frudiger, A.J. Effect of pretension in reconstructions of the anterior cruciate ligament with a Dacron prosthesis. A retrospective study. Knee Surg Sports Traumatol Arthrosc **3**, 202-8, 1996.

99. Roolker, W., Patt, T.W., van Dijk, C.N., Vegter, M., Marti, R.K. The Gore-Tex prosthetic ligament as a salvage procedure in deficient knees. Knee Surg Sports Traumatol Arthrosc **8**, 20-5, 2000.

100. Noth, U., Schupp, K., Heymer, A., Kall, S., Jakob, F., Schutze, N., Baumann, B., Barthel, T., Eulert, J., Hendrich, C. Anterior cruciate ligament constructs fabricated from human mesenchymal stem cells in a collagen type I hydrogel. Cytotherapy **7**, 447-55, 2005.

101. Bryant, S.J., Anseth, K.S. Controlling the spatial distribution of ECM components in degradable PEG hydrogels for tissue engineering cartilage. J Biomed Mater Res A **64**, 70-9, 2003.

102. Rydholm, A.E., Bowman, C.N., Anseth, K.S. Degradable thiol-acrylate photopolymers: polymerization and degradation behavior of an in situ forming biomaterial. Biomaterials **26**, 4495-506, 2005.

103. Temenoff, J., Park, H., Jabbari, E., Conway, D., Sheffield, T., Ambrose, C., Mikos, A. Thermally cross-linked oligo(poly(ethylene glycol) fumarate) hydrogels support osteogenic differentiation of encapsulated marrow stromal cells in vitro. Biomacromolecules **5**, 5-10, 2004.

104. Shin, H., Ruhe, P., Mikos, A., Jansen, J. In vivo bone and soft tissue response to injectable, biodegradable oligo(poly(ethylene glycol) fumarate) hydrogels. Biomaterials **24**, 3201-3211, 2003.

105. Shin, H., Temenoff, J., Mikos, A. In vitro cytotoxicity of unsaturated oligo[poly(ethylene glycol) fumarate] macromers and their cross-linked hydrogels. Biomacromolecules **4**, 522-560, 2003.

106. Jo, S., Shin, H., Shung, A., Fisher, J., Mikos, A. Synthesis and characterization of oligo(poly(ethylene glycol) fumarate) macromer. Macromolecules **34**, 2839-44, 2001.

107. Temenoff, J., Athanasiou, K., LeBaron, R., Mikos, A. Effect of poly(ethylene glycol) molecular weight on tensile and swelling properties of oligo(poly(ethylene glycol) fumarate) hydrogels for cartilage tissue engineering. J Biomed Matr Res **59**, 429-37, 2002.

108. Shin, H., Jo, S., Mikos, A.G. Modulation of marrow stromal osteoblast adhesion on biomimetic oligo[poly(ethylene glycol) fumarate] hydrogels modified with Arg-Gly-Asp peptides and a poly(ethyleneglycol) spacer. J Biomed Mater Res **61**, 169-79, 2002.

109. Hern, D.L., Hubbell, J.A. Incorporation of adhesion peptides into nonadhesive hydrogels useful for tissue resurfacing. J Biomed Mater Res **39**, 266-76, 1998.

110. Temenoff, J.S., Park, H., Jabbari, E., Sheffield, T.L., LeBaron, R.G., Ambrose, C.G., Mikos, A.G. In vitro osteogenic differentiation of marrow stromal cells encapsulated in biodegradable hydrogels. J Biomed Mater Res A **70**, 235-44, 2004.

111. Shin, H., Jo, S., Mikos, A. Modulation of marrow stromal osteoblast adhesion on biomimetic oligo[poly(ethylene glycol) fumarate] hydrogels modified with Arg-Gly-Asp peptides and a poly(ethylene glycol) spacer. J Biomed Matr Res **61**, 169-79, 2002.

112. West, J.L., Hubbell, J.A. Polymeric biomaterials with degradation sites for proteases involved in cell migration. Macromolecules **32**, 241-44, 1999.

113. Lee, S.H., Moon, J.J., Miller, J.S., West, J.L. Poly(ethylene glycol) hydrogels conjugated with a collagenase-sensitive fluorogenic substrate to visualize collagenase activity during three-dimensional cell migration. Biomaterials **28**, 3163-70, 2007.

114. Steinbrink, D.R., Bond, M.D., Van Wart, H.E. Substrate specificity of beta-collagenase from Clostridium histolyticum. J Biol Chem **260**, 2771-6, 1985.

115. GM6001 Product data sheet. Enzo Life Sciences; 2010.
116. Trieb, K., Blahovec, H., Brand, G., Sabeti, M., Dominkus, M., Kotz, R. In vivo and in vitro cellular ingrowth into a new generation of artificial ligaments. Eur Surg Res **36**, 148-51, 2004.

117. Lee, C.H., Shin, H.J., Cho, I.H., Kang, Y.-M., Kim, I.A., Park, K.-D., Shin, J.-W. Nanofiber alignment and direction of mechanical strain affect the ECM production of human ACL fibroblast. Biomaterials **26**, 1261-1270, 2004.

118. Triantafillopoulos, I.K., Banes, A.J., Bowman, K.F., Jr., Maloney, M., Garrett, W.E., Jr., Karas, S.G. Nandrolone decanoate and load increase remodeling and strength in human supraspinatus bioartificial tendons. Am J Sports Med **32**, 934-43, 2004.

119. Butler, D.L., Juncosa, N., Dressler, M.R. Functional efficacy of tendon repair processes. Annu Rev Biomed Eng **6**, 303-29, 2004.

120. Schulze-Tanzil, G., Mobasheri, A., Clegg, P.D., Sendzik, J., John, T., Shakibaei, M. Cultivation of human tenocytes in high-density culture. Histochem Cell Biol **122**, 219-28, 2004.

121. Karamuk, E., Mayer, J., Raeber, G. Tissue engineered composite of a woven fabric scaffold with tendon cells, response on mechanical simulation in vitro. Compos Sci Tech **64**, 885-891, 2004.

122. Yang, Z., Xie, H., Li, T. Tissue engineering of the musculo-skeletal system--basic research and clinical applications. Hand Surg **5**, 49-55, 2000.

123. Cristino, S., Grassi, F., Toneguzzi, S., Piacentini, A., Grigolo, B., Santi, S., Riccio, M., Tognana, E., Facchini, A., Lisignoli, G. Analysis of mesenchymal stem cells grown on a three-dimensional HYAFF 11-based prototype ligament scaffold. J Biomed Mater Res A **73A**, 275-283, 2005.

124. Caplan, A.I. Review: Mesenchymal stem cells: Cell-based reconstructive therapy in orthopedics. Tissue Eng **11**, 1198-211, 2005.

125. Doroski, D.M., Levenston, M.E., Temenoff, J.S. Cyclic tensile culture promotes fibroblastic differentiation of marrow stromal cells encapsulated in poly(ethylene glycol)-based hydrogels. Tissue Eng Part A **16**, 3457-66, 2010.

126. Nieponice, A., Maul, T., Cumer, J., soletti, L., Vorp, D. Mechanical stimulation induces morphological and phenotypic changes in bone marrow-derived progenitor cells within a three-dimensional fibrin matrix. J Biomed Matr Res A **81**, 523-30, 2007.

127. Lee, I., Wang, J., Lee, Y., Young, T. The differentiation of mesenchymal stem cells by mechanical stress or/and co-culture system. Biochem Biophys Res Commun **352**, 147-52, 2007.

128. Hannafin, J., Attia, E., Henshaw, R., Warren, R., Bhargava, M. Effect of cyclic strain and plating matrix on cell proliferation and integrin expression by ligament fibroblasts. J Orthop Res **24**, 149-58, 2006.

129. Park, J., Chu, J., Cheng, C., Chen, F., Chen, D., Li, S. Differential effects of equiaxial and uniaxial strain on mesenchymal stem cells. Biotechnol Bioeng **88**, 359-68, 2004.

130. Webb, K., Hitchcock, R., Smeal, R., Li, W., Gray, S., Tresco, P. Cyclic strain increases fibroblast proliferation, matrix accumulation, and elastic modulus of fibroblast-seeded polyurethane constructs. J Biomech **39**, 1136-44, 2006.

131. Bojsen-Moller, J., Brogaard, K., Have, M., Stryger, H., Kjaer, M., Aagaard, P., Magnusson, S. Passive knee joint range of motion is unrelated to the mechanical properties of the patellar tendon. Scand J Med Sci Sports, 2006.

132. Maganaris, C., Paul, J. Tensile properties of the in vivo human gastrocnemius tendon. J Biomech **35**, 1639-46, 2002.

133. Screen, H.R., Shelton, J.C., Bader, D.L., Lee, D.A. Cyclic tensile strain upregulates collagen synthesis in isolated tendon fascicles. Biochem Biophys Res Commun **336**, 424-9, 2005.

134. Waggett, A., Benjamin, M., Ralphs, J. Connexin 32 and 43 gap junctions differentially modulate tenocyte response to cyclic mechanical load. Eur J Cell biol **85**, 1145-54, 2006.

135. Henshaw, D., Attia, E., Bhargava, M., Hannafin, J. Canine ACL fibroblast integrin expression and cell alignment in response to cyclic tensile strain in three-dimensional collagen gels. J Orthop Res **24**, 481-90, 2006.

136. Barkhausen, T., van Griensven, M., Zeichen, J., Bosch, U. Modulation of cell functions of human tendon fibroblasts by different repetitive cyclic mechanical stress patterns. Exp Toxicol Pathol **55**, 153-8, 2003.

137. Lavagnino, M., Arnoczky, S.P., Tian, T., Vaupel, Z. Effect of amplitude and frequency of cyclic tensile strain on the inhibition of MMP-1 mRNA expression in tendon cells: an in vitro study. Connect Tissue Res **44**, 181-7, 2003.

138. Yang, G., Crawford, R., Wang, J. Proliferation and collagen production of human patellar tendon fibroblasts in response to cyclic uniaxial stretching in serum-free conditions. J Biomech **37**, 1543-50, 2004.

139. Connelly, J. Regulatory mechanisms in the chondrogenesis of mesenchymal progenitors: The roles of cyclic tensile loading and cell-matrix interactions. Department of Bioengineering, Georgia Institute of Technology, Atlanta, 2007.

140. Khatod, M., Akeson, W.H., Amiel, D. Ligament injury and repair. In: Pedowitz R.A., O'Connor J.J., Akeson W.H., eds. Daniel's Knee Injuries. Philadelphia, PA: Lippincott Williams and Wilkins, 2003, pp. 185-201.

141. Fox, S.I. Human Physiology. Boston: McGraw Hill; 2002.

142. Zhang, J., Bai, S., Zhang, X., Nagase, H., Sarras, M.P., Jr. The expression of novel membrane-type matrix metalloproteinase isoforms is required for normal development of zebrafish embryos. Matrix Biol **22**, 279-93, 2003.

143. Kerkela, E., Bohling, T., Herva, R., Uria, J.A., Saarialho-Kere, U. Human macrophage metalloelastase (MMP-12) expression is induced in chondrocytes during fetal development and malignant transformation. Bone **29**, 487-93, 2001.

144. Gepstein, A., Shapiro, S., Arbel, G., Lahat, N., Livne, E. Expression of matrix metalloproteinases in articular cartilage of temporomandibular and knee joints of mice during growth, maturation, and aging. Arthritis Rheum **46**, 3240-50, 2002.

145. Murphy, G., Nagase, H. Progress in matrix metalloproteinase research. Mol Aspects Med **29**, 290-308, 2008.

146. Tang, Z., Yang, L., Xue, R., Zhang, J., Wang, Y., Chen, P.C., Sung, K.L. Differential expression of matrix metalloproteinases and tissue inhibitors of metalloproteinases in anterior cruciate ligament and medial collateral ligament fibroblasts after a mechanical injury: involvement of the p65 subunit of NF-kappaB. Wound Repair Regen **17**, 709-16, 2009.

147. Chakraborti, S., Mandal, M., Das, S., Mandal, A., Chakraborti, T. Regulation of matrix metalloproteinases: An overview. Molec and Cell Biochem **253**, 269-85, 2003.

148. Van Wart, H.E., Birkedal-Hansen, H. The cysteine switch: a principle of regulation of metalloproteinase activity with potential applicability to the entire matrix metalloproteinase gene family. Proc Natl Acad Sci U S A **87**, 5578-82, 1990.

149. Sternlicht, M.D., Werb, Z. How matrix metalloproteinases regulate cell behavior. Annu Rev Cell Dev Biol **17**, 463-516, 2001.

150. Hadler-Olsen, E., Fadnes, B., Sylte, I., Uhlin-Hansen, L., Winberg, J.O. Regulation of matrix metalloproteinase activity in health and disease. FEBS J **278**, 28-45.

151. Woessner, J.F., Jr. The family of matrix metalloproteinases. Ann N Y Acad Sci **732**, 11-21, 1994.

152. Barrett, A.J., Starkey, P.M. The interaction of alpha 2-macroglobulin with proteinases. Characteristics and specificity of the reaction, and a hypothesis concerning its molecular mechanism. Biochem J **133**, 709-24, 1973.

153. Baker, A.H., Edwards, D.R., Murphy, G. Metalloproteinase inhibitors: biological actions and therapeutic opportunities. J Cell Sci **115**, 3719-27, 2002.

154. Wang, J.H. Mechanobiology of tendon. J Biomech **39**, 1563-82, 2006.

155. Chung, L., Dinakarpandian, D., Yoshida, N., Lauer-Fields, J.L., Fields, G.B., Visse, R., Nagase, H. Collagenase unwinds triple-helical collagen prior to peptide bond hydrolysis. EMBO J **23**, 3020-30, 2004.

156. Mitchell, P.G., Magna, H.A., Reeves, L.M., Lopresti-Morrow, L.L., Yocum, S.A., Rosner, P.J., Geoghegan, K.F., Hambor, J.E. Cloning, expression, and type II collagenolytic activity of matrix metalloproteinase-13 from human osteoarthritic cartilage. J Clin Invest **97**, 761-8, 1996.

157. Monovich, L.G., Tommasi, R.A., Fujimoto, R.A., Blancuzzi, V., Clark, K., Cornell, W.D., Doti, R., Doughty, J., Fang, J., Farley, D. and others. Discovery of potent, selective, and orally active carboxylic acid based inhibitors of matrix metalloproteinase-13. J Med Chem **52**, 3523-38, 2009.

158. Lovejoy, B., Welch, A.R., Carr, S., Luong, C., Broka, C., Hendricks, R.T., Campbell, J.A., Walker, K.A., Martin, R., Van Wart, H. and others. Crystal structures of MMP-1 and -13 reveal the structural basis for selectivity of collagenase inhibitors. Nat Struct Biol **6**, 217-21, 1999.

159. Butler, D.L., Dressler, M., Awad, H. Functional tissue engineering: Assessment of function in tendon and ligament repair. In: Guilak F., Butler D., Goldstein S., Mooney D., eds. Functional Tissue Engineering. New York, NY: Springer, 2003, pp. 213-26.

160. Kessler, M.A., Behrend, H., Henz, S., Stutz, G., Rukavina, A., Kuster, M.S. Function, osteoarthritis and activity after ACL-rupture: 11 years follow-up results of conservative versus reconstructive treatment. Knee Surg Sports Traumatol Arthrosc **16**, 442-8, 2008.

161. Deng, D., Liu, W., Xu, F., Yang, Y., Zhou, G., Zhang, W.J., Cui, L., Cao, Y. Engineering human neo-tendon tissue in vitro with human dermal fibroblasts under static mechanical strain. Biomaterials **30**, 6724-30, 2009.

162. Chokalingam, K., Juncosa-Melvin, N., Hunter, S.A., Gooch, C., Frede, C., Florert, J., Bradica, G., Wenstrup, R., Butler, D.L. Tensile stimulation of murine stem cell-collagen sponge constructs increases collagen type I gene expression and linear stiffness. Tissue Eng Part A **15**, 2561-70, 2009.

163. Benhardt, H.A., Cosgriff-Hernandez, E.M. The role of mechanical loading in ligament tissue engineering. Tissue Eng Part B Rev **15**, 467-75, 2009.

164. Saber, S., Zhang, A.Y., Ki, S.H., Lindsey, D.P., Smith, R.L., Riboh, J., Pham, H., Chang, J. Flexor tendon tissue engineering: Bioreactor cyclic strain increases construct strength. Tissue Eng Part A **16**, 2085-90, 2010.

165. Lee, I.C., Wang, J.H., Lee, Y.T., Young, T.H. The differentiation of mesenchymal stem cells by mechanical stress or/and co-culture system. Biochem Biophys Res Commun **352**, 147-52, 2007.

166. Goshima, J., Goldberg, V.M., Caplan, A.I. The osteogenic potential of culture-expanded rat marrow mesenchymal cells assayed in vivo in calcium phosphate ceramic blocks. Clin Orthop Relat Res, 298-311, 1991.

167. Krych, A.J., Jackson, J.D., Hoskin, T.L., Dahm, D.L. A meta-analysis of patellar tendon autograft versus patellar tendon allograft in anterior cruciate ligament reconstruction. Arthroscopy **24**, 292-8, 2008.

168. Cukierman, E., Pankov, R., Stevens, D.R., Yamada, K.M. Taking cell-matrix adhesions to the third dimension. Science **294**, 1708-12, 2001.

169. Vanderploeg, E.J. Mechanotransduction in engineered cartilaginous tissues: in vitro oscillatory tensile loading [PhD thesis]. Department of Mechanical Engineering, Georgia Institute of Technology, Atlanta, Ga, 2006.

170. Temenoff, J.S., Park, H., Jabbari, E., Conway, D.E., Sheffield, T.L., Ambrose, C.G., Mikos, A.G. Thermally cross-linked oligo(poly(ethylene glycol) fumarate) hydrogels support osteogenic differentiation of encapsulated marrow stromal cells in vitro. Biomacromolecules **5**, 5-10, 2004.

171. Connelly, J.T., Mouw, J.K., Vanderploeg, E.J., Levenston, M.E. Cyclic tensile loading influences differentiation of bovine bone marrow stromal cells in a TGF-beta dependent manner. Abstract presented at the Orthopaedic Research Society Meeting, Washington, DC, 2005. Abstract no. 0946.

172. Connelly, J.T., Mouw, J.K., Vanderploeg, E.J., Levenston, M.E. Cyclic tensile loading alters gene expression and matrix synthesis of bone marrow stromal cells.

Abstract presented at the Orthopaedic Research Society Meeting, Chicago, Il, 2006. Abstract no. 0999.

173. Jo, S., Shin, H., Shung, A., Fisher, P., Mikos, A.G. Synthesis and characterization of oligo(poly(ethylene glycol) fumarate) macromer. Macromolecules **34**, 2839-2844, 2001.

174. Connelly, J.T., Vanderploeg, E.J., Mouw, J.K., Wilson, C., Levenston, M.E. Tensile loading modulates BMSC differentiation and the development of engineered fibrocartilage constructs. Tissue Eng Part A **16**, 1913-23, 2010.

175. Titushkin, I., Cho, M. Distinct membrane mechanical properties of human mesenchymal stem cells determined using laser optical tweezers. Biophys J **90**, 2582-91, 2006.

176. Nieponice, A., Maul, T.M., Cumer, J.M., Soletti, L., Vorp, D.A. Mechanical stimulation induces morphological and phenotypic changes in bone marrow-derived progenitor cells within a three-dimensional fibrin matrix. J Biomed Mater Res A **81**, 523-30, 2007.

177. McBeath, R., Pirone, D.M., Nelson, C.M., Bhadriraju, K., Chen, C.S. Cell shape, cytoskeletal tension, and RhoA regulate stem cell lineage commitment. Dev Cell **6**, 483-95, 2004.

178. Shin, H., Quinten Ruhe, P., Mikos, A.G., Jansen, J.A. In vivo bone and soft tissue response to injectable, biodegradable oligo(poly(ethylene glycol) fumarate) hydrogels. Biomaterials **24**, 3201-11, 2003.

179. Kuo, C.K., Tuan, R.S. Mechanoactive tenogenic differentiation of human mesenchymal stem cells. Tissue Eng Part A **14**, 1615-27, 2008.

180. Juncosa-Melvin, N., Matlin, K.S., Holdcraft, R.W., Nirmalanandhan, V.S., Butler, D.L. Mechanical stimulation increases collagen type I and collagen type III gene expression of stem cell-collagen sponge constructs for patellar tendon repair. Tissue Eng **13**, 1219-26, 2007.

181. Salinas, C.N., Anseth, K.S. The influence of the RGD peptide motif and its contextual presentation in PEG gels on human mesenchymal stem cell viability. J Tissue Eng Regen Med **2**, 296-304, 2008.

182. Ghazanfari, S., Tafazzoli-Shadpour, M., Shokrgozar, M.A. Effects of cyclic stretch on proliferation of mesenchymal stem cells and their differentiation to smooth muscle cells. Biochem Biophys Res Commun **388**, 601-5, 2009.

183. Abousleiman, R.I., Reyes, Y., McFetridge, P., Sikavitsas, V. Tendon tissue engineering using cell-seeded umbilical veins cultured in a mechanical stimulator. Tissue Eng Part A **15**, 787-95, 2009.

184. Gong, Z., Niklason, L.E. Small-diameter human vessel wall engineered from bone marrow-derived mesenchymal stem cells (hMSCs). FASEB J **22**, 1635-48, 2008.

185. Kearney, E.M., Prendergast, P.J., Campbell, V.A. Mechanisms of strain-mediated mesenchymal stem cell apoptosis. J Biomech Eng **130**, 061004, 2008.

186. Temenoff, J.S., Athanasiou, K.A., LeBaron, R.G., Mikos, A.G. Effect of poly(ethylene glycol) molecular weight on tensile and swelling properties of oligo(poly(ethylene glycol) fumarate) hydrogels for cartilage tissue engineering. J Biomed Mater Res **59**, 429-37, 2002.

187. Cruise, G.M., Scharp, D.S., Hubbell, J.A. Characterization of permeability and network structure of interfacially photopolymerized poly(ethylene glycol) diacrylate hydrogels. Biomaterials **19**, 1287-94, 1998.

188. Bryant, S.J., Anseth, K.S. Hydrogel properties influence ECM production by chondrocytes photoencapsulated in poly(ethylene glycol) hydrogels. J Biomed Mater Res **59**, 63-72, 2002.

189. Kinneberg, K.R., Nirmalanandhan, V.S., Juncosa-Melvin, N., Powell, H.M., Boyce, S.T., Shearn, J.T., Butler, D.L. Chondroitin-6-sulfate incorporation and mechanical stimulation increase MSC-collagen sponge construct stiffness. J Orthop Res, 2010.

190. Khatod, M., Amiel, D. Ligament biochemistry and physiology. In: Pedowitz R.A., O'Connor J.J., Akeson W.H., eds. Daniel's Knee Injuries. Philadelphia, PA: Lippincott Williams & Wilkins, 2003, pp. 31-42.

191. Jarvinen, T.A., Jozsa, L., Kannus, P., Jarvinen, T.L., Hurme, T., Kvist, M., Pelto-Huikko, M., Kalimo, H., Jarvinen, M. Mechanical loading regulates the expression of tenascin-C in the myotendinous junction and tendon but does not induce de novo synthesis in the skeletal muscle. J Cell Sci **116**, 857-66, 2003.

192. Mackie, E.J., Ramsey, S. Expression of tenascin in joint-associated tissues during development and postnatal growth. J Anat **188 ( Pt 1)**, 157-65, 1996.

193. Ge, Z., Goh, J.C., Lee, E.H. The effects of bone marrow-derived mesenchymal stem cells and fascia wrap application to anterior cruciate ligament tissue engineering. Cell Transplant **14**, 763-73, 2005.

194. Qiu, Y., Lim, J.J., Scott, L., Jr., Adams, R.C., Bui, H.T., Temenoff, J.S. PEG-based hydrogels with tunable degradation characteristics to control delivery of marrow stromal cells for tendon overuse injuries. Acta Biomater.

195. Chen, J., Horan, R.L., Bramono, D., Moreau, J.E., Wang, Y., Geuss, L.R., Collette, A.L., Volloch, V., Altman, G.H. Monitoring mesenchymal stromal cell developmental stage to apply on-time mechanical stimulation for ligament tissue engineering. Tissue Eng **12**, 3085-95, 2006.

196. Canal, T., Peppas, N.A. Correlation between mesh size and equilibrium degree of swelling of polymeric networks. J Biomed Mater Res **23**, 1183-93, 1989.

197. Park, Y., Lutolf, M.P., Hubbell, J.A., Hunziker, E.B., Wong, M. Bovine primary chondrocyte culture in synthetic matrix metalloproteinase-sensitive poly(ethylene glycol)-based hydrogels as a scaffold for cartilage repair. Tissue Eng **10**, 515-22, 2004.

198. Lutolf, M.P., Weber, F.E., Schmoekel, H.G., Schense, J.C., Kohler, T., Muller, R., Hubbell, J.A. Repair of bone defects using synthetic mimetics of collagenous extracellular matrices. Nat Biotechnol **21**, 513-8, 2003.

199. Engler, A.J., Sen, S., Sweeney, H.L., Discher, D.E. Matrix elasticity directs stem cell lineage specification. Cell **126**, 677-89, 2006.

200. Timmer, M.D., Jo, S., Wang, C., Ambrose, C.G., Mikos, A.G. Characterization of the cross-linked structure of fumarate-based degradable polymer networks. Macromolecules **35**, 4373-4379, 2002.

201. Raeber, G.P., Lutolf, M.P., Hubbell, J.A. Molecularly engineered PEG hydrogels: a novel model system for proteolytically mediated cell migration. Biophys J **89**, 1374-88, 2005.

202. Raeber, G.P., Lutolf, M.P., Hubbell, J.A. Mechanisms of 3-D migration and matrix remodeling of fibroblasts within artificial ECMs. Acta Biomater **3**, 615-29, 2007.

203. Kim, J., Park, Y., Tae, G., Lee, K.B., Hwang, S.J., Kim, I.S., Noh, I., Sun, K. Synthesis and characterization of matrix metalloprotease sensitive-low molecular weight hyaluronic acid based hydrogels. J Mater Sci Mater Med **19**, 3311-8, 2008.

204. Lutolf, M.P., Lauer-Fields, J.L., Schmoekel, H.G., Metters, A.T., Weber, F.E., Fields, G.B., Hubbell, J.A. Synthetic matrix metalloproteinase-sensitive hydrogels for the conduction of tissue regeneration: engineering cell-invasion characteristics. Proc Natl Acad Sci U S A **100**, 5413-8, 2003.

205. Patterson, J., Hubbell, J.A. Enhanced proteolytic degradation of molecularly engineered PEG hydrogels in response to MMP-1 and MMP-2. Biomaterials **31**, 7836-45, 2010.

206. Brink, K.S., Yang, P.J., Temenoff, J.S. Degradative properties and cytocompatibility of a mixed-mode hydrogel containing oligo[poly(ethylene glycol)fumarate] and poly(ethylene glycol)dithiol. Acta Biomater **5**, 570-9, 2009.

207. Diederichs, S., Freiberger, F., van Griensven, M. Effects of repetitive and short time strain in human bone marrow stromal cells. J Biomed Mater Res A **88**, 907-15, 2009.

208. Connelly, J.T. Regulatory mechanisms in the chondrogenesis of mesenchymal progenitors: The roles of cyclic tensile loading and cell-matrix interations [PhD thesis]. Department of Biomedical Engineering, Georiga Institute of Technology, Atlanta, Ga, 2007.

209. Park, J.S., Chu, J.S., Cheng, C., Chen, F., Chen, D., Li, S. Differential effects of equiaxial and uniaxial strain on mesenchymal stem cells. Biotechnol Bioeng **88**, 359-68, 2004.

210. Zhang, L., Tran, N., Chen, H.Q., Kahn, C.J., Marchal, S., Groubatch, F., Wang, X. Time-related changes in expression of collagen types I and III and of tenascin-C in rat bone mesenchymal stem cells under co-culture with ligament fibroblasts or uniaxial stretching. Cell Tissue Res **332**, 101-9, 2008.

211. Hering, T.M. Regulation of chondrocyte gene expression. Front Biosci **4**, D743-61, 1999.

212. Svoboda, K.K. Chondrocyte-matrix attachment complexes mediate survival and differentiation. Microsc Res Tech **43**, 111-22, 1998.

213. Kinneberg, K.R., Nirmalanandhan, V.S., Juncosa-Melvin, N., Powell, H.M., Boyce, S.T., Shearn, J.T., Butler, D.L. Chondroitin-6-sulfate incorporation and mechanical stimulation increase MSC-collagen sponge construct stiffness. J Orthop Res, [Epub ahead of print].

214. Chiquet-Ehrismann, R., Chiquet, M. Tenascins: regulation and putative functions during pathological stress. J Pathol **200**, 488-99, 2003.

215. Chiquet-Ehrismann, R., Kalla, P., Pearson, C.A., Beck, K., Chiquet, M. Tenascin interferes with fibronectin action. Cell **53**, 383-90, 1988.

216. Wang, J.H., Thampatty, B.P., Lin, J.S., Im, H.J. Mechanoregulation of gene expression in fibroblasts. Gene **391**, 1-15, 2007.

217. Iqbal, J., Zaidi, M. Molecular regulation of mechanotransduction. Biochem Biophys Res Commun **328**, 751-5, 2005.

218. Pollard, T.D., Earnshaw, W.C. Cell Biology. Philadelphia: Elsevier Science; 2002.

219. Halfon, S., Abramov, N., Grinblat, B., Ginis, I. Markers Distinguishing Mesenchymal Stem Cells from Fibroblasts Are Downregulated with Passaging. Stem Cells Dev.

220. Dominici, M., Le Blanc, K., Mueller, I., Slaper-Cortenbach, I., Marini, F., Krause, D., Deans, R., Keating, A., Prockop, D., Horwitz, E. Minimal criteria for defining multipotent mesenchymal stromal cells. The International Society for Cellular Therapy position statement. Cytotherapy **8**, 315-7, 2006.